64-5

AIR FORCE INSTITUTE OF TECHNOLOGY

AIR UNIVERSITY
UNITED STATES AIR FORCE

SCHOOL OF ENGINEERING

WRIGHT-PATTERSON AIR FORCE BASE, OHIO

AF-WP-O-OCT 63 3,500

INVESTIGATION OF PHOTOMETRIC DATA RECEIVED FROM AN ARTIFICIAL EARTH SATELLITE

Eugene Michael Vallerie III

Captain USAF

GA/Phys/63-13

AF-WP-O-SEP 63 23

INVESTIGATION OF PHOTOMETRIC DATA RECEIVED FROM AN ARTIFICIAL EARTH SATELLITE

THESIS

Presented to the Faculty of the School of Engineering
of the Air Force Institute of Technology
Air University
in Partial Fulfillment of the
Requirements for the Degree of
Master of Science

by

Eugene Michael Vallerie III
Captain USAF
Graduate Astronautics

August 1963

Preface

The suggestion that this study be undertaken was made by Mr. Kenneth Kissell of the General Physics Research Laboratory, Aerospace Research Laboratories. As an astronomer, Mr. Kissell is extremely interested in all the happenings of the heavens. A long time satellite observer, he suggested that there are many unanswered questions about the variations in the reflected light intensity from satellites. After my first observation of a tumbling satellite, my interest also was aroused. Mr. Kissell's ideas, guidance, and timely prodding were invaluable in the completion of this thesis.

I am deeply indebted to Dr. W. L. Lehmann, Head of the Physics Department of the Air Force Institute of Technology, for his gracious consent to the undertaking of this investigation as a graduate thesis.

I wish to express my appreciation to Mr. Rosenburger and Master Sergeant Jarvis of the Reconnaisence Laboratory, Aeronautical Systems Division, for their assistance in maintaining and operating the tracking facilities.

My special thanks go to the wives of the personnel involved, who have been inconvenienced many evenings

and early mornings while the experimental data was being collected.

Eugene Michael Vallerie III

Contents

Contents

Contents

List of Figures

List of Figures

List of Tables

Abstract

A theory is developed relating the axis of rotation about the center of mass and the orientation of the longitudinal axis of a cylindrical satellite to the variation in light intensity observed by a tracking station. Photometric recordings of the light data received from an artificial earth satellite are made using the equipment at the USAF Sulfur Grove, Ohio tracking station.

The theory is applied to the experimental data received from revolution 257 of satellite 1962 Beta Alpha 2, an Agena B rocket body. The right ascension and declination of the axis of rotation and the longitudinal axis of this satellite are found. Using the orientation of the longitudinal axis found by the developed theory, the variation of light intensity due to orientation is calculated. The effect of changing the phase angle and the right ascension of the longitudinal axis is calculated and compared with the experimental data.

GA/Phys/63-13

INVESTIGATION OF PHOTOMETRIC DATA RECEIVED FROM AN ARTIFICIAL EARTH SATELLITE

I. Introduction

Since visual observations of satellites first began, observers have noticed the reflected light from many of the satellites presents periodic fluctuations during a transit. Early observations of the Russian satellites 1957 β 1 (Ref 8: 163-165) and 1958 δ 1 (Ref 9: 83) indicated a periodic light fluctuation. Satellite observers have now become familiar with the periodic light fluctuations of many satellites (Ref 6: 145). This variation of light intensity depends upon the following factors (Ref 1: 3):

a) the phase angle or angle between the sun, satellite, and observer,

b) the period of rotation of the satellite about its center of mass,

c) the angle that the axis of rotation makes with the plane containing the sun, satellite, and observer,

d) the geometric shape of the satellite,

e) the reflectivity of the satellite surface materials.

The sum of these factors yields a composite effect (Ref 1: 3), i.e., A portion of the total fluctuation, which may range up to seven stellar magnitudes, has a distinct contribution

from each of them. In order to study the contribution from each of these factors, the problem of extracting the individual effects from the composite effects must be solved.

Scope of Study

The purpose of this investigation was to make and interpret photometric recordings of various United States and Russian satellites. The observations were to be performed with the existing tracking and recording equipment located at the Sulfur Grove, Ohio tracking station.

The formulation of a simple analytical theory that may identify some of the variables causing the light fluctuations was to be accomplished and used to investigate the experimental data.

Previous Work

Even before the launching of the first earth satellite, the optical characteristics of a specular reflecting and a diffuse reflecting spherical satellite were predicted (Ref 14: 23-25).

Photometric observations of the Russian satellite 1957 β 1 were made at the U. S. Naval Ordnance Test Station, China Lake, California during March 1958 (Ref 8: 163-165) and of 1958 δ 1 from July 1958 to October 1958 (Ref 9: 83) by James Moore.

The rhythmic flashing of 1958 δ.1 was of enough significance to warrant the organization of Project Rotor to collect and analyze a large number of accurately observed flashes (Ref 5: 83). Many of the reports under Project Rotor included occasions where the fluctuations died out and the reflected light appeared steady (Ref 6: 146).

The Reconnaissance Laboratory, Aeronautical Systems Division, Wright-Patterson Air Force Base, had made photometric recordings of satellite light intensities at the Sulfur Grove, Ohio tracking station in 1962 as part of an equipment feasibility study and to experiment with new tracking techniques. Part of this equipment was used in this investigation.

V. M. Grigorevskij, a Russian astronomer at the Odessa Astronomical Observatory, had attempted to define the orientation of a satellite by using a visual estimation of the light fluctuations. The National Aeronautics and Space Administration's technical translation of his published articles were a major scource of background information (Ref 10: 1-16).

II. Theory

The amplitude of the light curve obtained during the transit of a satellite depends upon many factors. It is necessary to identify each of these factors and to find which are constant, which are variable, which are known, and which are unknown.

The factors considered to be of primary importance in determining the illuminance received by an observer will be discussed and the illuminance equations presented. By elimination of those factors which are known or constant, it is hoped to develop a simple theory for the solution of some of the unknown quantities.

Illumination by the Sun

The solar illuminance, "solar constant", above the atmosphere varies only slightly. There are no systematic or periodic variations larger than 0.2 per cent(Ref 7: 81). For this investigation the solar illuminance will be considered a constant. It has the value of 12,000 lumens/square foot but may be considered in any other appropriate energy units also. The symbol E_s will represent the solar constant in all equations. Any contribution of light arriving at the satellite from other means, such as the moon or earth will be considered negligible (Ref 12: 5).

Satellite Surface Characteristics

Since satellites may be composed of many types of metals, paints, and materials, the type of light reflection will be an unknown. A polished metal surface will give a specular type of reflection while a painted surface will reflect in a diffuse manner dictated by the type of paint. Actual satellite light reflections may be a combination of both diffuse and specular types. Separate equations will be presented for each type of reflection.

Geometrical Shape

The area of a satellite illuminated by the sun for a given orientation depends upon the geometrical size and shape. Shapes of satellites vary considerably and may contain many irregularities. For this investigation only a sphere and a cylinder will be considered in the mathematical calculations.

Orientation in Space

The orientation of a satellite will be considered a constant unless a rotation about the center of mass is present.

A stationary or non-rotating satellite will maintain the same orientation in an inertial reference frame throughout its transit. The phase angle ϕ , the angle

between the line of sight and the surface normal, δ_o , and the angle between the observer's surface normal and the sun's surface normal, ϵ , will all be variables. The angle between the surface normal and the sun line, δ_s , will remain a constant. The phase angle is shown in Figure 1. The other orientation angles are shown in Figure 2.

A satellite rotating about its center of mass has all of the forestated variables and, in addition, the angle between the surface normal and the sun line, δ_s , also becomes a variable during the transit.

Variation of Distance from the Observer

The illumination varies inversely with the square of the distance from the observer. In a typical transit slant range will increase and decrease by a factor of three. This contributes to a large variation of the illumination received by the observer. A correction may be applied to bring all illuminance to a standard reference range of 1000 kilometers in the following manner:

E = Reflected Light Illumination at 1000 Kilometers

E* = Reflected Light Illumination at Range (r)

$$E\,(1000)^2 = \text{constant} = E^*\,(r)^2$$

$$E = \frac{E^*\,(r)^2}{(1000)^2}$$

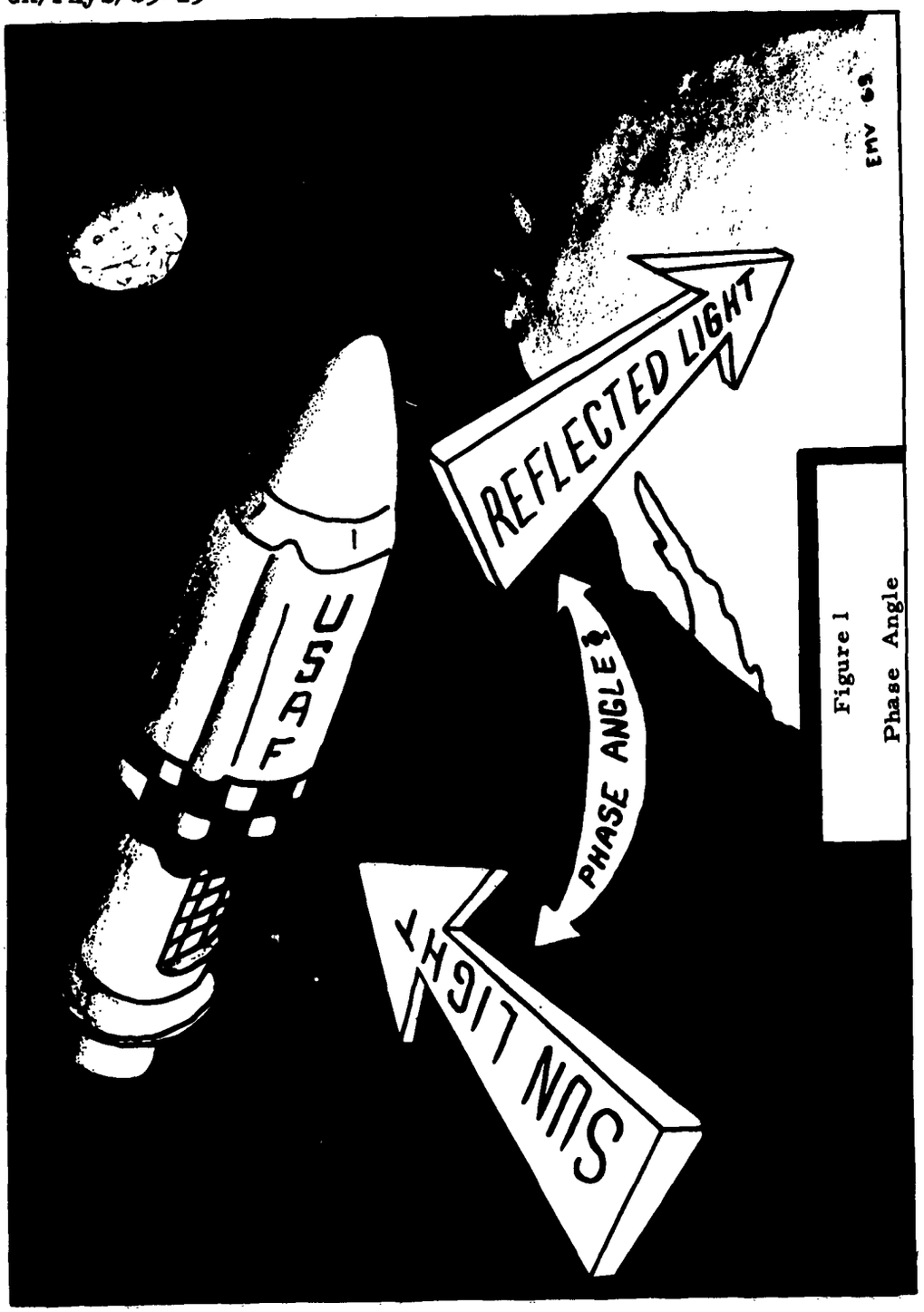

Figure 1
Phase Angle

(Adapted from Ref 7)

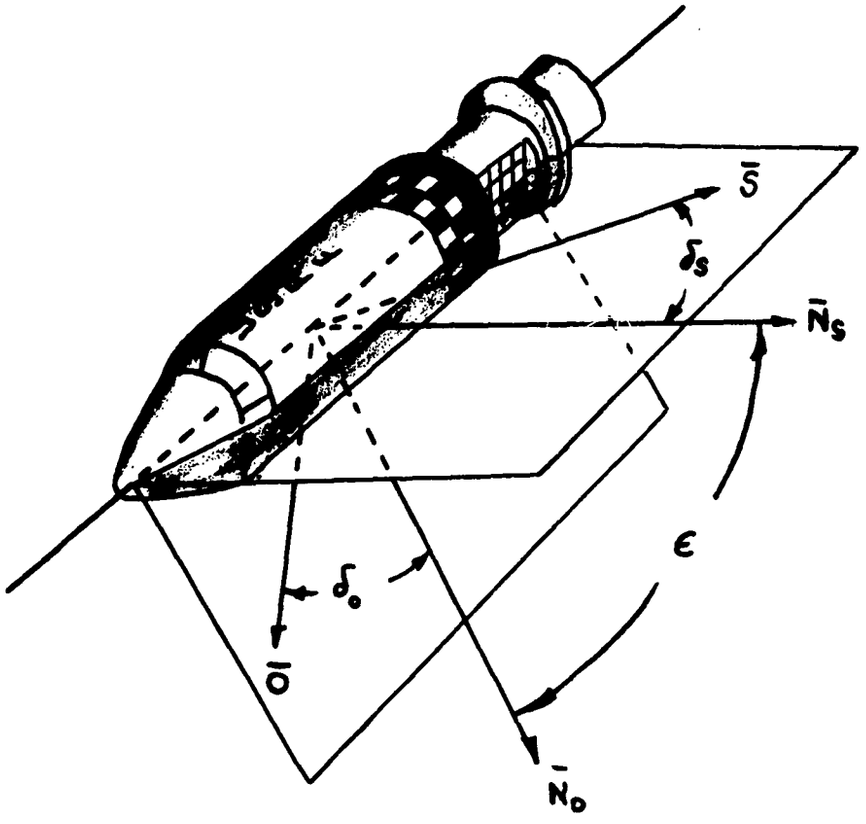

Figure 2

Orientation Angles

Atmospheric Absorption

The absorption of light by the atmosphere not only depends upon the distance the light must travel through the atmosphere but also upon the specific conditions of the atmosphere at the time of the observation. A reasonably good correction can be computed using the method set forth by Leendert Binnendijk in Properties of Double Stars (Ref 2: 239-244). The air mass traversed by the light from a star at any elevation is taken as the secant of the zenith distance z, with the air mass at the zenith taken as unity. Secant z is computed as a function of the hour angle t. Extinction stars are observed at regular time intervals and the extinction is plotted against air mass. A zenith correction was not applied in this investigation since atmosphere conditions usually deteriorated rapidly during and after a satellite transit. Magnitude reference stars were observed but not extinction stars. Zirker, Whipple and Davis (Ref 14: 28) take extinction as a constant .4 magnitude above 30° in elevation.

Reflected Light Equations

In expressing the reflected light equations the following symbols will be used:

E_s, illuminance at the satellite due to the source in lumens/square foot,

E_o, illuminance received by the observer in lumens/square foot,

a , ratio of reflected light to incident light,

b , radius of reflecting sphere or cylinder, feet,

h , length of cylinder, feet,

d , distance from satellite to observer, feet,

T , atmospheric absorption coefficient, ratio of light arriving at observer to reflected light,

ϕ , phase angle, see Figure 1,

δ_o , angle between line of sight and surface normal

δ_s , angle between sun line and surface normal

ϵ , angle between surface normals, see Figure 2.

Although the illuminance equations may be derived from geometrical optics principles, for shapes other than a sphere or cylinder these equations become quite cumbersome. Only the equations for a sphere and cylinder are developed below.

1) Specular Reflecting Sphere (Ref 14:24-25)

Let $2\alpha = \phi$ phase angle.

Consider the radiation incident on a spherical zone of the sphere whose angular radius is α and width $d\alpha$. Axis of the spherical zone is in the direction of the sun. The power incident on the zone is

$$dF = E_s \, 2\pi b^2 \sin\alpha \cos\alpha \, d\alpha$$

and falls on area

$2\pi\, d^2 \sin 2\alpha\, (2\, d\alpha)$ at a distance d from the sphere.

The observed illuminance is

$$E_o = \frac{2\pi\, b^2\, E_s \sin\alpha \cos\alpha\, d\alpha\; a\, T}{2\pi\, d^2 \sin 2\alpha\, (2\, d\alpha)} = \frac{b^2\, E_s\, a\, T}{4\, d^2}$$

2) Diffuse Reflecting Sphere (Ref 14: 24)

Lambert's Law for a diffuse surface gives the power radiated (dq) per unit solid angle from the surface element ds, in the direction making an angle δ_o with the surface normal as

$$dq = \frac{a}{\pi} E_s \cos\delta_s \cos\delta_o\, ds \qquad (1)$$

where

a = per cent reflected by surface

E_s = incident illuminance

δ_s = angle of incidence measured from surface normal.

The surface element expressed in terms of spherical co-ordinates b, Θ , ω is

$$ds = b^2 \cos\Theta\; d\Theta\; d\omega \qquad (2)$$

The polar axis is taken to be the direction from the center of the sphere (of radius b) to the observer.

$$\cos\delta_o = \cos\omega \cos(\Theta - \Phi) \qquad (3)$$

$$\cos\delta_s = \cos\omega \cos\Theta \qquad (4)$$

Substituting equations 2, 3, and 4 into 1 and integrating we obtain

$$q = \frac{a E_s b^2}{\pi} \int_{-\frac{\pi}{2}}^{\frac{\pi}{2}} \cos^3 \omega \; d\omega \int_{\phi - \frac{\pi}{2}}^{\frac{\pi}{2}} \cos(\theta - \phi)\cos\theta \; d\theta$$

$$= \frac{2 a E_s b^2}{3 \pi} \left[\sin\phi + (\pi - \phi)\cos\phi \right]$$

The observed illumination is

$$E_o = \frac{q T}{d^2} = \frac{2 a E_s T b^2}{3 \pi d^2} \left[\sin\Phi + (\pi - \Phi)\cos\Phi \right]$$

3) Specularly Reflecting Cylinder (Ref 3: 119)

In general, plane and cylindrical mirrors reflect light in narrow beams and the illuminance due to the mirror would be

$$E_o = E_s \frac{a h b T}{d^2} \cos \frac{\epsilon}{2}$$

4) Diffusely Reflecting Cylinder (Ref 12: 7)

Applying Lambert's Law as in the case of a diffuse sphere and integrating over the cylinder the illuminance at the observer would be

$$E_o = E_s \frac{a h b T}{2 \pi d^2} \left[(\pi - \epsilon)\cos\epsilon + \sin\epsilon \right] \cos\delta_o \cos\delta_s$$

Calculation of the Axis of Rotation About the Center of Mass

It is assumed that the axis of rotation about the center of mass of a cylindrical satellite is approximately perpendicular to the longitudinal axis of the cylinder.

The axis of rotation may be oriented with respect to the line of sight in three ways.

1) As shown in Figure 3A, the axis of rotation may be contained in a plane that is perpendicular to the line of sight. A rotation in this orientation will cause a maximum area change relative to the observer.

2) In Figure 3B, the axis of rotation lies along the line of sight. There will be no area change and therefore no variation of illumination due to axis of rotation orientation.

3) Figure 3C shows the axis of rotation at some angle Θ to the line of sight. The area change will then vary as the function $(1-\cos\Theta)$. The amplitude of the illuminance curve will vary as $A(1-\cos\Theta)$, where A is the maximum illuminance for that transit (Ref 10: 3).

At the point of greatest illuminance variation during a transit, the axis of rotation is contained in a plane that is perpendicular to the line of sight.

If the lines of sight for two different transits are expressed as vectors in an inertial reference frame, then the axis of rotation is contained in the intersection of the two planes that are perpendicular to the respective

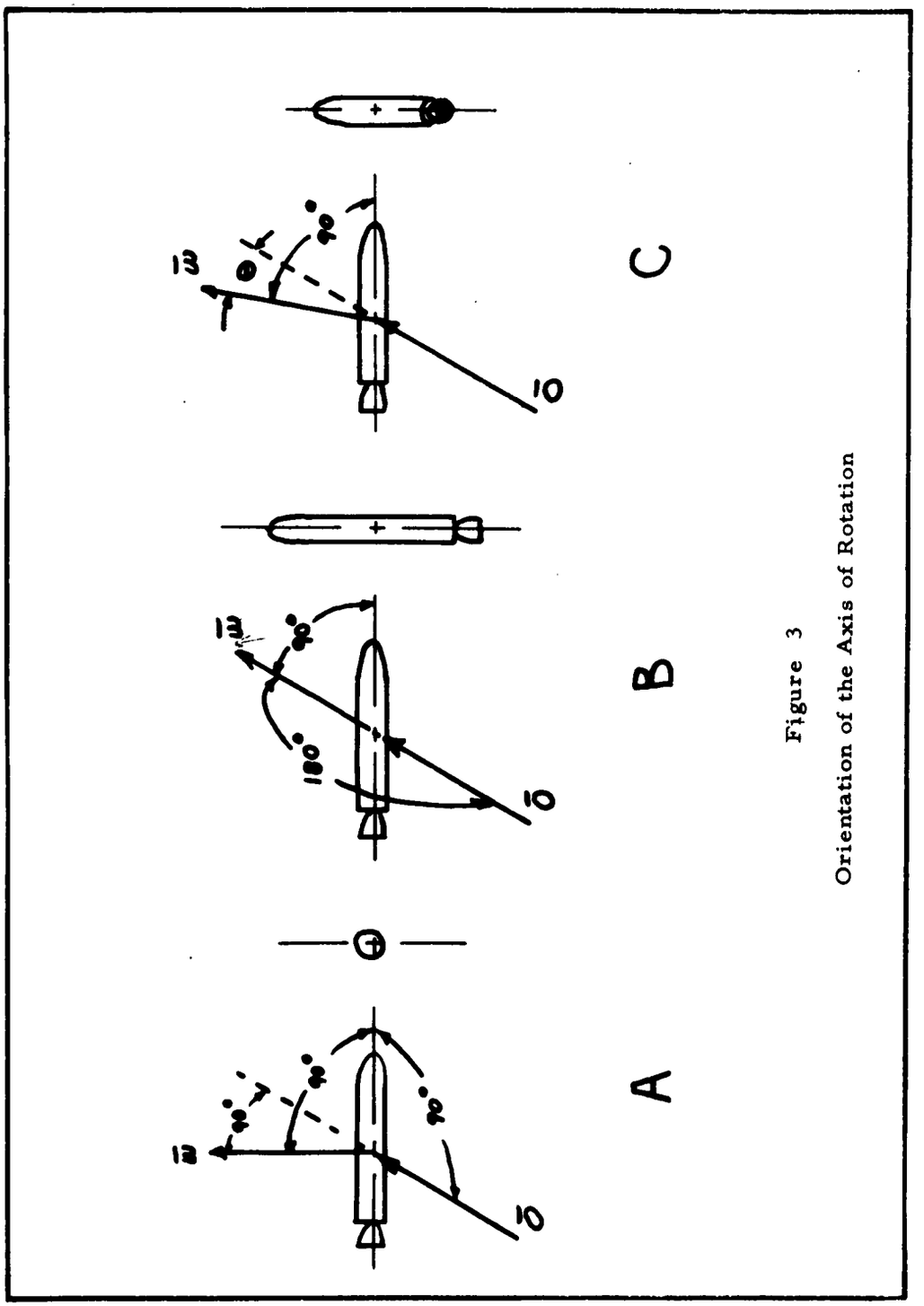

Figure 3
Orientation of the Axis of Rotation

lines of sight.

The vector product of the two line of sight vectors will define a vector that has the same orientation as the intersection of the two perpendicular planes containing the axis of rotation. This vector has the same direction cosines as the line containing the axis of rotation.

Example:

Line of sight vector of 1st transit is $\bar{O}_1$.

Line of sight vector of 2nd transit is $\bar{O}_2$.

Expressed in equatorial co-ordinates, the direction cosines of these vectors are as follows:

Vector $\bar{O}_1$	Vector $\bar{O}_2$
$\alpha_1 = \cos D_1 \cos \Psi_1$	$\alpha_2 = \cos D_2 \cos \Psi_2$
$\beta_1 = \cos D_1 \sin \Psi_1$	$\beta_2 = \cos D_2 \sin \Psi_2$
$\gamma_1 = \sin D_1$	$\gamma_2 = \sin D_2$

where Ψ is the right ascension and D the declination in the usual astronomical sense.

The vector product of $\bar{O}_1$, $\bar{O}_2$ is

$$\bar{O}_1 \times \bar{O}_2 = \begin{pmatrix} \beta_2\gamma_1 - \gamma_2\beta_1 \\ \gamma_2\alpha_1 - \alpha_2\gamma_1 \\ \alpha_2\beta_1 - \beta_2\alpha_1 \end{pmatrix}$$

The components of the vector product are

$$\alpha_3' = \beta_2\gamma_1 - \gamma_2\beta_1$$
$$\beta_3' = \gamma_2\alpha_1 - \alpha_2\gamma_1$$
$$\gamma_3' = \alpha_2\beta_1 - \beta_2\alpha_1$$

The direction cosines of the vector product are found by dividing the components of the vector product by the length. Therefore, the direction cosines of the axis of rotation in inertial space are

$$\alpha_3 = \frac{\alpha_3'}{\sqrt{\alpha_3'^2 + \beta_3'^2 + \gamma_3'^2}}$$

$$\beta_3 = \frac{\beta_3'}{\sqrt{\alpha_3'^2 + \beta_3'^2 + \gamma_3'^2}}$$

$$\gamma_3 = \frac{\gamma_3'}{\sqrt{\alpha_3'^2 + \beta_3'^2 + \gamma_3'^2}}$$

Since $\gamma_3 = \sin D_3$, the declination of the axis of rotation is found immediately. Solution of either

$$\alpha_3 = \cos D_3 \cos \Psi_3$$

or

$$\beta_3 = \cos D_3 \sin \Psi_3$$

gives the right ascension of the axis of rotation.

With the orientation of the axis of rotation now known, the plane of rotation in inertial space is also known. However, the direction of the rotation about this axis and in the plane of rotation is not yet known.

Calculation of the Orientation of the Longitudinal Axis of a Cylindrical Satellite

For the calculation of the orientation of the longitudinal axis of a cylindrical satellite during a transit, the variables of orientation for a diffuse cylinder will be used. The equation for a diffusely reflecting cylinder as previously stated is

$$E_o = E_s \frac{a\ h\ b\ T}{2\pi\ d^2} \left[(\pi - \epsilon)\cos\epsilon + \sin\epsilon \right] \cos\delta_o \cos\delta_s$$

The solar constant E_s, the reflectance a , the satellite size h and b are all constants. The atmospheric absorption T and the range d are independent of orientation. It is then assumed that the quantity $\left[(\pi - \epsilon)\cos\epsilon + \sin\epsilon \right] \cos\delta_o \cos\delta_s$ is dependent only upon the orientation of the satellite. Therefore, ϵ , $\cos\delta_o$, and $\cos\delta_s$ will be considered variables of orientation during a transit. At a particular point in a transit all of these variables take on a definite value.

The following notation for the solution of the variables of orientation will be used:

$\bar{A}$, unit vector along satellite longitudinal axis,

$\bar{O}$, unit vector along line of sight from satellite to observer,

$\bar{S}$, unit vector along sun line from satellite to sun,

$\bar{N}_o$, surface normal of cylinder that lies in plane containing $\bar{O}$ and $\bar{A}$,

$\bar{N}_s$, surface normal of cylinder that lies in plane containing $\bar{S}$ and $\bar{A}$,

δ_o, angle between the normal $\bar{N}_o$ and the vector $\bar{O}$,

δ_s, angle between the normal $\bar{N}_s$ and the vector $\bar{S}$,

ϵ, angle between the surface normals $\bar{N}_o$ and $\bar{N}_s$.

All of these quantities are shown in Figure 2.

The scalar product of $\bar{A}$ and $\bar{O}$ will give the cosine of the angle between them. This angle is $90^o - \delta_o$. Therefore,

$$\cos \delta_o = \sin \cos^{-1} \bar{A} \cdot \bar{O}.$$

In a similar manner

$$\cos \delta_s = \sin \cos^{-1} \bar{A} \cdot \bar{S}.$$

The vector product $\bar{A} \times \bar{O}$ results in a vector perpendicular to the plane of $\bar{A}$ and $\bar{O}$. This vector is also perpendicular to the normal $\bar{N}_o$. Division by $\cos \delta_o$ results in a unit vector perpendicular to the

normal $\bar{N}_o$.

$$\frac{\bar{A} \times \bar{O}}{\cos \delta_o} = \text{a unit vector perpendicular to the plane containing } \bar{N}_o.$$

Similarly,

$$\frac{\bar{A} \times \bar{S}}{\cos \delta_s} = \text{a unit vector perpendicular to the plane containing } \bar{N}_s.$$

The angle between the two unit vectors is the same as the angle between the normals $\bar{N}_o$ and $\bar{N}_s$, for the sides are mutually perpendicular. Therefore,

$$\cos \epsilon = \frac{\bar{A} \times \bar{O}}{\cos \delta_o} \cdot \frac{\bar{A} \times \bar{S}}{\cos \delta_s}$$

By vector identity,

$$\cos \epsilon = \frac{(\bar{A} \cdot \bar{A})(\bar{O} \cdot \bar{S}) - (\bar{O} \cdot \bar{A})(\bar{A} \cdot \bar{S})}{\cos \delta_o \quad \cos \delta_s}$$

$$\cos \epsilon = \frac{(\bar{O} \cdot \bar{S}) - (\bar{O} \cdot \bar{A})(\bar{A} \cdot \bar{S})}{\cos \delta_o \quad \cos \delta_s}$$

The quantity $(\bar{O} \cdot \bar{S})$ is equal to the cosine of the angle between the observer's vector and the sun vector and is known as the phase angle Φ. Thus

$$\cos \epsilon = \frac{\cos \Phi - \sin \delta_o \sin \delta_s}{\cos \delta_o \quad \cos \delta_s}$$

If the direction cosines of the three unit vectors $\bar{A}$, $\bar{O}$, and $\bar{S}$ are expressed in equatorial co-ordinates, then the variables ϵ , δ_o, and δ_s can be expressed as functions of equatorial co-ordinates. The direction cosines of a unit vector are as follows:

$$\alpha = \cos D \cos \Psi$$
$$\beta = \cos D \sin \Psi$$
$$\gamma = \sin D$$

where Ψ is the right ascension and D the declination in equatorial co-ordinates.

Substitution in the equation for $\cos \delta_o$ is performed as follows:

$$\cos \delta_o = \sin \cos^{-1} \bar{A} \cdot \bar{O}$$

$$\bar{A} \cdot \bar{O} = \begin{bmatrix} \alpha_a \\ \beta_a \\ \gamma_a \end{bmatrix} \cdot \begin{bmatrix} \alpha_o \\ \beta_o \\ \gamma_o \end{bmatrix} = \alpha_a \alpha_o + \beta_a \beta_o + \gamma_a \gamma_o$$

$$\alpha_a \alpha_o = \cos D_a \cos \Psi_a \cos D_o \cos \Psi_o$$

$$\beta_a \beta_o = \cos D_a \sin \Psi_a \cos D_o \sin \Psi_o$$

$$\gamma_a \gamma_o = \sin D_a \sin D_o$$

$$\bar{A} \cdot \bar{O} = \cos D_a \cos \Psi_a \cos D_o \cos \Psi_o + \cos D_a \sin \Psi_a \cos D_o \sin \Psi_o + \sin D_a \sin D_o$$

Then,

$$\cos\delta_o = \sin\cos^{-1}\left[\cos(\Psi_a-\Psi_o)\cos D_a\cos D_o + \sin D_a\sin D_o\right]$$

Similarly

$$\cos\delta_s = \sin\cos^{-1}\left[\cos(\Psi_a-\Psi_s)\cos D_a\cos D_s + \sin D_a\sin D_s\right]$$

In the expression of the cosine of the angle between the two surface normals, ϵ, the phase angle Φ must also be solved for in equatorial coordinates. The phase angle Φ is equal to the supplement of the angle between the sun, observer, and the satellite. This is angle SAO in Figure 4. Angle SOA, the supplement of Φ, is first found by projection on the celestial sphere and the solution of a spherical triangle. This procedure is used since the distance between the observer and the satellite is small compared to the distance between the observer and the sun. It can be assumed that the line from the observer to the sun, line OS, is parallel to the line from the satellite to the sun, line AS in Figure 4.

$$\text{Phase Angle } \Phi = 180 - \cos^{-1}\left[\cos(90-D_s)\cos(90-D_o) + \sin(90-D_s)\sin(90-D_o)\cos(\Psi_o-\Psi_s)\right]$$

It is observed that unknown quantities in all of the preceding expressions are the right ascension Ψ_a and the declination D_a of the longitudinal axis of the cylindrical satellite. An estimate of these two unknowns can be achieved by using the point of maximum light

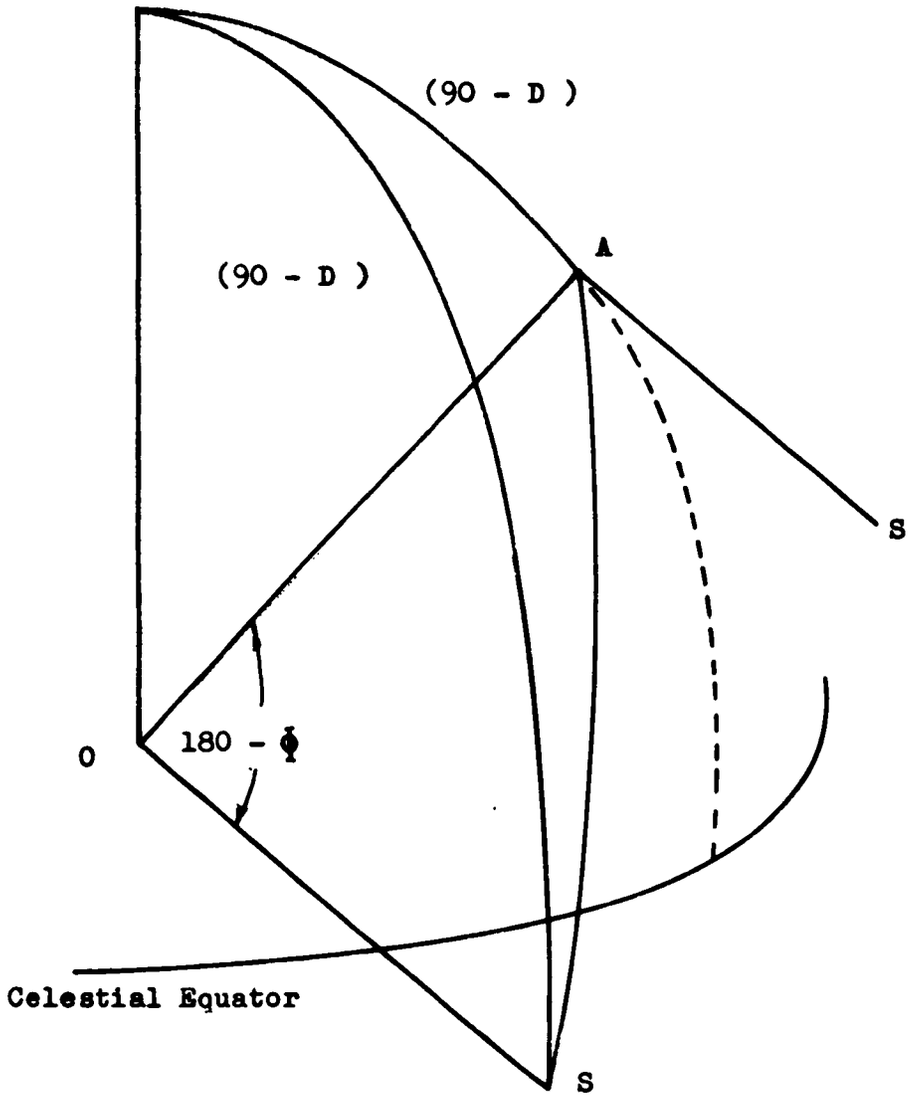

Figure 4

Projection of Phase Angle Supplement

variation during a transit, as was used in determining the orientation of the axis of rotation.

At the point of maximum light variation it was assumed that the longitudinal axis of the satellite was contained in the plane of the line-of-sight vector $\bar{O}$ and the sun line vector $\bar{S}$. The angle between these two vectors is the phase angle Φ . Normals $\bar{N}_o$ and $\bar{N}_s$ then coincide and the angle ϵ between them is zero. For maximum reflection, both specular and diffuse, the surface normals bisect the phase angle Φ and δ_o equals δ_s . This orientation is shown in Figure 5.

Projection of these quantities on the celestial sphere and the solution of the resulting spherical triangles results in the determination of the right ascension and declination of the longitudinal axis of the satellite. The spherical triangles are illustrated in Figure 6.

Direction of Rotation About the Center of Mass

Although the line containing the axis of rotation of a cylindrical satellite has previously been found, the direction of the axis along this line is not known.

If the longitudinal axis makes a given angle with the line-of-sight at the maximum light variation, after one period of revolution with respect to the sun, the longitudinal axis will not make the same angle θ_1 with the line-of-sight due to the motion of the satellite in space.

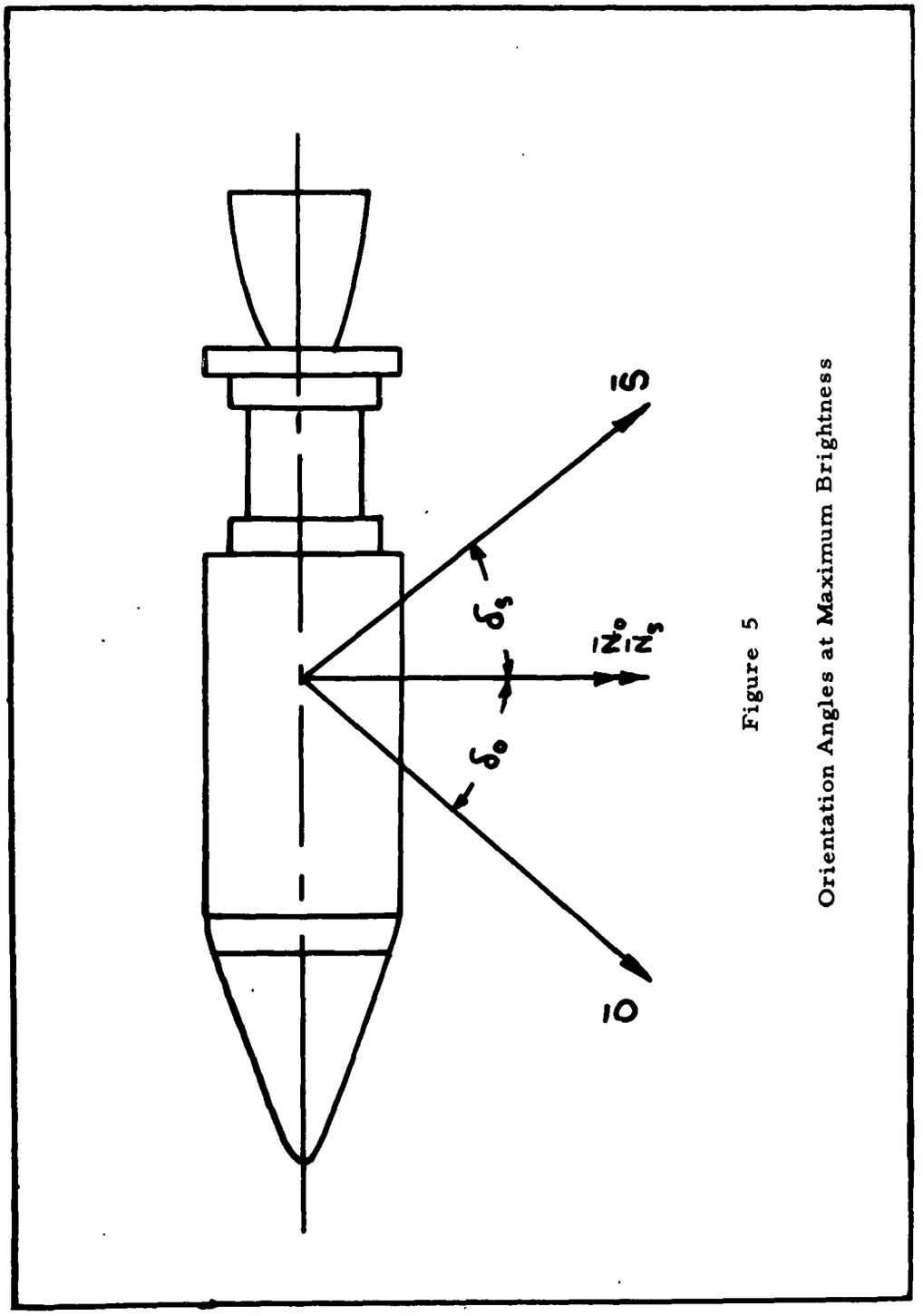

Figure 5

Orientation Angles at Maximum Brightness

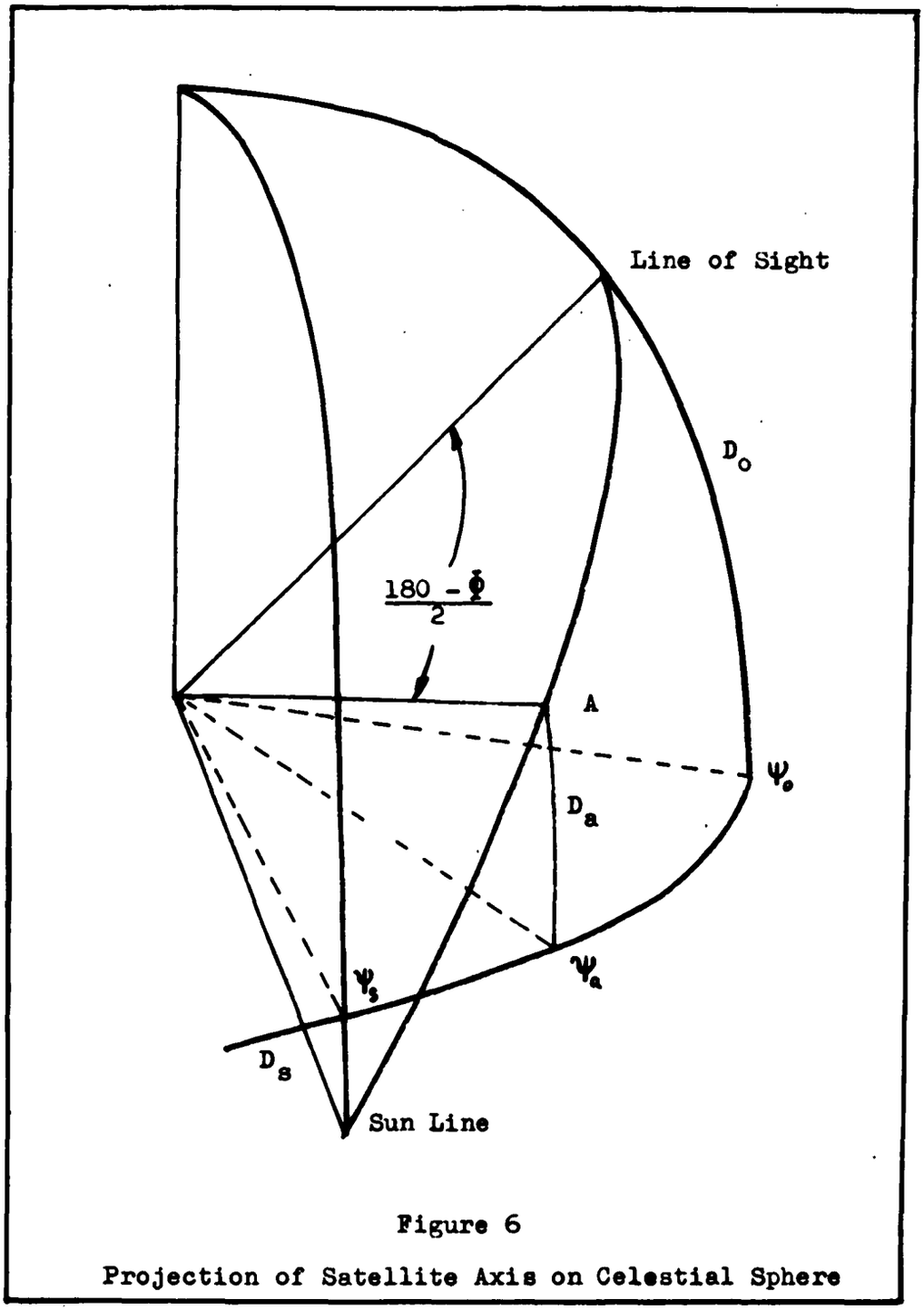

Figure 6

Projection of Satellite Axis on Celestial Sphere

In order for the longitudinal axis to make the same angle θ_1 (rotate through one period with respect to the line of sight), it must turn through one period with respect to the sun plus or minus the quantity $\left[\frac{\sigma}{360} \text{ X Period}\right]$. The sign will be dependent upon the direction of rotation of the satellite (Ref 10: 9). Figure 7A shows one period of a cylindrical rotating satellite with respect to the sun. It is obvious that after one period the satellite does not make the same angle with the line of sight. In Figure 7B, the satellite returns to the same orientation with respect to the line of sight but has turned through an angle greater or less than one period depending on the direction of rotation and the direction of the sun.

If the absolute period of a satellite is known, then an increase or decrease of the period during a transit will reveal the direction of rotation.

If a satellite had a true period of 10 seconds and the measured apparent period (average for one transit) was 10.01 seconds, then after 1000 revolutions there would be a difference of one period between the integral numberof revolutions made by the true period and that of the apparent period.

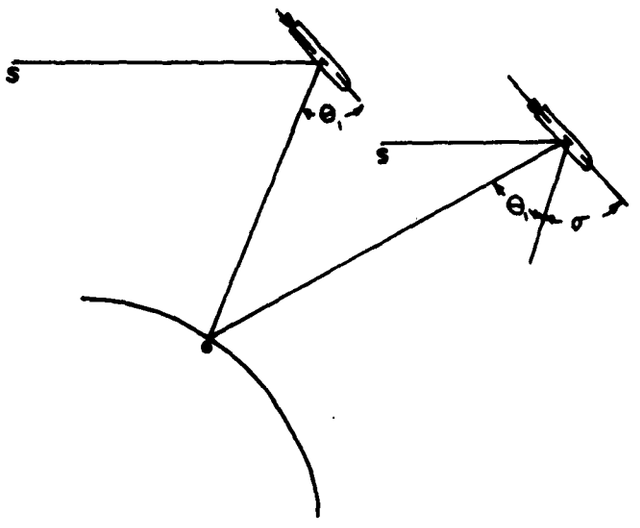

Figure 7A

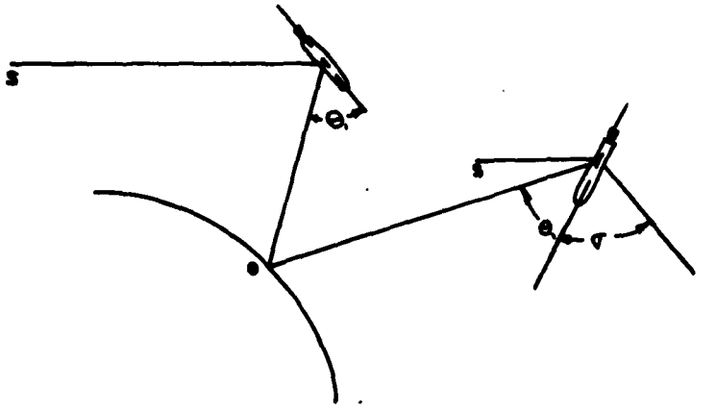

Figure 7B

Period of Revolution

From photometric data it is possible to measure the apparent period (average of one transit) to within .01 seconds. It is possible to assign an integral number of revolutions to a corresponding point in the orbit so the apparent period can be compared with the true period if the percentage of increase or decrease of the angular rate is greater than .01/period.

III. Description of Apparatus

The equipment used to make photometric recordings was originally used by the Aerial Reconnisance Laboratory, ASD, for the study of scintillation effects during a satellite transit. Since August 1962 the equipment has been turned over to Mr. Kenneth Kissell, ARL, to continue experiments in satellite photometry.

Basic Overall System

The apparatus consists of a 12-inch Cassegrain optical system of 60-inch focal length mounted on a modified Baker-Nunn satellite camera triaxial mount. Light is focused on an RCA type 7029 photomultiplier and the voltage is recorded on an Ampex tape recorder. Voltage is simultaneously applied to a Honeywell Visicorder for visual representation. A block diagram of the equipment is shown in Figure 8.

Optics

Aquisition and tracking of the satellite is done visually with an auxillary telescope with a 2.2 degree field of view. Gathering of the light for the phototube is done by a Perkin Elmer 12-inch Cassegrain theodolite of 60-inch focal length. Figure 9 shows a simlified drawing of the theodolite system.

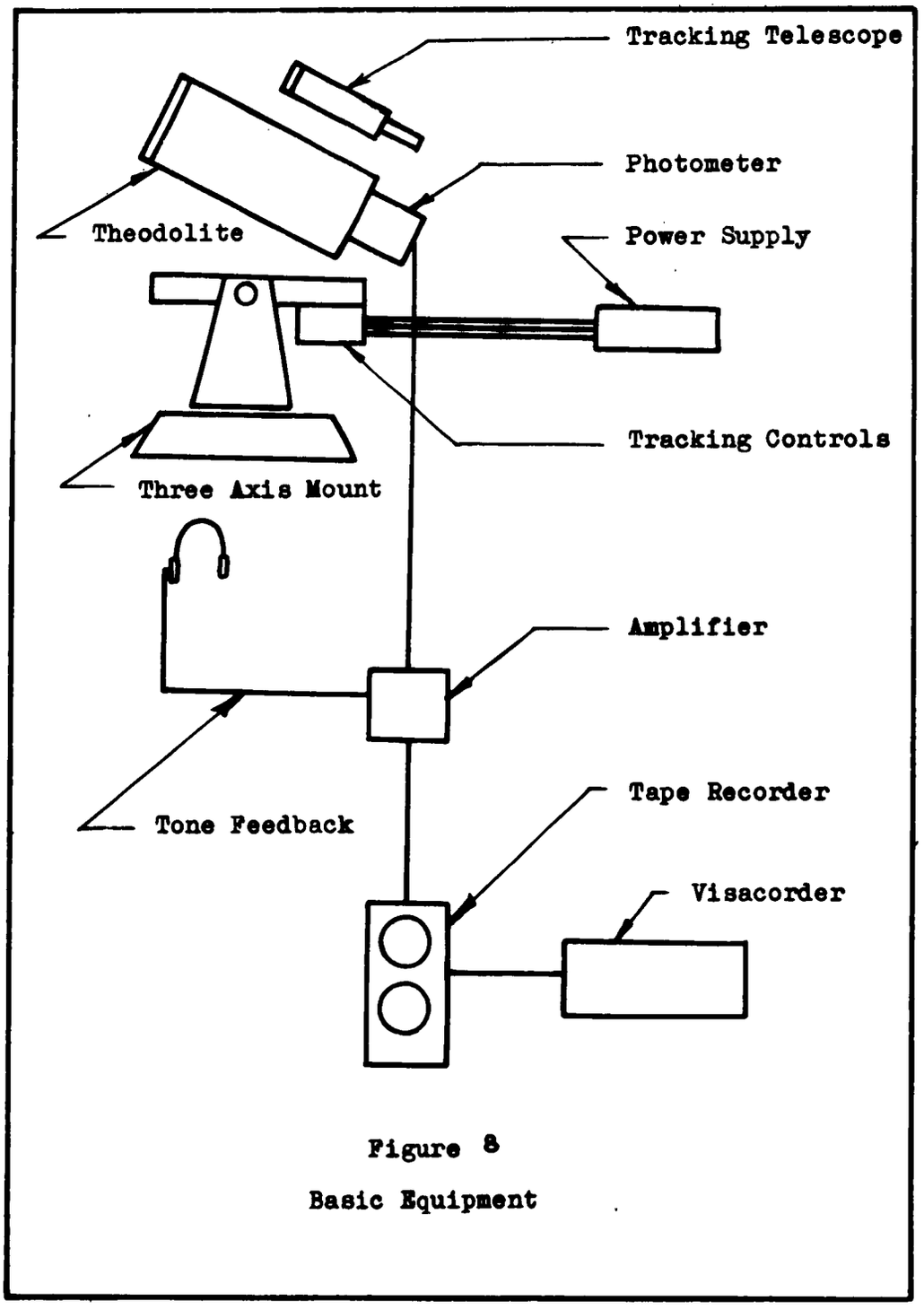

Figure 8

Basic Equipment

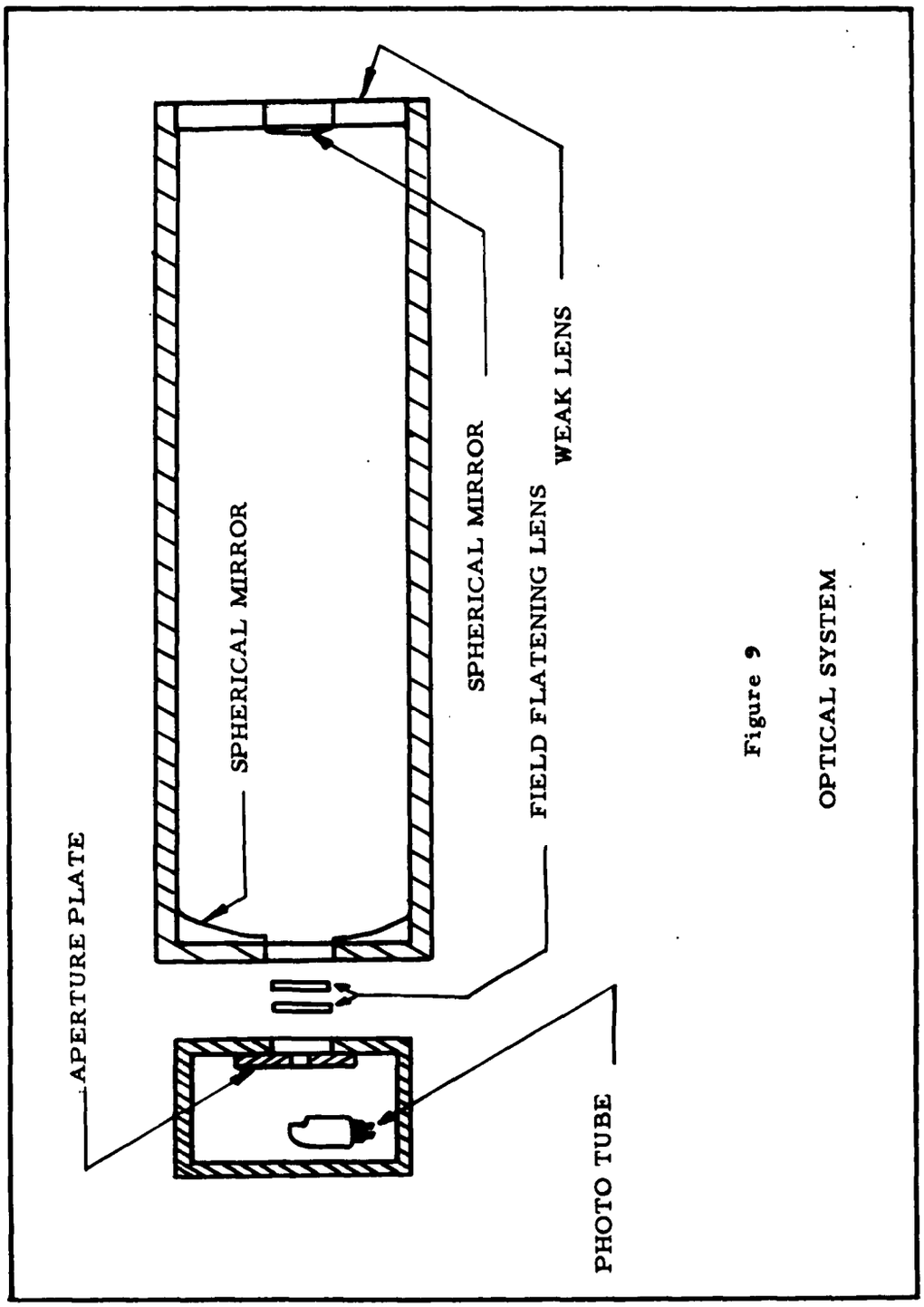

Figure 9

OPTICAL SYSTEM

Triaxial Mount

The modified Baker-Nunn satellite camera mount allows movement of the telescope field through an approximation of the satellite track across the sky. The optical system and triaxial mount are shown in Figures 10 and 11.

Photo Multiplier

The photo multiplier used is an RCA 10-stage, dormer-window type 7029 with extremely high cathode sensitivity. A dimensional outline and base diagram is shown below in Figure 12. The spectral sensitivity curve is contained in Figure 13.

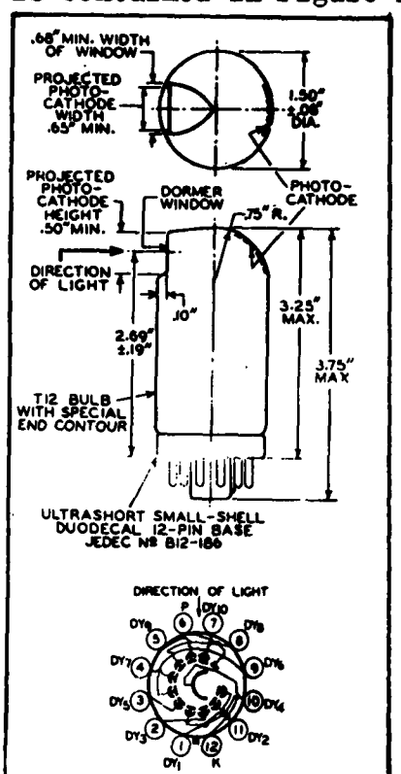

Figure 12

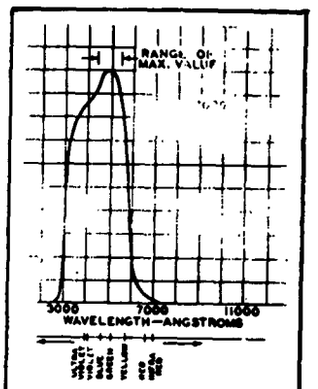

Figure 13

Tape Recorder

For permanent recordings a frequency-modulated tape recorder is used. It is manufactured by Ampex Corporation and is model 3560, serial number 55M155.

Visicorder

Visual recording is done on a Honeywell Visicorder, Figure 16. The paper used in the recorder is a direct print linagraph paper made by the Eastman Kodak Company.

Figure 10
Optical System and Triaxial Mount

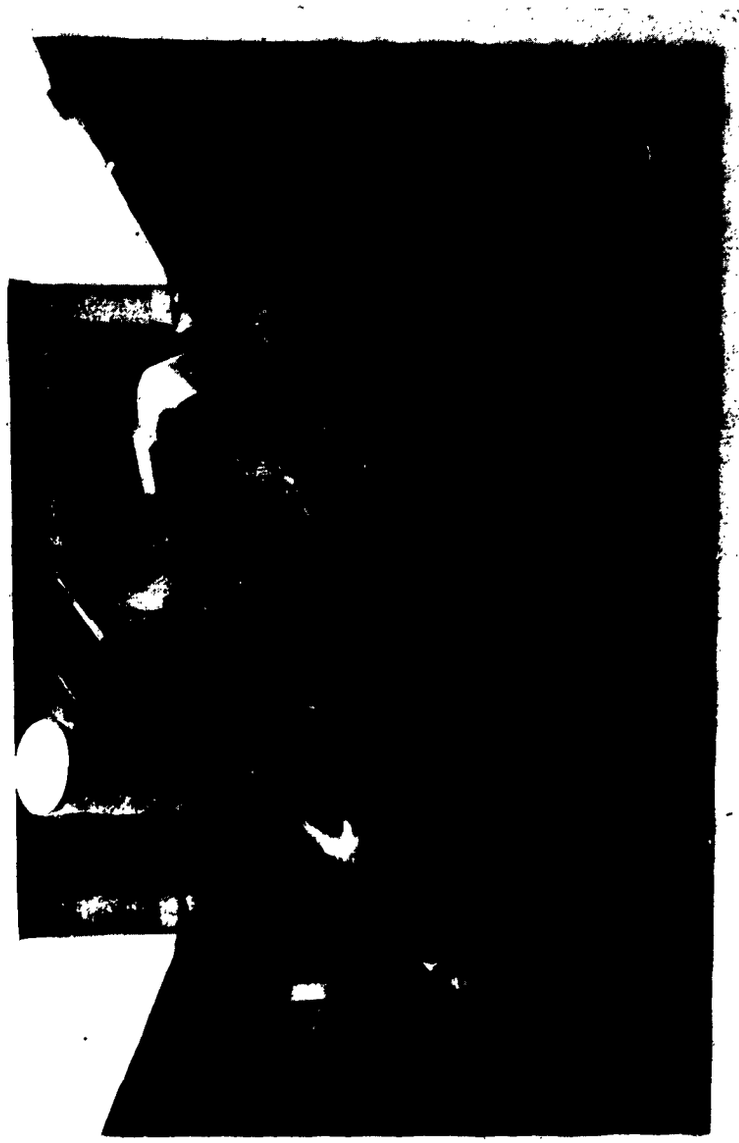

Figure 11

Optical System and Triaxial Mount

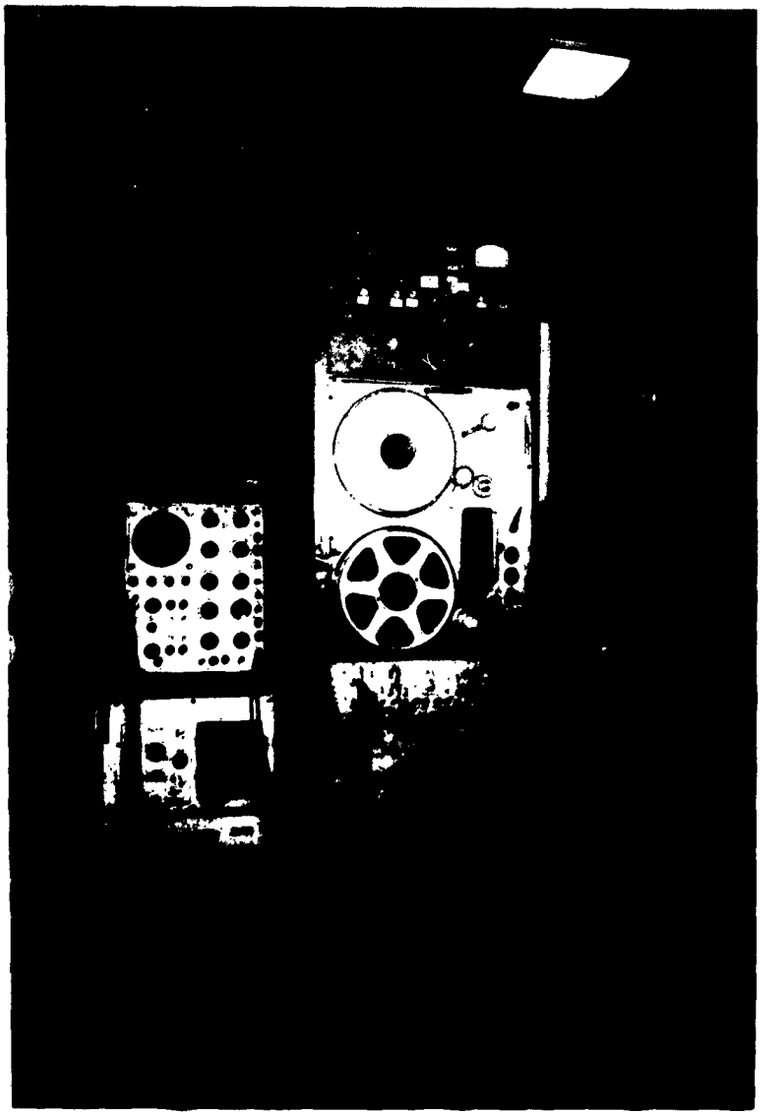

Figure 14

Tape Recorder

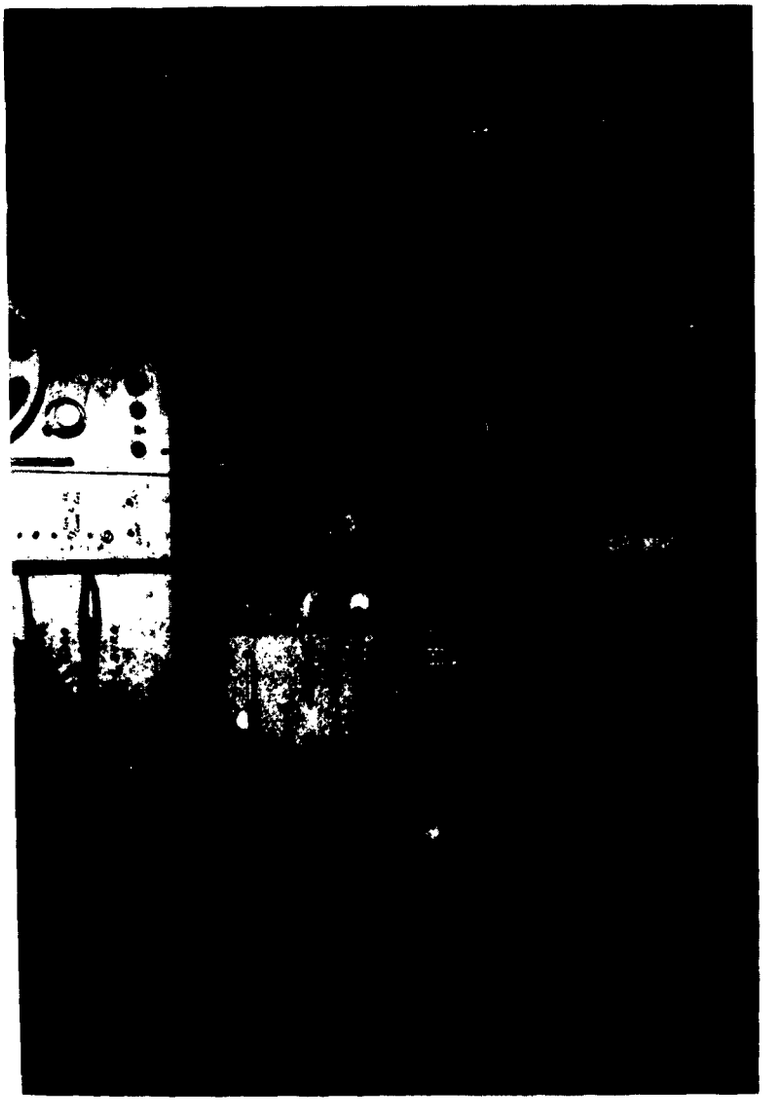

Figure 15

Communications Panel and Power Supply

Figure 16
Visicorder

IV. Tracking and Recording Procedure

Tracking information is received from SPADATS, Ent Air Force Base, Colorado or from Spacetrack R & D Facility, Hanscom Field, Mass. by TWX in the form of Look Angles giving day, time, elevation, azimuth, range, sun elevation, and illumination. Illumination is the angle of the sun with respect to the satellite's horizon. A negative illumination means the satellite is in the earth's shadow and is not illuminated. If Look Angles data are not available, a bulletin of equatorial crossings from SPADATS or the Smithsonian Astrophysical Observatory is used and the look angles are calculated using the procedure set forth by Paul R. Measel and Kenneth E. Kissell (Ref 4: 1-16).

This information is then recalculated for aligning the triaxial mount for azimuth, gimbal and platform angles.

The lowest point in elevation available is then selected as the aquisition point. At aquisition the satellite may pass into the field of the auxillary visual telescope but not into the photometer. Manual tracking speed (platform angular velocity) and gimbal angle are adjusted until the satellite enters the field of the photometer. Acceptance of the satellite by the photometer aperture is indicated by a change of frequency of an audio tone feedback from the photometer.

Manual tracking is accomplished during the transit by control of the platform angular rate and the gimbal angle.

The photometer signals are recorded on the tape recorder and simultaniously on the Visicorder paper. An instantaneous graphical recording is made. Time marks from station WWV are applied to the graphical recording by the recording equipment operator. At the end of the satellite transit, brightness recordings of several stars of known magnitude are made as a reference.

V. Analysis of Data

As a satellite is injected into orbit the carrier rocket body the payload has just separated from also attains orbital velocity. The Agena B rocket body that placed the Canadian satellite Alouette into orbit is an example of this occurence. Primarily this rocket body, known as 1962 Beta Alpha 2, and two Russian rocket bodies, 1963-10B and 1962 Beta Theta 2, were used as objects for obtaining experimental light curves.

Reduction to Linear Form

The response of the photomultiplier is logarithmic in form and the raw experimental data on a light curve are adjusted to linear form by taking the anti log of the voltage. Several of the experimental curves are contained in Appendix B. The raw data peak voltages contained in the curves of 1962 Beta Alpha 2, revolutions 257 and 270, were reduced to linear form and are shown in Tables I and II of Appendix A.

Range and Background Corrections

After the peak voltages are reduced to linear form, the background voltage in linear form is then subtracted. The range correction is now applied to bring the data in or out to a standard 1000 km reference. This eliminates any variation in the light curve due to range changes. A graph of the peak voltages of revolution

257, satellite 1962 Beta Alpha 2, before the range correction and also after the range correction are shown in Figures 17 and 18 of Appendix A. A problem occurs in reducing minimum voltages of a light curve if they are equal to or below the background level voltage. It is then impossible to separate the two quantities.

Conversion to Equatorial Coordinates

The elevation and azimuth are both plotted against time from the tracking information. This facilitates finding the elevation and azimuth for any point on the light curve. For 1962 Beta Alpha 2, revolutions 257 and 270, the elevation and azimuth of the peak voltages were converted to right ascension and declination using the standard conversion equations. Thesevalues are listed in Tables III and IV in Appendix A.

The Air Almanac was used for the location of the First Point of Aries and the right ascension and declination of the sun (Ref 13: 581).

Calculation of the Axis of Rotation

Calculation of the axis of rotation about the center of mass for 1962 Beta Alpha 2 was attempted using the maximum points of light variation found on the light curves for revolutions 257 and 270. The procedure was the same as previously discussed (p. 13). The vector product of the lines of sight of the maximum variation points was divided by the length to arrive at the direction cosines of the line containing the axis of rotation. The line

containing the axis of rotation was found to have a right ascension of 08^{o} 52' and a declination of 18^{o} 48'. The calculations are shown in Appendix A. It should be remembered that the theory was derived for a cylinder whose axis of rotation was perpendicular to the longitudinal axis. The actual axis of rotation of 1962 Beta Alpha 2 most likely meets these ideal conditions only approximately.

In the transit of 1962 Beta Alpha 2 on 15 April 1963 the brightness minima rise from the beginning of the transit to the middle of the transit over an output voltage range of 0.8 volts. The peak voltages remain fairly constant. It is quite possible that the diffuse reflection minima are increasing with a decrease in range since this occurs near minimum range on all tracks. However, the minimum range on most observed transits lies between 1100km and 1150 km but none have the large rise that the transit of 15 April 1963 has. For this revolution it is most likely caused by the movement of the axis of rotation from being close to perpendicular to the line of sight at the begining of the transit to coincidence with the line of sight at the middle of the transit and then a continuation toward perpendicularity again at the end of the transit. This would cause a large variation between peak and minimum voltages, a small variation, and then back to a large variation.

Calculation of the Longitudinal Axis

The orientation of the longitudinal axis of 1962 Beta Alpha 2 was calculated using the maximum voltage point of revolution 257 and the theory previously discussed. It was assumed that the longitudinal axis was contained inthe plane of the phase angle and that the normal to the satellite surface bisected the phase angle. Without these assumptions the solution of the spherical triangles shown in Figure 6 would not be possible. The calculations shown in Appendix A produced a right ascension of 237° 38' and a declination of 18° 14' for the orientation of the longitudinal axis.

Comparison of the Experimental Light Curves With the Calculated Light Curves

After finding the orientation of the satellite longitudinal axis, the remaining orientation variables, δ_o , δ_s , and ϵ were solved for using the equations that were developed in the section on theory. These variables are shown in Table V in Appendix A.

Another assumption was made at this point. It was assumed that the satellite made one half period of revolution about its center of mass between two consecutive peak voltages. As explained in the section on the calculation of the direction of spin, page 23, this is not entirely

accurate. The period according to the experimental curve was actually increasing. This assumption would not have much of an effect on the overall shape of the curve but would slightly shift it.

Calculation of the function $\left[(\pi - \epsilon)\cos\epsilon + \sin\epsilon\right]\cos\delta_o \cos\delta_s$ was first accomplished assuming the reflection was diffuse in nature. After plotting this function, Figure 21 and 22 in Appendix A, it was found that it did not yield agreement to the general shape of the reduced experimental light curve. It was then decided to calculate the function $\cos\frac{\epsilon}{2}$ to see if the reflection was of a specular type. After plotting the function $\cos\frac{\epsilon}{2}$, it was observed that this calculated curve and the experimental curve had the same general shape. The graphs of this function are shown in Appendix A, Figure 23 and 24. First the phase angle was varied, and then the satellite axis was varied to see what effect each has on the calculated curve and to test the sensitivity to the derived axes.

Figure 25, Appendix A, is a graph of the function $\cos\frac{\epsilon}{2}$ calculated with an increased phase angle of 2 degrees. This increase lowered the overall light uniformily. A decrease of the phase angle of 30 minutes is plotted in Figure 26, Appendix A. This decrease raised the curve of the function $\cos\frac{\epsilon}{2}$ such that it went above 1.00.

Variation of the satellite axis produced a different effect on the calculated curve. A decrease in the right ascension of 5 degrees from 237° 38' to 232° 38' shifted the function $\cos \frac{\epsilon}{2}$ to the left and the maximum variation point coincided with the experimental peak voltage. This graph is shown in Figure 27, Appendix A. An increase in the right ascension of the longitudinal axis of 5 degrees to 242° 38' shifted the function $\cos \frac{\epsilon}{2}$ to the right. A graph of this function is also contained in Appendix A and is Figure 28.

Period of Revolution

The approximate period of revolution of 1962 Beta Alpha 2 could be found directly from the experimental light curve. The period during the October 1962 transits varied from 24 to 26 seconds with an average of 25 seconds or 12.5 seconds for the half period, time between peaks.

In April 1963 the light curves show a period for one revolution reduced almost in half. The curves for 13, 14, and 15 April 1963 give average half periods of 6.63, 6.70, and 7.16 seconds respectively. The 15 June 1963 curve gives the average half period of 7.19 seconds.

What had caused the rotation about the center of mass to increase between October 1962 and April 1963 can only be speculated upon. Mr. Gary McCue, a member of the

Western Satellite Research Network, confirmed this rotational period decrease and suggested that the cause may lie in a corrosive puncture of the pressurized helium bottles by the nitric acid propellant. Rapid rotation rises have been observed in other satellites (Ref 15).

The period of revolution of the Russian rocket bodies, 1963-10B and 1962 Beta Theta 2, is surprisingly low. The April 28 1963 transit of 1963-10B shows an average period of .46 seconds and .40 seconds for the average period during the transit of 3 May 63 is shown. The transit of 1962 Beta Theta 2 on 7 May 1963 shows an average period of 1.62 seconds. In order for these massive Russian rocket bodies to have a rotational velocity of this magnitude, they must be purposely spun after separation of the payload. Structural loads above 12g are developed and may cause a break up of the rocket body.

Expansion of the light curve data obtained from 1962 Beta Theta 2 shows a definite asymetrical period. This may be caused by the axis of rotation being at an angle much less that 90 degrees with the longitudinal axis. A satisfactory theory for investigating the period with the axis of rotation at an angle other than 90 degrees to the longitudinal axis has not yet been completed and therefore an interpretation of this asymetrical period has not been undertaken.

VI. Conclusions and Recommendations

Conclusion

From the experimental data, using the theory derived for a cylinder, an estimate of the orientation of the axis of rotation and the longitudinal axis of a satellite can be found. It has also been shown that the optical characteristics of a particular satellite can be recorded, prese rved, and compared with each other and with other satellites over a long period of time.

This investigation has proven conclusively that the recording of photometric data received from an artificial earth satellite can assist in identifying some of the unknown quantities related to the orientation and optical characteristics of the satellite.

Recommendations

Only a portion of the experimental data were reduced and thoroughly examined. Other light curves of satellite 1962 Beta Alpha 2 should be used to calculate the axis of rotation about the center of mass, orientation of the longitudinal axis, and the direction of spin. These results should be compared with each other and with the data found in this investigation.

The simple theory derived in this investigation

should be improved, expanded, and computer programmed.

It is definitly recommended that the compiling of a catalogue of the optical characteristics of various satellites be started. A comparison of the optical characteristics of an unknown object could quickly classify if not identify the object. This would be a valuable aid to satellite observers throughtout the world.

Bibliography

1. Abott, W. N. Optical Earth Satellite Observations. Scientific Report No. 2. Griffiss Air Force Base, Rome, New York: Rome Air Development Center, February 1958.

2. Binnendijk, Leendert. Properties of Double Stars. Philadelphia: University of Pennsylvania Press, 1960.

3. Chorvinsky, M., et al. Optical Phenomena In Space. Technical Report 61-163. Griffiss Air Force Base, Rome, New York: Rome Air Development Center.

4. Measel, Paul R., and Kenneth E. Kissell. A Method For The Prediction Of Satellite Positions and Visibilities. Report distributed by Smithsonian Astrophysical Observatory Moonwatch Project.

5. Melin, Marshall. "The Tumbling of 1958 δ 1". Sky and Telescope, XVIII: 82-83 (December 1958).

6. Melin, Marshall. "More About Project Rotor". Sky and Telescope, XVIII: 145-146 (January 1959).

7. Menzel, Donald H. Our Sun. Cambridge: Harvard University Press, 1959.

8. Moore, J. G. "Photometric Observations of the Second Soviet Satellite (1957 β 1)". Publications of the Astronomical Society of the Pacific. 71: 163-165 (April 1959).

9. Moore, J. G. "Photometric Observations of Satellite 1958 δ 1". Sky and Telescope, XVIII: 83(December 1958).

10. National Aeronautics and Space Administration. Optical Observation of Artificial Earth Satellites. Technical Translation F-11. Washington, D.C.: February 1961.

11. Radio Corporation of America. RCA Photosensitive Devices and Cathode-Ray Tubes. Harrison, New Jersey, 1960.

12. Stiles, George J. Prediction of Apparent Magnitude of Distant Missiles in Sunlight. Memorandum Report No. 1008. Aberdeen Proving Ground, Maryland: Ballistic Research Laboratories, June 1956.

13. United States Naval Observatory. The Air Almanac. September-December 1962. Washington, D.C.: Department of the Navy, 1961.

14. Zirker, J. B., F. L. Whipple and R. J. Davis. "Time Available for the Optical Observation of an Earth Satellite." Scientific Uses of Earth Satellites. Edited by James Van Allen. Ann Arbor: The University of Michigan Press, 1956.

15. Private communication with Mr. Gary McCue of the Western Satellite Research Network, California.

Appendix A

Calculated Data

Table I

Linearized Light Curve Data, Revolution 257,
Satellite 62 Beta Alpha 2

Peak	Volts	Sky Volts	E Total	E Sky	E Sat.	Range Km	$(\text{Range})^2 \times 10^6$	E Sat. 1000Km
1	1.50	.10	31.62	1.25	30.37	1800	3.24	98.3
2	1.65	.08	44.67	1.20	43.47	1750	3.06	133.01
3	1.50	.06	31.62	1.14	30.48	1700	2.89	88.08
4	off track					1660	2.75	
5	1.55	.05	35.48	1.12	34.36	1620	2.62	90.02
6	1.60	.05	39.81	1.12	38.69	1580	2.49	96.30
7	1.70	.05	50.12	1.12	49.00	1550	2.40	117.60
8	1.80	.05	63.10	1.12	61.98	1510	2.28	141.30
9	1.75	.05	56.23	1.12	55.11	1470	2.16	119.00
10	1.60	.05	39.81	1.12	38.69	1430	2.04	78.9
11	1.55	.05	35.48	1.12	34.36	1400	1.96	67.3
12	1.68	.05	47.86	1.12	46.74	1390	1.93	90.2
13	1.75	.05	56.23	1.12	55.11	1380	1.90	104.7

Table I

Linearized Light Curve Data, Revolution 257
Satellite 62 Beta Alpha 2

Peak	Volts	Sky Volts	E Total	E Sky	E Sat.	Range Km	$(\text{Range})^2 \times 10^{-6}$	E Sat. 1000Km
14	1.75	.05	56.23	1.12	55.11	1370	1.87	103.0
15	1.72	.05	52.48	1.12	51.36	1360	1.84	94.5
16	1.65	.05	44.67	1.12	43.55	1350	1.82	79.2
17	1.55	.05	35.48	1.12	34.36	1360	1.84	63.2
18	1.68	.05	47.86	1.12	46.74	1370	1.87	87.4
19	1.60	.08	39.81	1.20	38.61	1380	1.90	73.3
20	1.60	.11	39.81	1.28	38.53	1400	1.96	75.5
21	off track					1420	2.01	
22	1.60	.15	39.81	1.41	38.40	1450	2.10	80.6
23	1.50	.16	31.62	1.41	30.21	1480	2.19	66.1
24	1.48	.17	30.20	1.41	28.79	1510	2.28	65.4
25	1.20	.18	15.85	1.51	14.34	1550	2.40	34.4
26	1.00	.20	10.00	1.58	8.42	1600	2.56	21.5

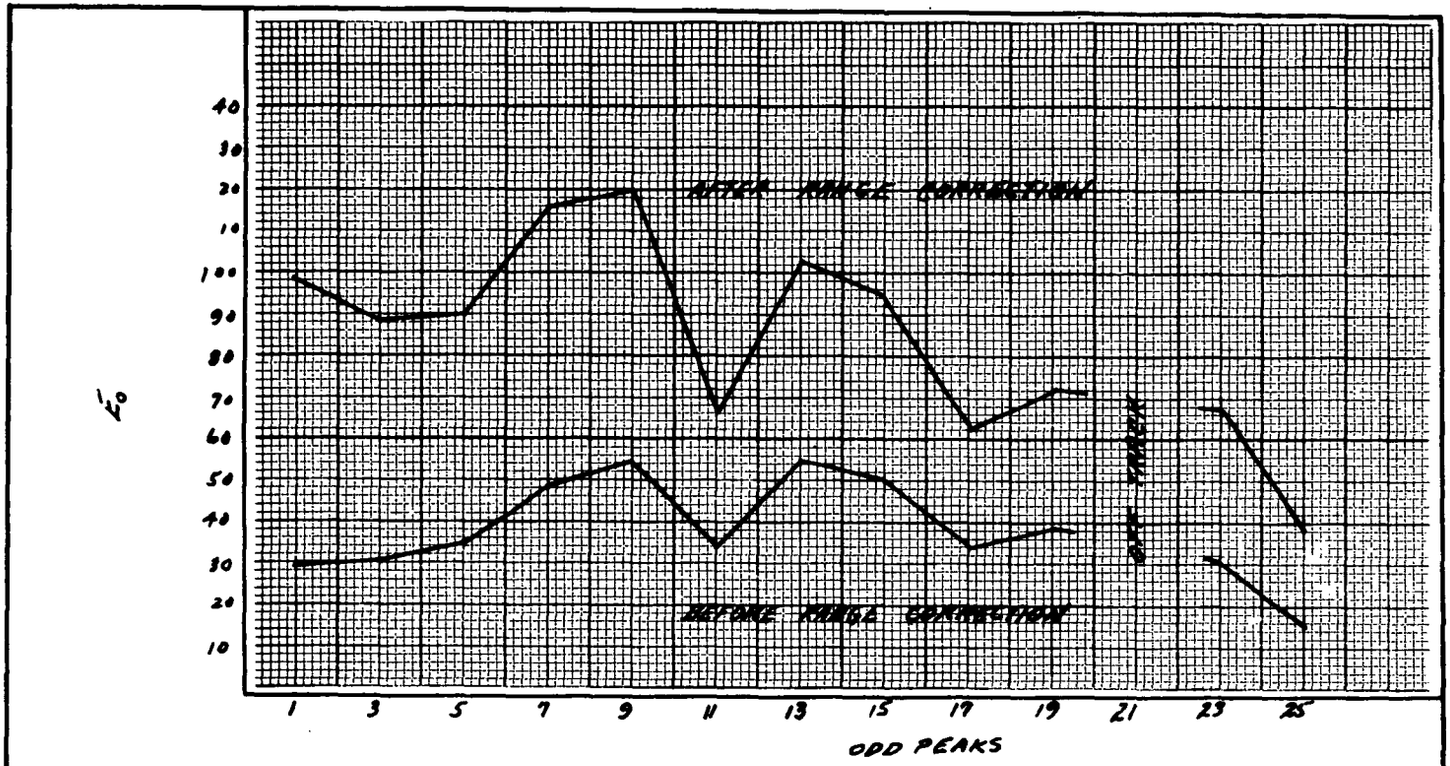

Figure 17
Linearized Data
Satellite 1962 Beta Alpha 2, Revolution 257
Odd Voltage Peaks Track 18 Oct 62

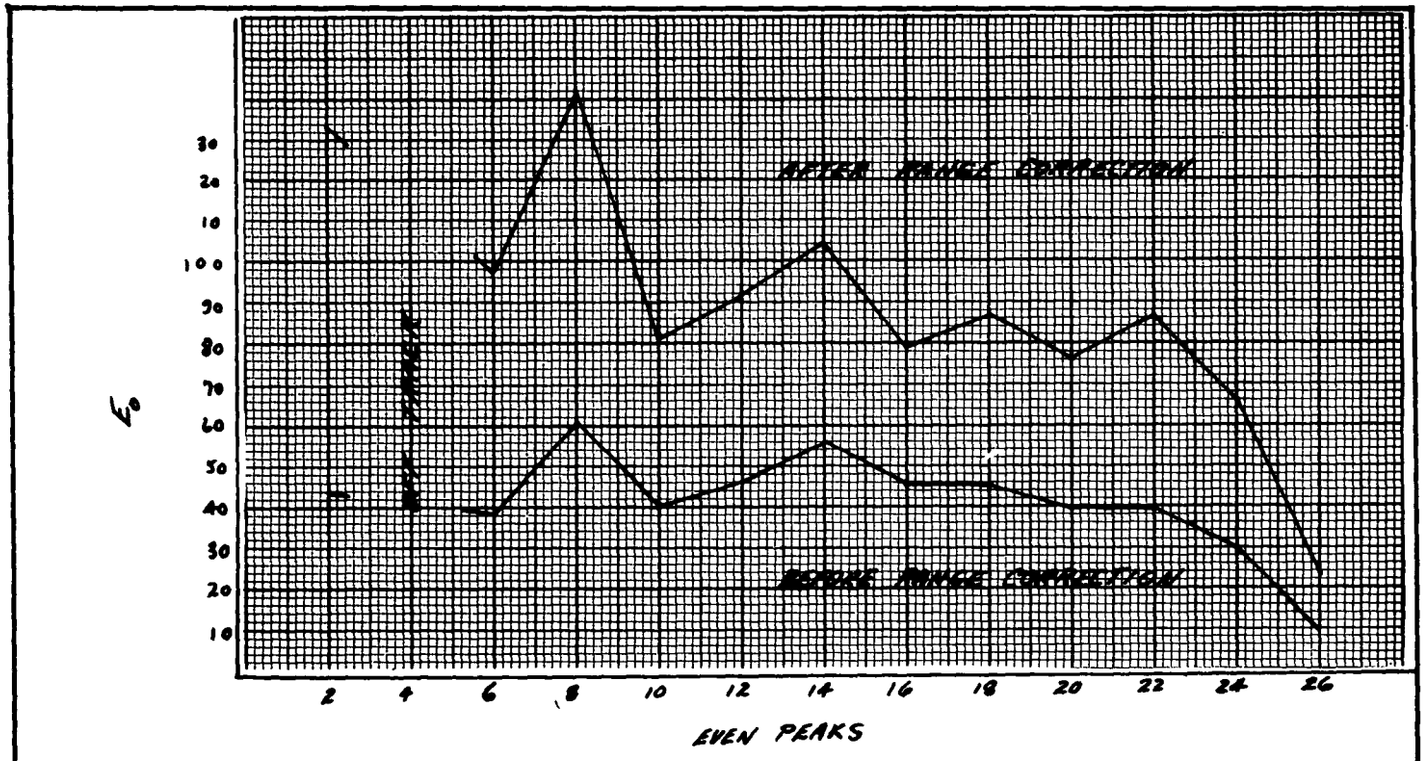

Figure 18
Linearized Data
Satellite 1962 Beta Alpha 2, Revolution 257
Even Voltage Peaks Track 18 Oct. 62

Table II

Linearized Light Curve Data, Revolution 270,

Satellite 62 Beta Alpha 2

Peak	Volts	Sky Volts	E Total	E Sky	E Sat.	Range Km	$(\text{Range})^2 \times 10^{-6}$	E Sat. 1000Km
1	1.45	.07	28.18	1.17	27.01	1530	2.34	63.2
2	off track	.06		1.14		1480	2.19	
3	1.50	.05	31.62	1.12	30.04	1430	2.04	61.2
4	1.65	.05	44.67	1.12	43.55	1380	1.90	82.7
5	1.55	.05	35.48	1.12	34.36	1330	1.76	60.4
6	1.65	.05	44.67	1.12	43.55	1290	1.66	72.2
7	1.64	.05	43.65	1.12	42.53	1260	1.58	67.1
8	1.70	.05	50.12	1.12	49.00	1240	1.53	74.9
9	1.75	.05	56.23	1.12	55.11	1210	1.46	80.4
10	1.75	.05	56.23	1.12	55.11	1180	1.39	76.6
11	1.65	.05	44.67	1.12	43.55	1160	1.34	58.3
12	1.73	.05	53.70	1.12	52.58	1150	1.32	69.4
13	1.77	.05	58.88	1.12	57.76	1150	1.32	76.2
14	1.80	.05	63.10	1.12	61.98	1160	1.34	83.0

Table II (Cont.)

Linearized Light Curve Data, Revolution 270

Satellite 62 Beta Alpha 2

Peak	Volts	Sky Volts	E Total	E Sky	E Sat.	Range Km	$(\text{Range})^2 \times 10^{-6}$	E Sat. 1000Km
15	1.75	.05	56.23	1.12	55.11	1170	1.36	74.9
16	1.75	.05	56.23	1.12	55.11	1190	1.41	77.7
17	1.68	.05	47.86	1.12	46.74	1220	1.48	69.1
18	1.82	.06	66.07	1.14	64.93	1250	1.56	101.2
19	1.60	.06	39.81	1.14	38.67	1280	1.63	63.0
20	1.70	.07	50.12	1.17	48.95	1310	1.71	83.7
21	1.52	.08	33.11	1.20	31.91	1350	1.82	58.0
22	1.60	.09	39.81	1.23	38.58	1400	1.96	75.6
23	1.45	.10	28.18	1.25	26.93	1450	2.10	56.5
24	1.52	.11	33.11	1.28	31.83	1500	2.25	71.6
25	off track.12			1.31		1550	2.40	
26	1.35	.13	22.39	1.34	21.05	1600	2.56	53.8
27	1.25	.14	17.78	1.38	16.40	1650	2.72	44.6

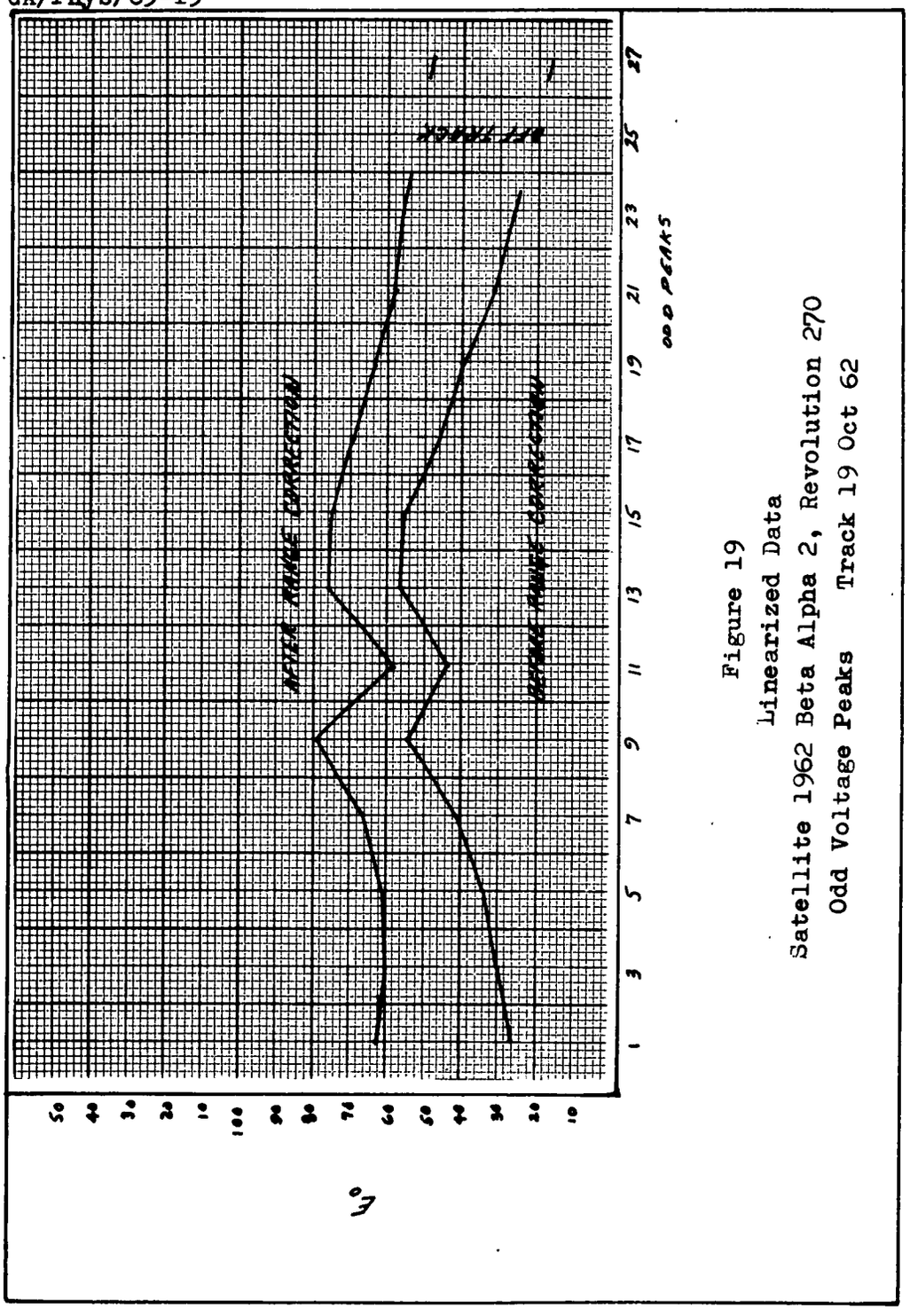

Figure 19
Linearized Data
Satellite 1962 Beta Alpha 2, Revolution 270
Odd Voltage Peaks Track 19 Oct 62

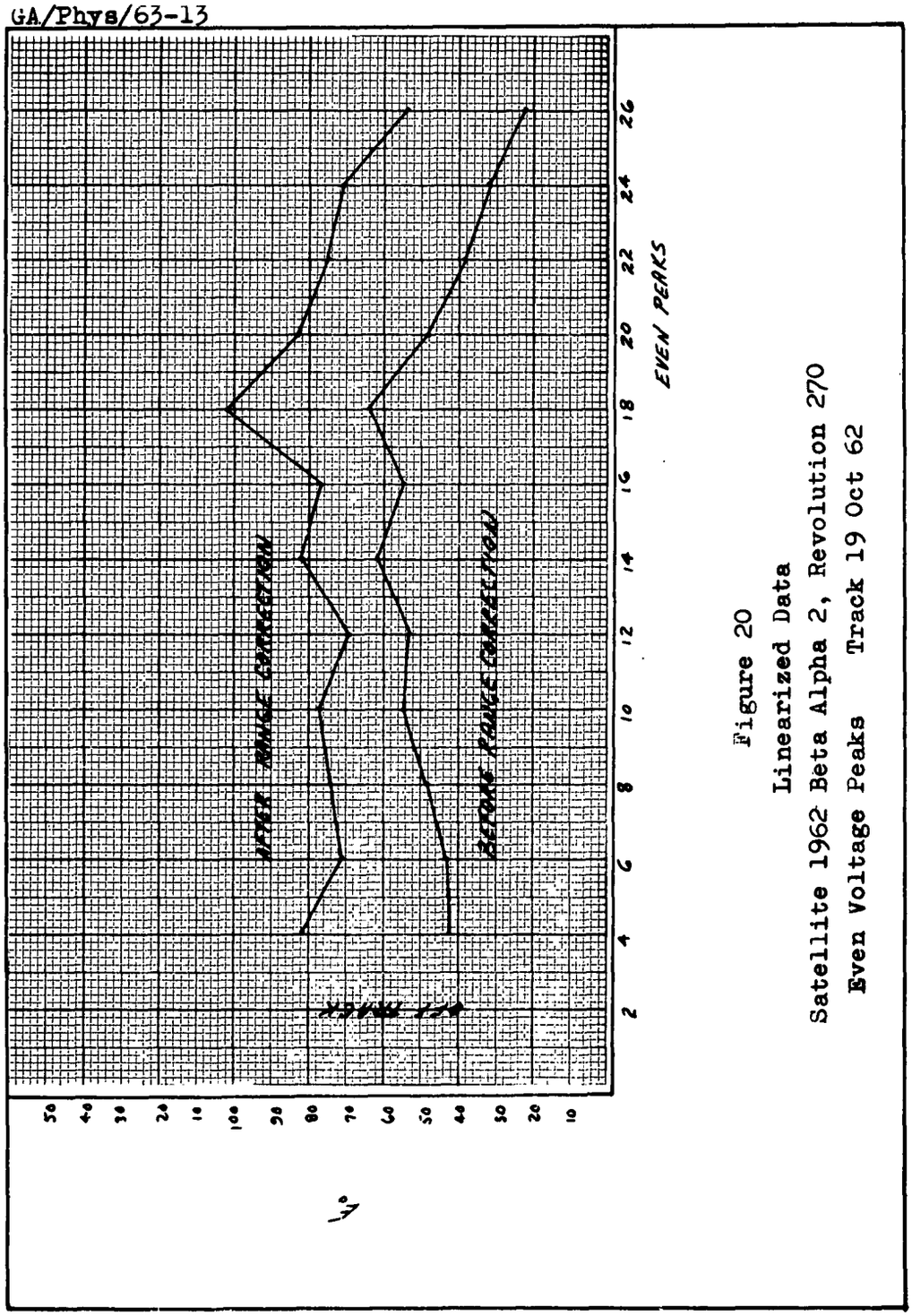

Figure 20
Linearized Data
Satellite 1962 Beta Alpha 2, Revolution 270
Even Voltage Peaks Track 19 Oct 62

Table III

Right Ascension and Declination of the Line of Sight

for Satellite 62 Beta Alpha 2 Rev. 257

Peak	LHA Ψ_a	GHA Υ	RA Ψ_a	Dec. D_a	Sine D_a	Cosine D_a
	° ′	° ′	° ′	° ′		
1	93 55	52 35	235 34	55 10	.82079	.57119
2	89 28	52 39	239 05	54 32	.81440	.58023
3	85 08	52 42	243 28	52 56	.79790	.60274
4	81 43	52 45	246 56	51 01	77837	.62909
5	77 23	52 48	251 19	49 35	.76137	.64834
6	73 59	52 51	254 46	47 02	.73178	.68157
7	70 31	52 54	258 17	44 36	.70224	.71203
8	67 12	52 58	261 40	42 15	.67227	.74022
9	64 01	53 01	264 54	39 57	.64218	.76661
10	61 10	53 04	267 48	37 41	.61124	.79140
11	57 53	53 07	271 08	34 07	.56077	.82790
12	54 48	53 10	274 16	30 38	.50940	.86045
13	51 59	53 13	276 58	27 10	.45655	.88968
14	49 04	53 16	280 06	23 52	.40467	.91449
15	46 56	53 19	282 17	21 01	.35862	.93348
16	45 05	53 23	284 12	17 56	.30802	.95142
17	43 06	53 27	286 15	14 57	.25794	.96615
18	41 19	53 29	288 04	11 41	.20239	.97928
19	39 20	53 32	290 06	08 28	.14716	.98910
20	37 27	53 36	292 03	04 56	.08592	.99630
21	35 20	53 39	294 13	01 27	.02534	.99968
22	33 13	53 42	296 23	-02 22	-.04140	.99915
23	31 31	53 45	298 08	-05 44	-.09988	.99500
24	29 20	53 48	300 22	-08 36	-.14967	.98876
25	26 45	53 52	303 01	-10 57	-.19001	.98179
26	24 00	53 55	305 49	-13 11	-.22817	.97365

Table IV

Right Ascension and Declination of the Line of Sight
Satellite 62 Beta Alpha 2, Revolution 270

Peak	LHA ψ_a	GHA γ	RA ψ_o	Dec. D_a	Sine D_a	Cosine D_a
1	257° 36′	321° 02′	339° 20′	79° 26′	.98304	.18338
2	270 45	321 05	326 14	78 32	.98004	.19880
3	282 50	321 08	314 12	77 26	.97604	.21758
4	292 17	321 11	304 48	75 15	.96705	.25460
5	298 57	321 13	298 10	72 22	.95301	.30292
6	303 55	321 17	293 16	69 44	.93809	.34639
7	306 57	321 20	290 17	66 13	.91508	.40328
8	311 18	321 23	285 59	63 46	.89700	.44203
9	313 00	321 27	284 21	58 13	.85005	.52671
10	315 49	321 30	281 35	54 00	.80902	.58779
11	318 10	321 33	279 27	50 10	.76791	.64056
12	320 43	321 36	276 47	46 09	.72116	.69227
13	322 40	321 40	274 54	42 23	.67409	.73865
14	323 43	321 43	273 53	38 46	.62615	.77970
15	324 48	321 47	272 53	34 08	.56112	.82773
16	325 11	321 50	272 33	28 57	.48405	.87504
17	326 00	321 53	271 47	24 20	.41204	.91116
18	326 44	321 56	271 06	19 49	.33901	.94078
19	327 15	321 59	270 38	16 16	.28011	.95997
20	326 40	322 02	271 16	13 36	.23514	.97196
21	328 53	322 05	269 06	08 24	.14608	.98927
22	329 40	322 08	268 22	05 00	.08716	.99619
23	327 28	322 12	270 38	03 06	.05408	.99854
24	324 00	322 15	274 09	01 47	.03112	.99952
25	321 00	322 18	277 12	00 28	.00814	.99997
26	320 06	322 21	278 09	00 28	.00814	.99997
27	316 34	322 23	281 33	-00 59	-.01716	.99985

GA/Phys/63-13

Calculation of the Axis of Rotation

Satellite 62 Beta Alpha 2 Revolution 257 & 270

Revolution 257		Revolution 270
$D_1 = 41^\circ 54'$		$D_2 = 19^\circ 49'$
$\Psi_1 = 261^\circ 40'$		$\Psi_2 = 271^\circ 47'$
$\sin \Psi_1 = -.98791$		$\sin \Psi_2 = -.99952$
$\cos \Psi_1 = -.15500$		$\cos \Psi_2 = .03112$
$\sin D_1 = .66783$		$\sin D_2 = .33901$
$\cos D_1 = .74431$		$\cos D_2 = .94078$
$\alpha_1 = -.11536$		$\alpha_2 = .02927$
$\beta_1 = -.73531$		$\beta_2 = -.93626$
$\gamma_1 = .66783$		$\gamma_2 = .33901$
$\beta_2 \gamma_1 = -.62526$	$\gamma_2 \alpha_1 = -.03910$	$\alpha_2 \beta_1 = -.02152$
$\gamma_2 \beta_1 = -.24927$	$\gamma_1 \alpha_2 = .019547$	$\alpha_1 \beta_2 = .10800$
$\alpha_3' = -.37599$	$\beta_3' = -.05864$	$\gamma_3' = -.12952$
$\alpha_3'^2 = .141368$	$\alpha_3 = .93536$	
$\beta_3'^2 = .003438$		
$\gamma_3'^2 = .016775$	$\beta_3 = .14588$	
$x = .161581$		
$\sqrt{x} = -.40197$	$\gamma_3 = .32221$	
$\sin D_3 = .32221$	$D_3 = 18^\circ 48'$	$\cos D_3 = .94665$
$\cos \Psi_3 = .98807$	$\Psi_3 = 08^\circ 52'$	

GA/Phys/63-13

Calculation of the Longitudinal Axis of Satellite 62 Beta Alpha 2

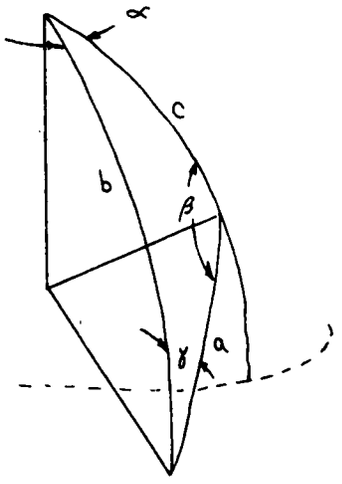

$$\cos a = \cos b \cos c + \sin b \sin c \cos \alpha$$

$\alpha = 51^\circ 06'$

$b = 99^\circ 23'$

$c = 47^\circ 45'$

$a = 69^\circ 34'$

phase angle

$\phi = 180^\circ - a = 110^\circ 26'$

$\gamma = 37^\circ 56'$

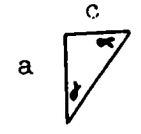

$$\cos \alpha = \cos a \cos \gamma$$

$\alpha = 37^\circ 20'$

$$\sin c = \tan a \operatorname{ctn} \alpha$$

$c = 12^\circ 31'$

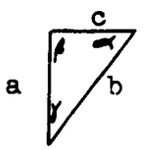

$$\cos b = \cos a \cos c$$
$$b = 15^\circ 36'$$

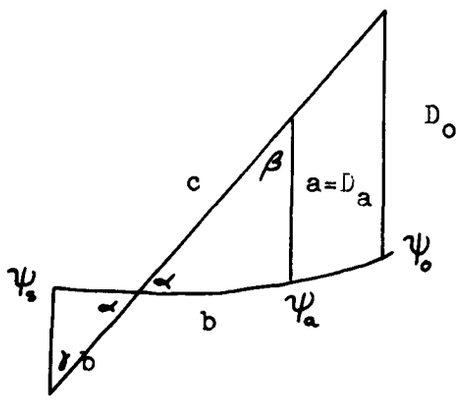

$$38^\circ 47' - 15^\circ 36' = 23^\circ 11'$$

$$\sin a = \sin \quad \sin c$$
$$a = 18^\circ 14' = D_a = \text{declination}$$

$$\sin b = \tan a \operatorname{ctn} \alpha$$
$$b = 14^\circ 33'$$

$$\psi_s + 12^\circ 31' + 14^\circ 33' = \psi_a$$
$$\psi_a = 237^\circ 38' = \text{right ascension}$$

Table V

Orientation Variables

Satellite 62 Beta Alpha 2, Rev. 257

Peak	$\psi_a - \psi_o$	Φ	δ_o	ϵ	$\frac{[(\pi-\epsilon)\cos\epsilon + \sin\epsilon]}{(\cos\delta_o \cos\delta_s)}$	$\cos\frac{\epsilon}{2}$
1	2° 04′	112° 11′	53° 02′	48° 40′	.85082	.91116
2	- 1 27	111 38	53 41	44 30	.87873	.92554
3	- 5 50	111 34	55 00	39 42	.89915	.94058
4	- 9 18	111 49	56 26	31 17	.94035	.96301
5	-13 41	111 03	56 47	29 51	.94573	.96630
6	-17 08	111 12	57 57	23 32	.95716	.97899
7	-20 39	110 57	58 29	17 16	.97738	.98867
8	-24 02	110 29	58 29	10 58	1.0025	.99551
9	-27 16	109 41	58 01	05 48	1.0292	.99872
10	-30 10	108 55	57 16	04 42	1.0520	.99916
11	-33 30	108 10	56 13	10 51	1.0667	.99553
12	-36 38	107 12	54 36	17 42	1.0807	.98809
13	-39 20	106 17	52 49	23 46	1.0884	.97857
14	-42 28	104 43	50 07	29 23	1.1081	.96727
15	-44 39	103 39	47 59	33 42	1.1137	.95707
16	-46 34	102 45	45 23	39 30	1.1033	.94118
17	-48 37	102 33	43 25	44 37	1.0760	.92510
18	-50 26	101 36	40 59	48 11	1.0690	.91283
19	-52 28	99 22	38 12	48 49	1.1039	.91056
20	-54 25	98 12	35 16	52 21	1.0920	.89739
21	-56 35	96 40	32 04	55 17	1.0855	.88580
22	-58 45	95 13	28 39	58 33	1.0683	.87221
23	-60 30	94 04	25 43	62 03	1.0346	.85687
24	-62 44	92 23	22 33	63 51	1.0279	.84866
25	-65 23	90 44	19 12	65 21	1.0243	.84635
26	-68 11	87 58	15 12	65 27	1.0409	.84588
	$\psi_a - \psi_s$			δ_s		
Sun	27° 04′			51° 35′		

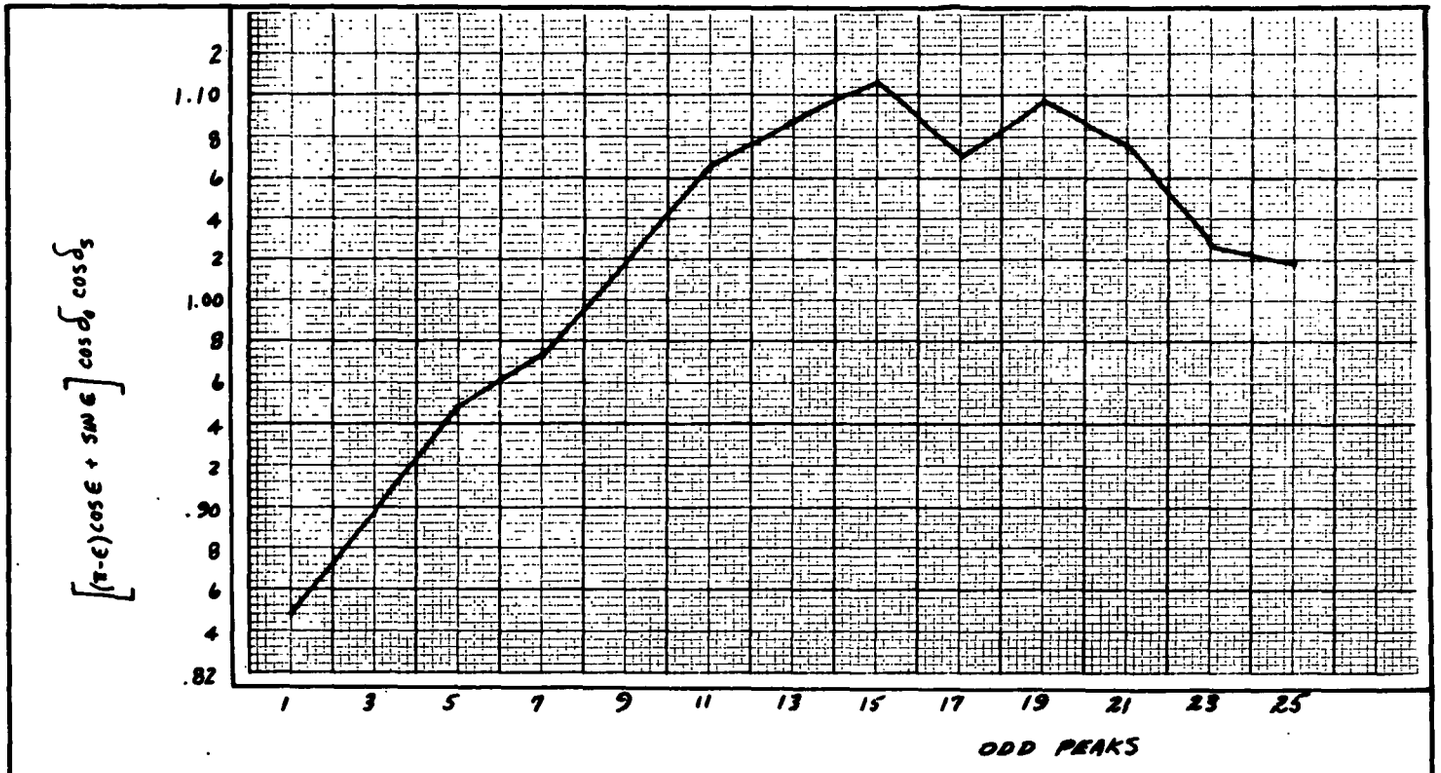

Figure 21
Diffuse Variation Function
Satellite 1962 Beta Alpha 2
Odd Peaks Revolution 257

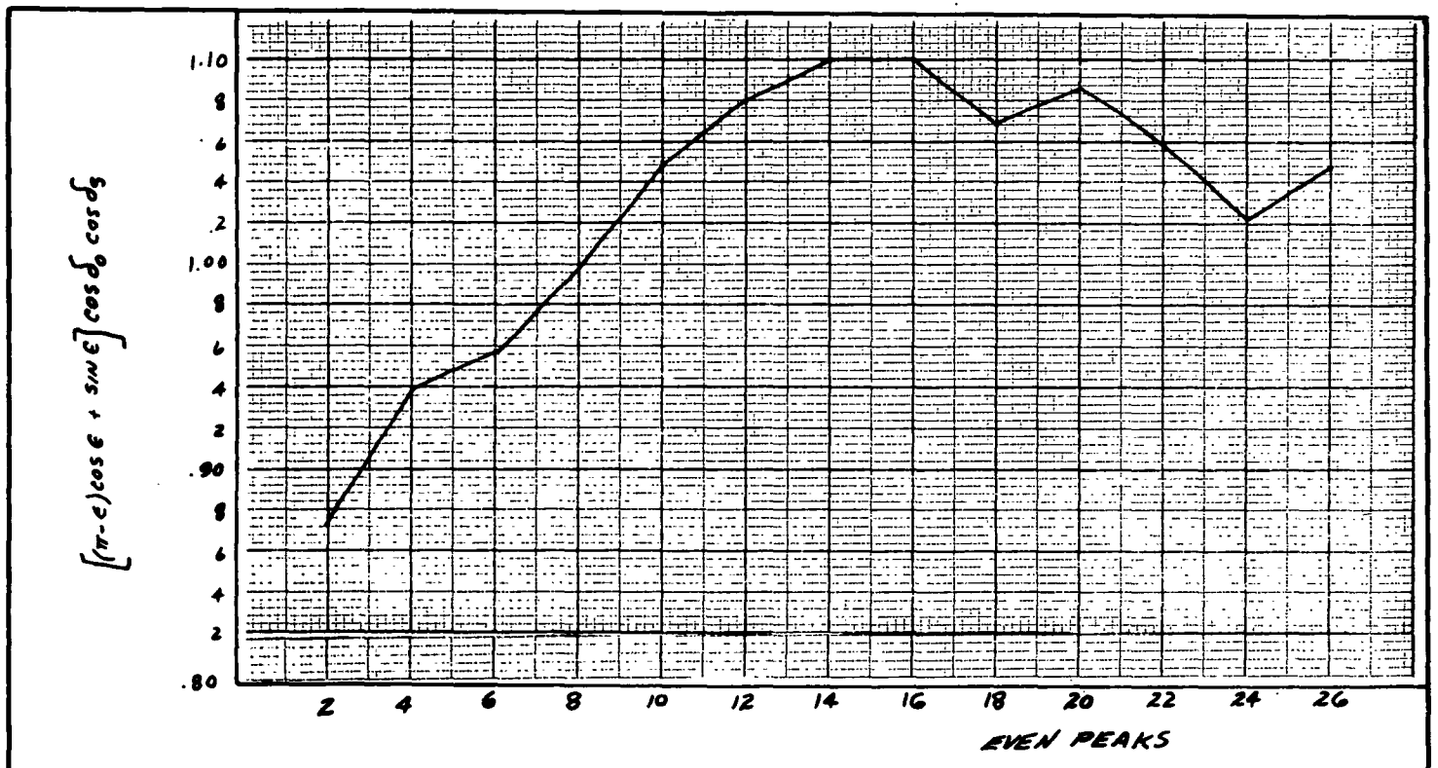

Figure 22
Diffuse Variation Function
Satellite 1962 Beta Alpha 2
Even Peaks Revolution 257

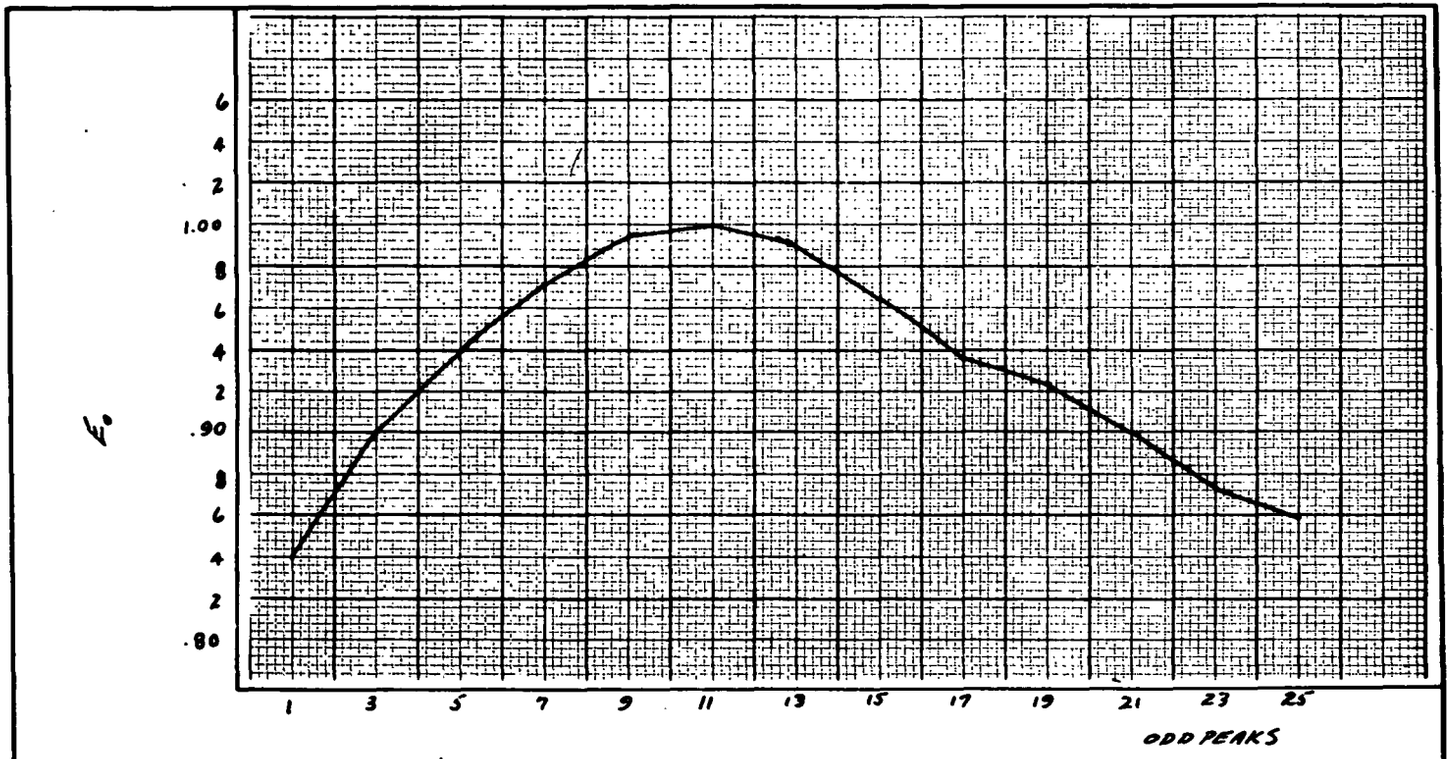

Figure 23
Specular Variation Function
Satellite 1962 Beta Alpha 2
Odd Peaks Revolution 257

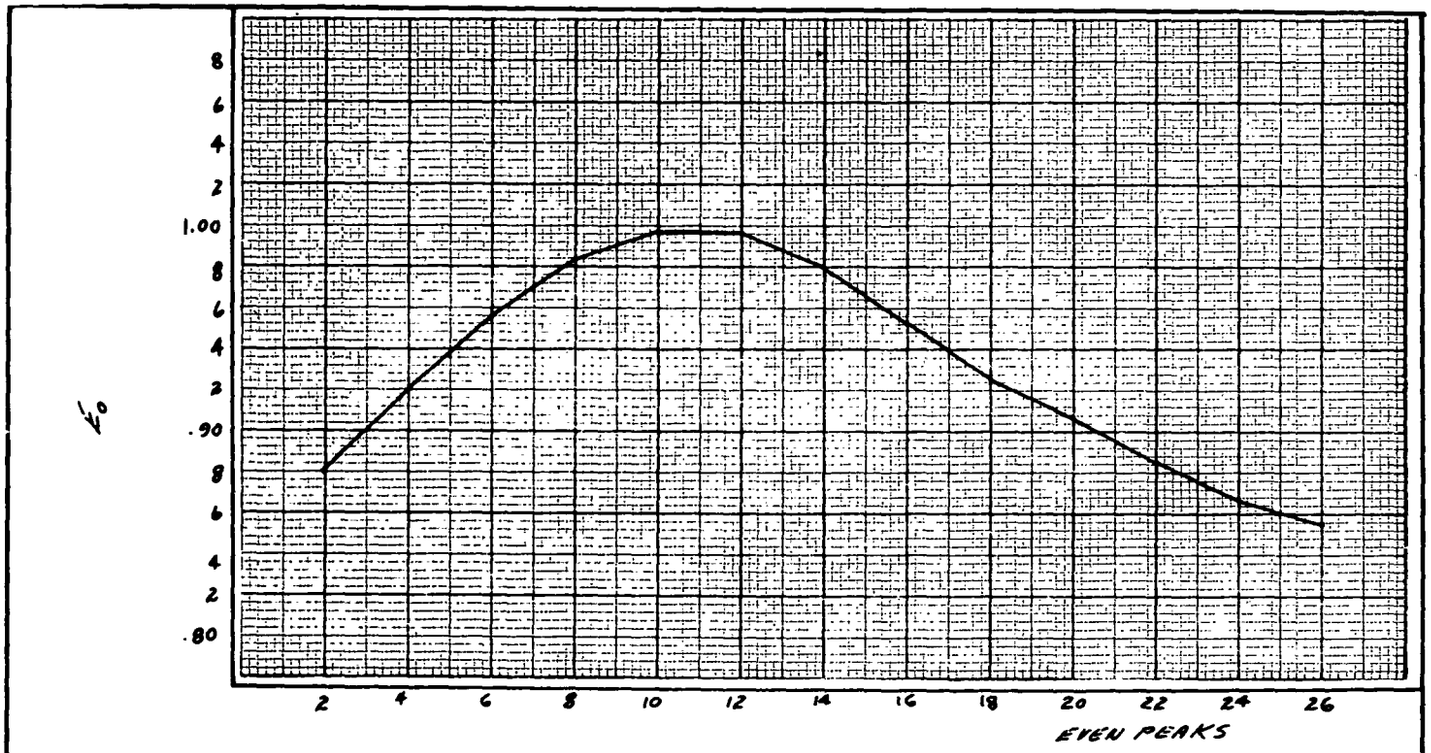

Figure 24
Specular Variation Function
Satellite 1962 Beta Alpha 2
Even Peaks Revolution 257

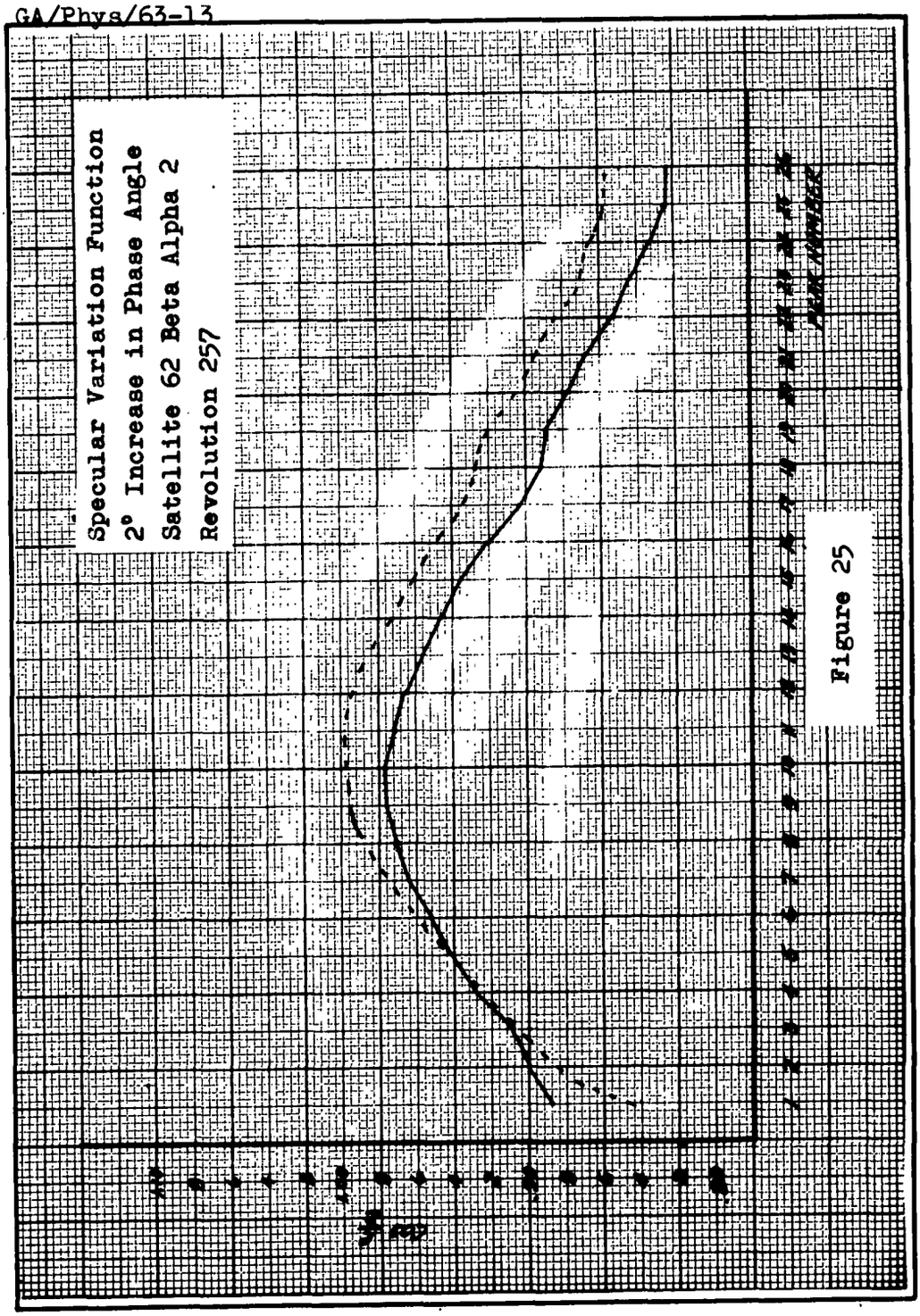
Specular Variation Function
2° Increase in Phase Angle
Satellite 62 Beta Alpha 2
Revolution 257

Figure 25

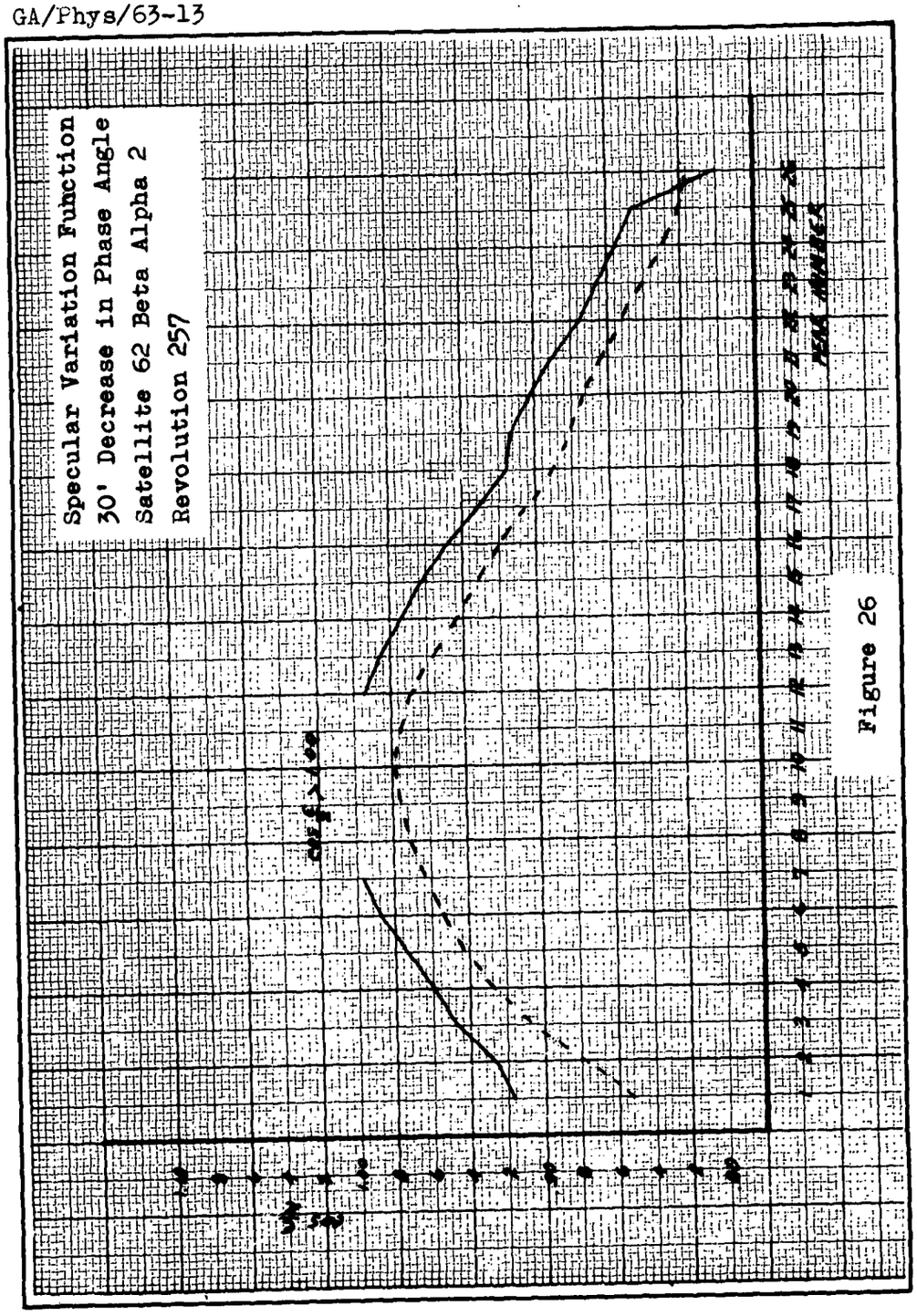
Specular Variation Function
30' Decrease in Phase Angle
Satellite 62 Beta Alpha 2
Revolution 257

Figure 26

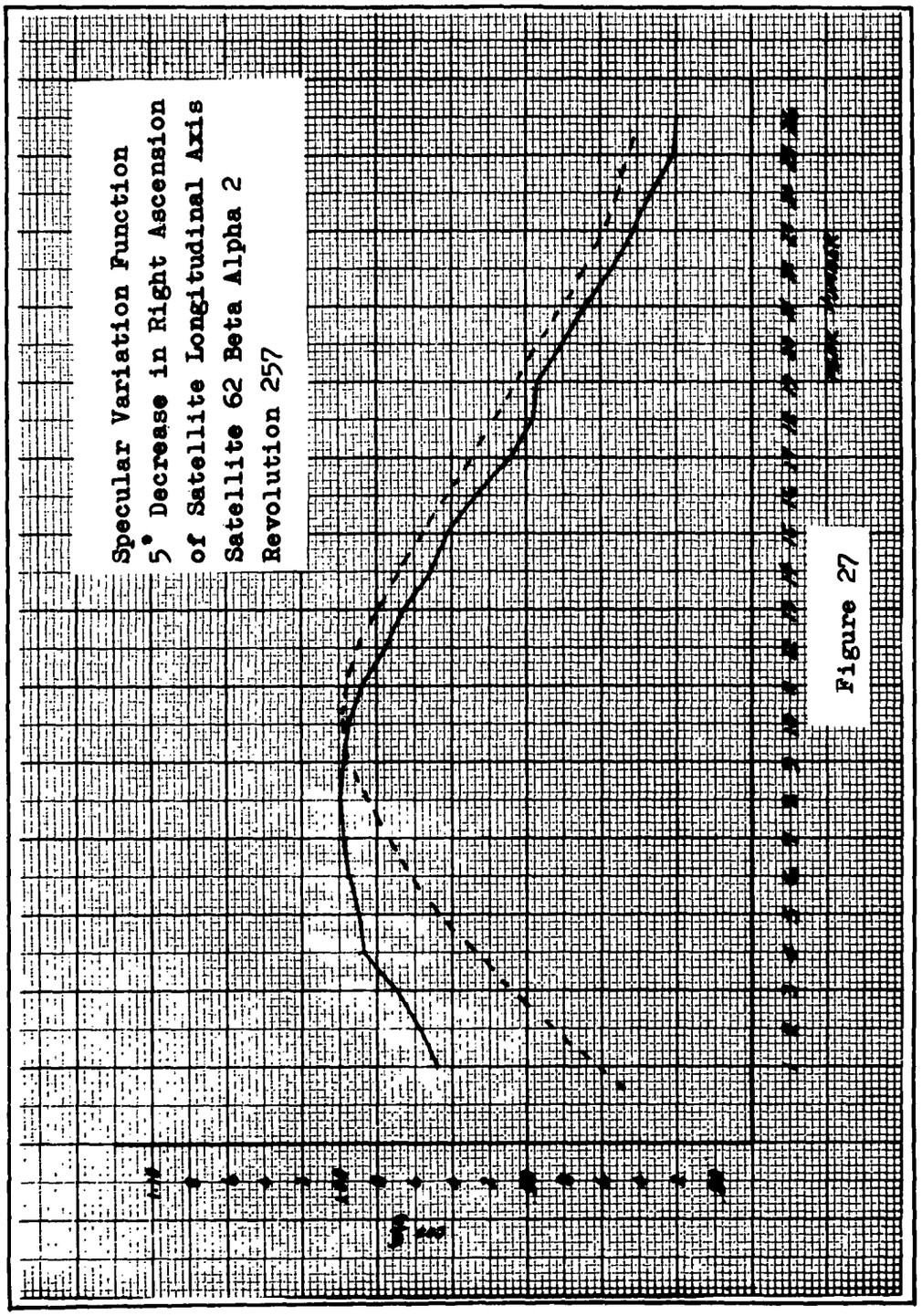
Specular Variation Function
5° Decrease in Right Ascension
of Satellite Longitudinal Axis
Satellite 62 Beta Alpha 2
Revolution 257

Figure 27

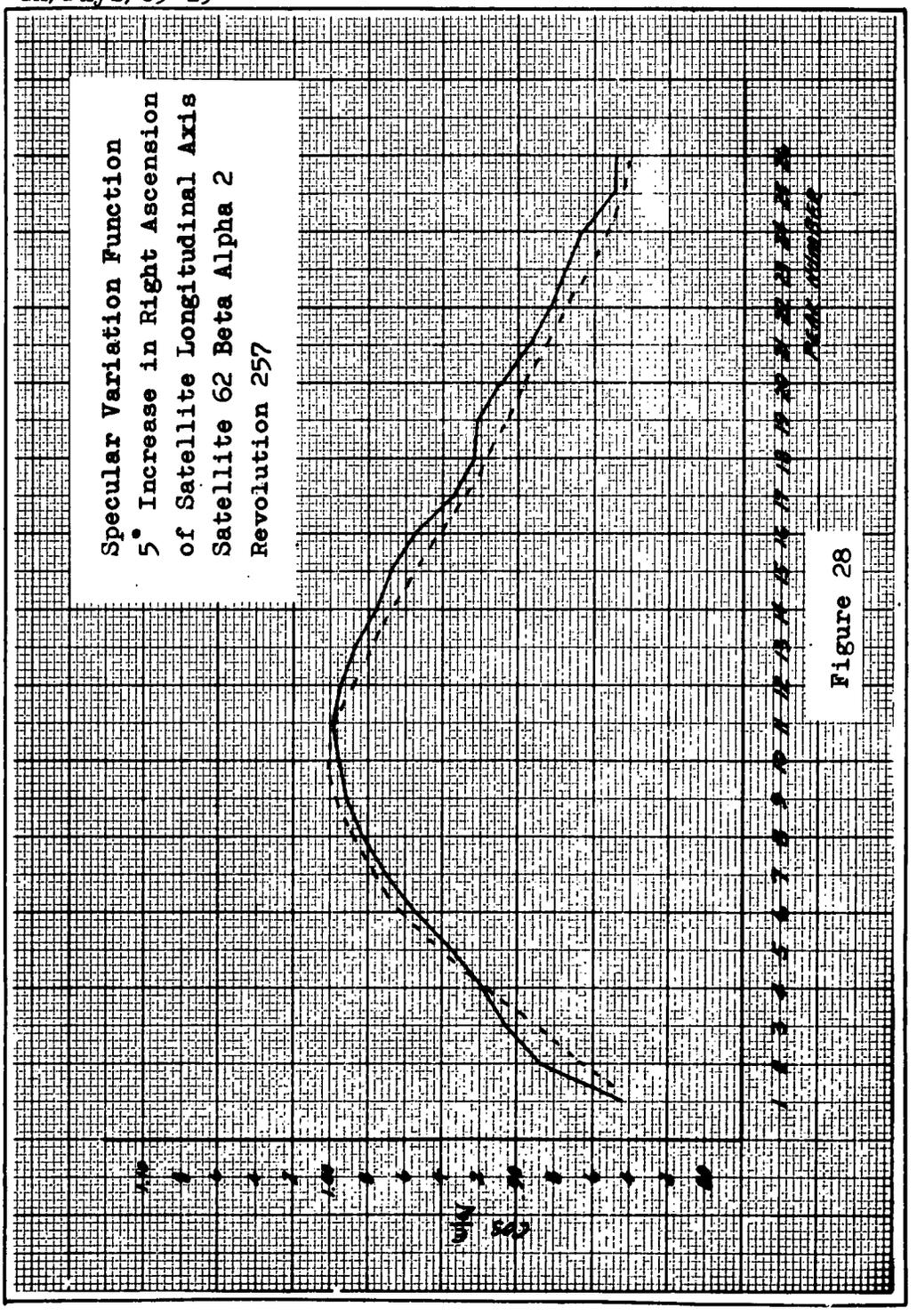
Specular Variation Function
5° Increase in Right Ascension
of Satellite Longitudinal Axis
Satellite 62 Beta Alpha 2
Revolution 257

Figure 28

Appendix B

Experimental Data

Table VI

Tracking Data Satellite 62 Beta Alpha 2

Revolution 257

SGWADCTV 241 62B-ALPHA2 SAT. NO. 426 ELEM. 2

STARTED AT REVOLUTION NO. 156 VISUAL PASSES

REV NO.	ZEBRA TIME DAY	HR	MIN.	ELEV ANG.	AZIM ANG.	RANGE KM.	SUNS ELEV	ILLUMI NATION
257	291	01	40.54	1.8	341.8	3573	-32.4	16.6
257	291	01	41.55	5.4	340.0	3213	-32.6	14.8
257	291	01	42.55	9.5	337.5	2859	-32.8	13.1
257	291	01	43.55	14.2	334.2	2515	-33.0	11.4
257	291	01	44.55	19.7	329.6	2189	-33.2	9.7
257	291	01	45.55	26.1	322.9	1891	-33.4	8.1
257	291	01	46.56	33.5	312.7	1638	-33.5	6.6
257	291	01	47.56	40.8	296.6	1451	-33.7	5.2
257	291	01	48.56	45.1	273.4	1364	-33.9	3.8
257	291	01	49.56	43.4	248.0	1395	-34.1	2.5
257	291	01	50.56	37.1	228.4	1536	-34.3	1.3
257	291	01	51.57	29.5	215.6	1762	-34.5	0.2
257	291	01	52.57	22.5	207.3	2043	-34.6	-0.8
257	291	01	53.57	16.6	201.8	2359	-34.8	-1.6
257	291	01	54.57	11.5	197.9	2697	-35.0	-2.4
257	291	01	55.57	7.1	195.0	3049	-35.2	-3.0
257	291	01	56.57	3.3	192.7	3409	-35.4	-3.5

GA/Phys/63-13

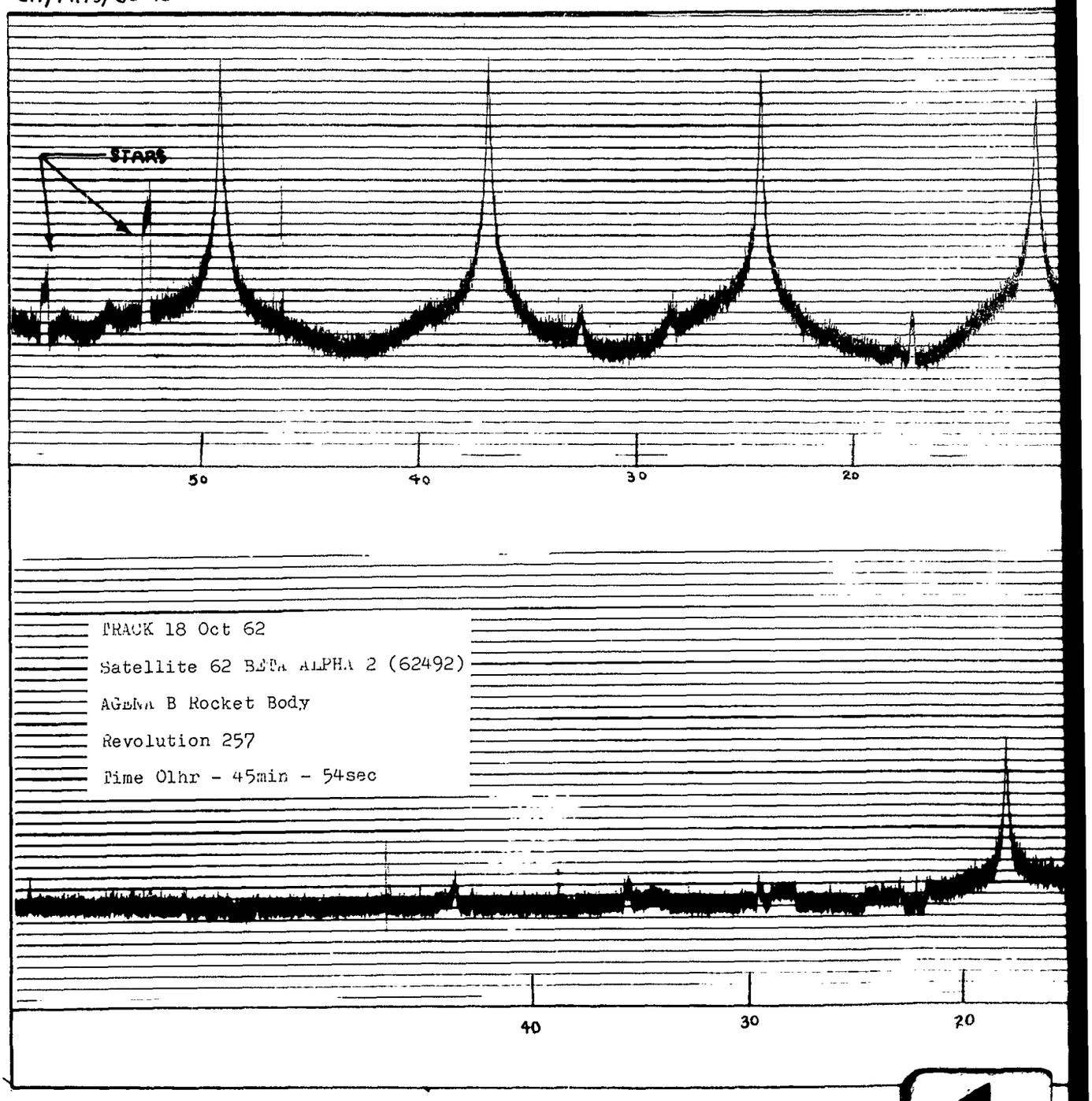

1

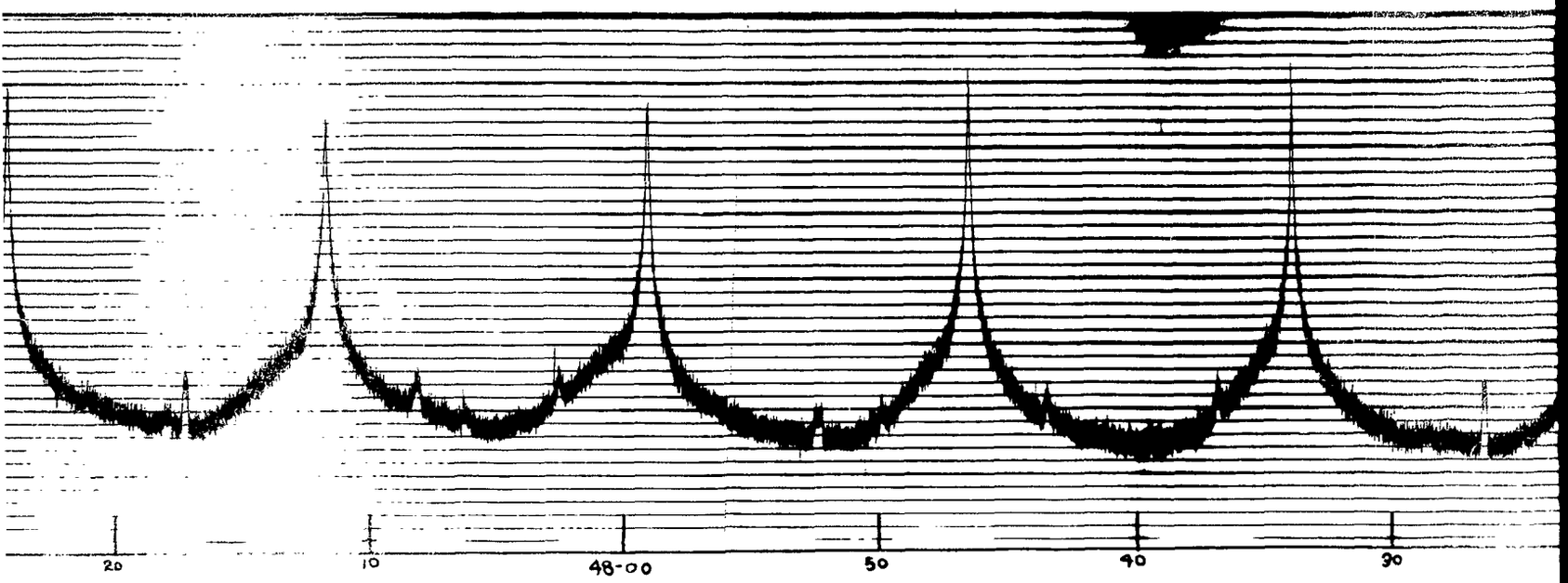

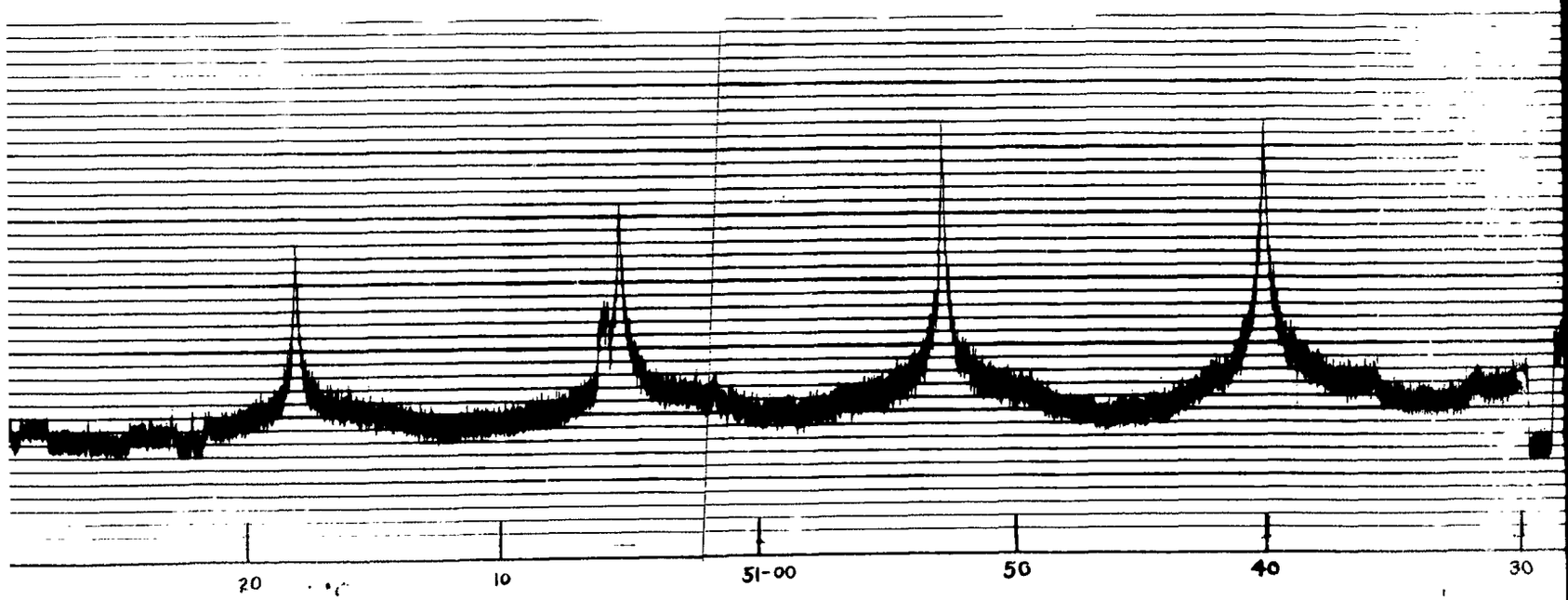

2

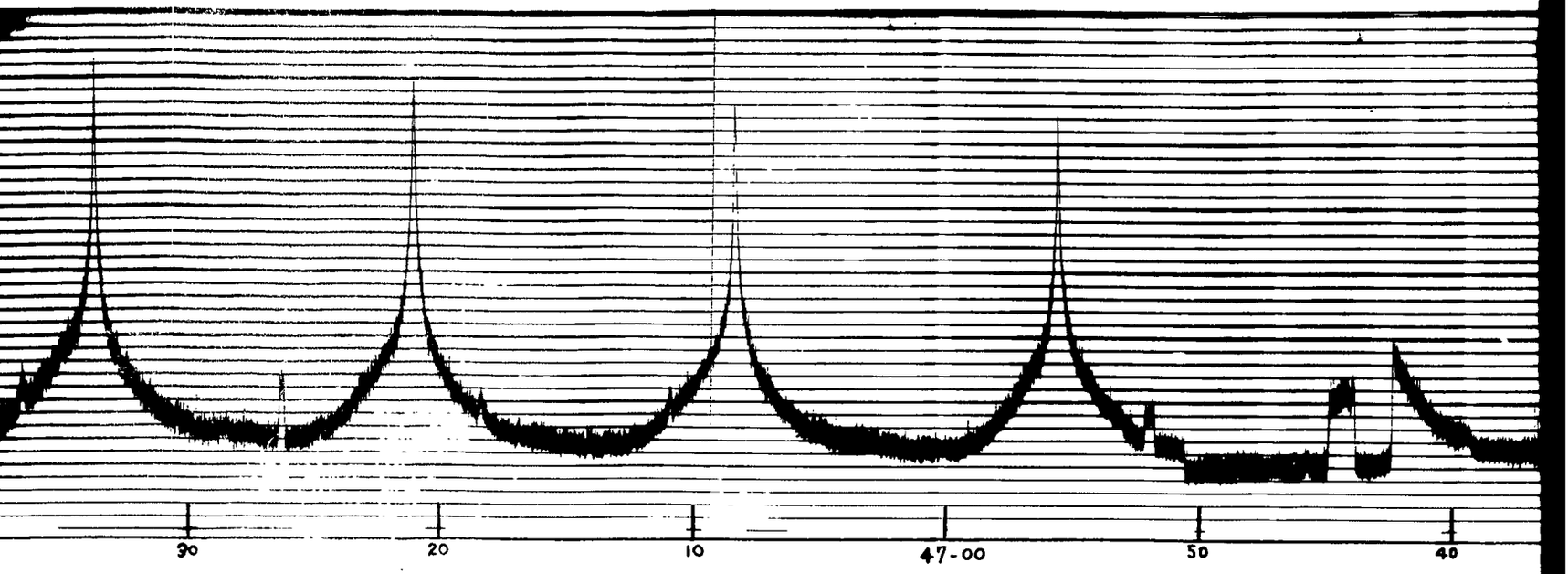

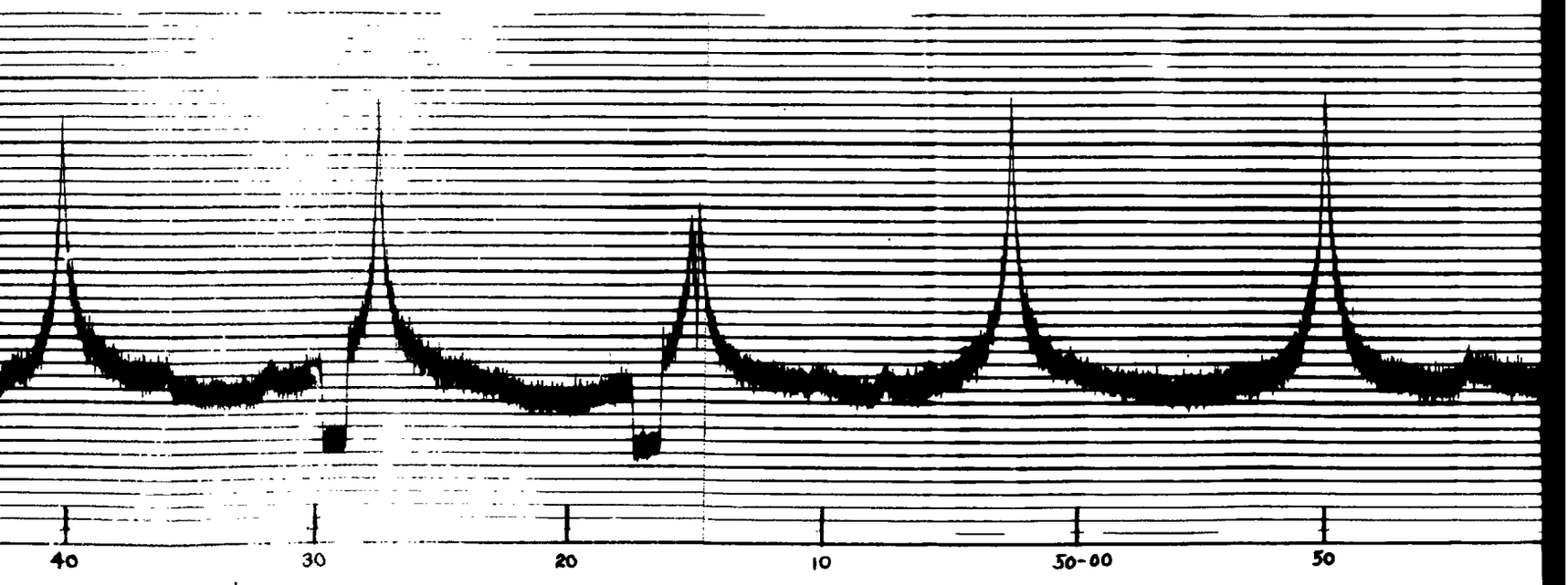

3

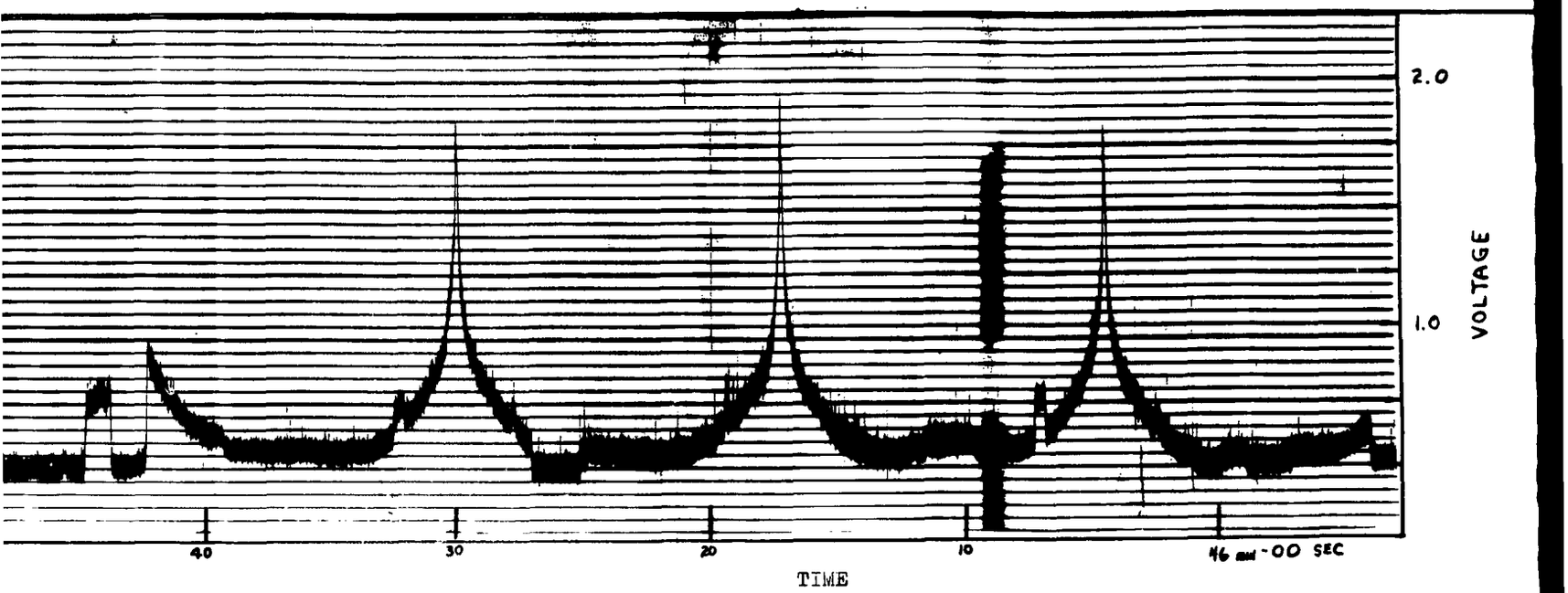
2.0
1.0
VOLTAGE
40
30
20
10
46 and -00 SEC
TIME

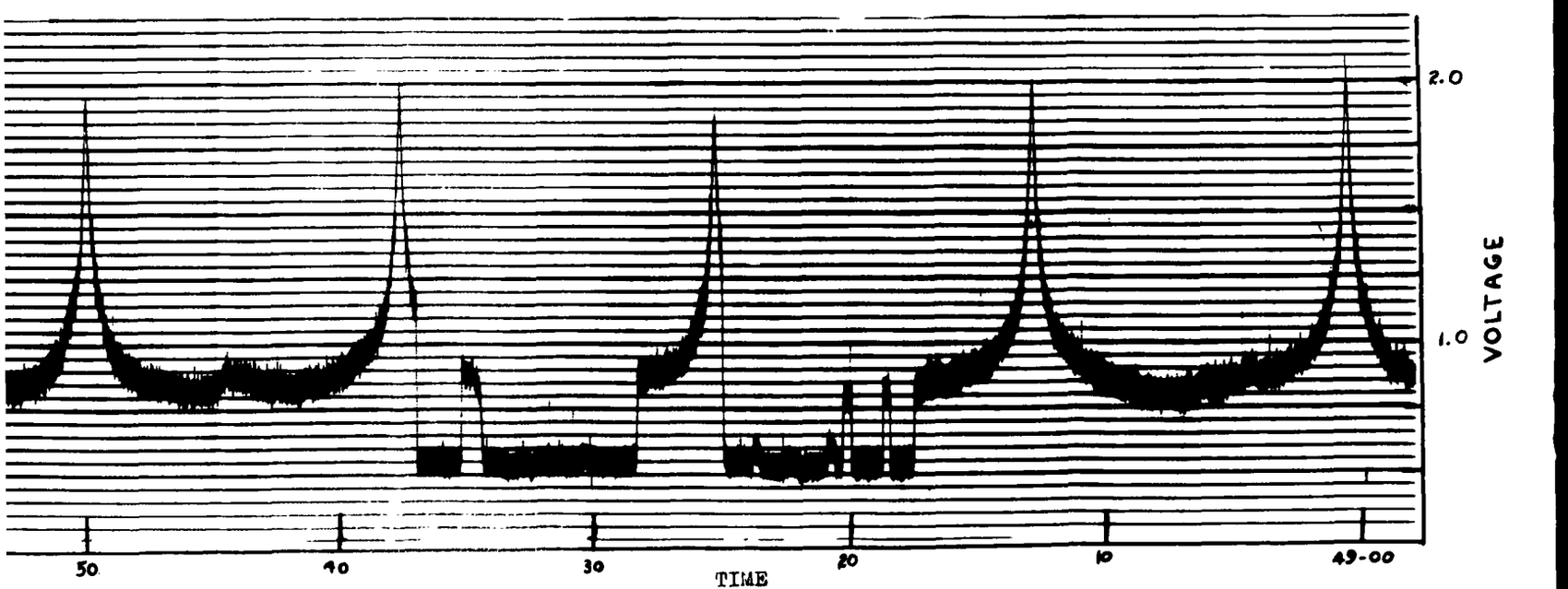
2.0
1.0
VOLTAGE
50
40
30
20
10
49-00
TIME

4

GA/Phys/63-13

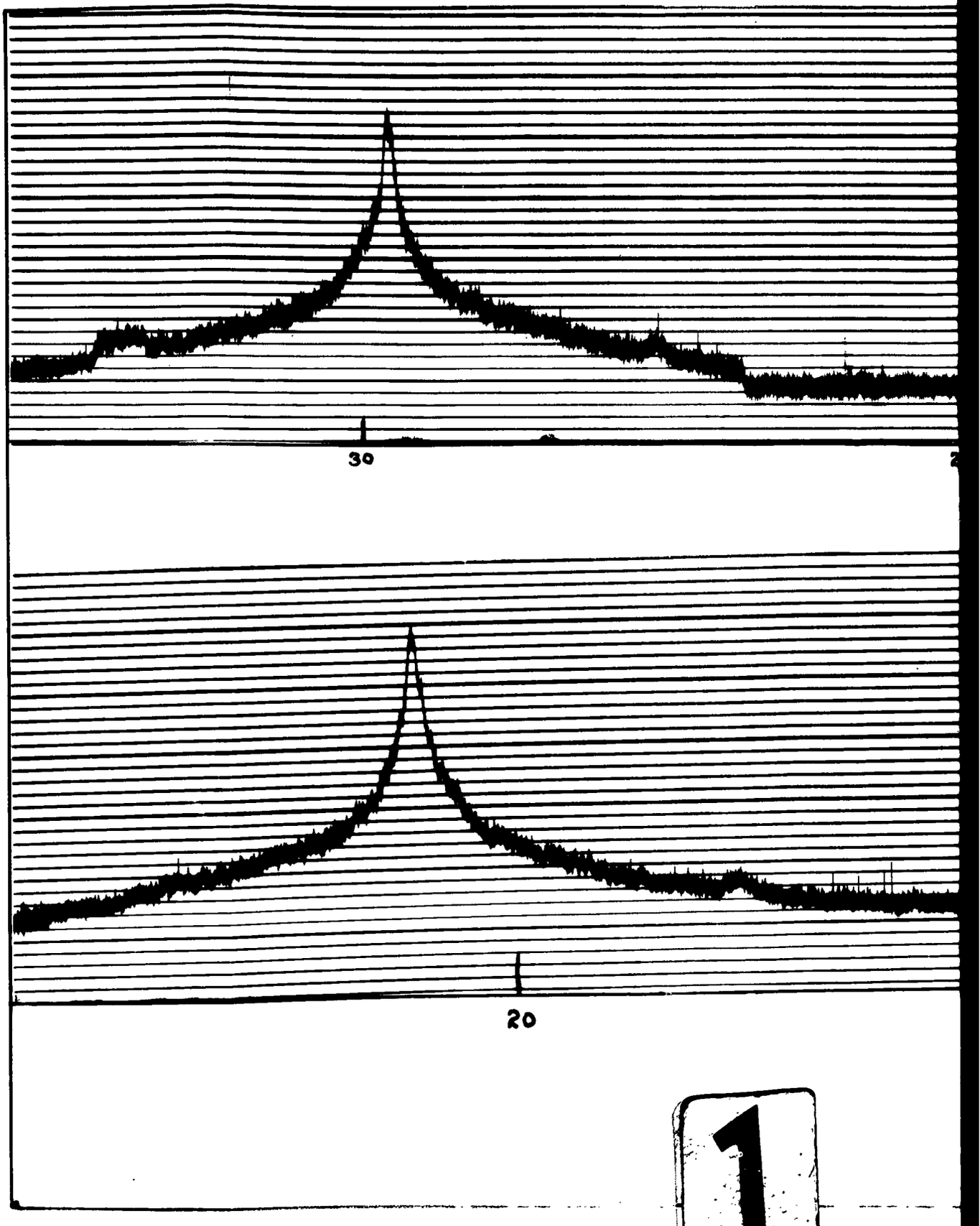

1

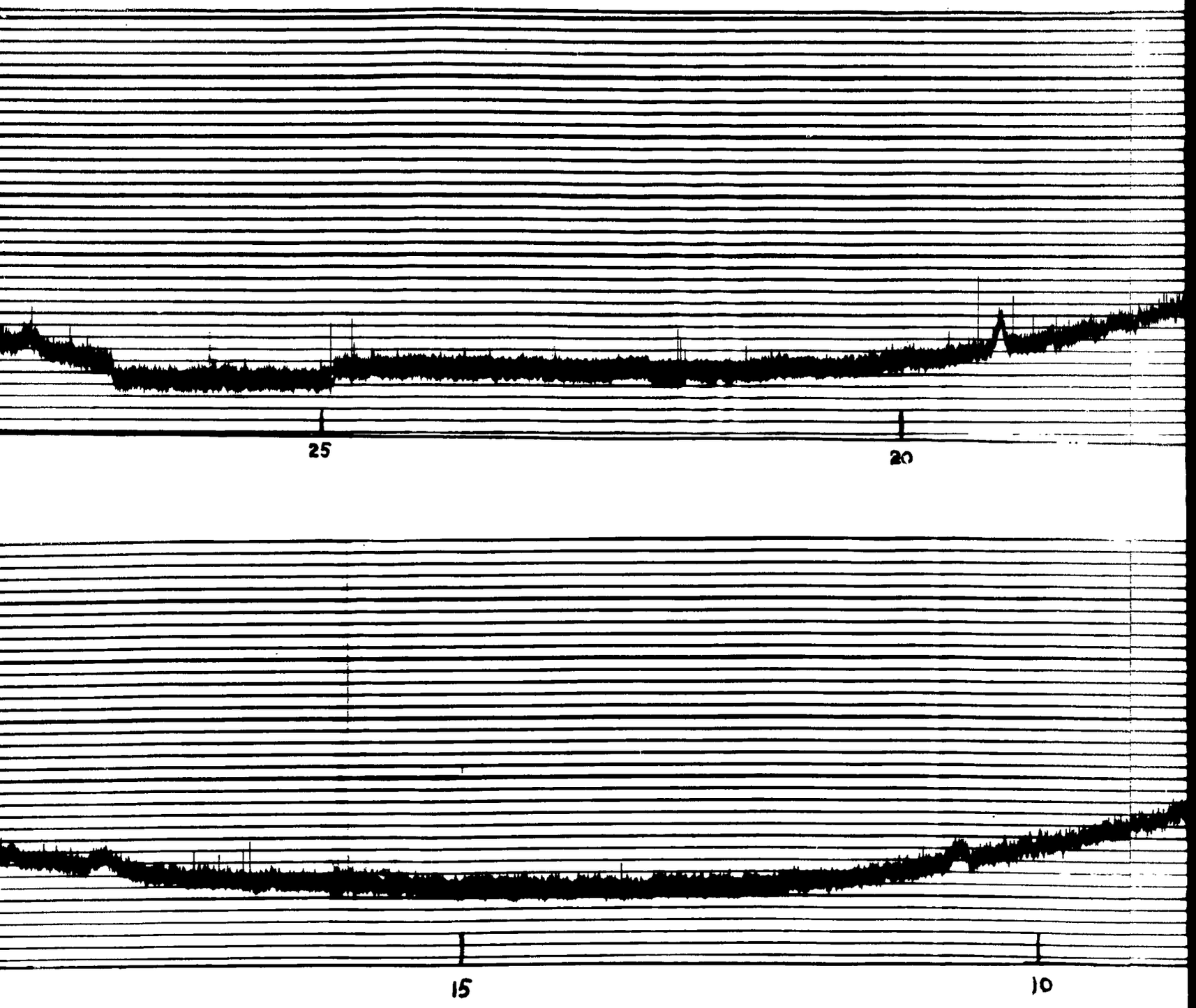
25
20
15
10

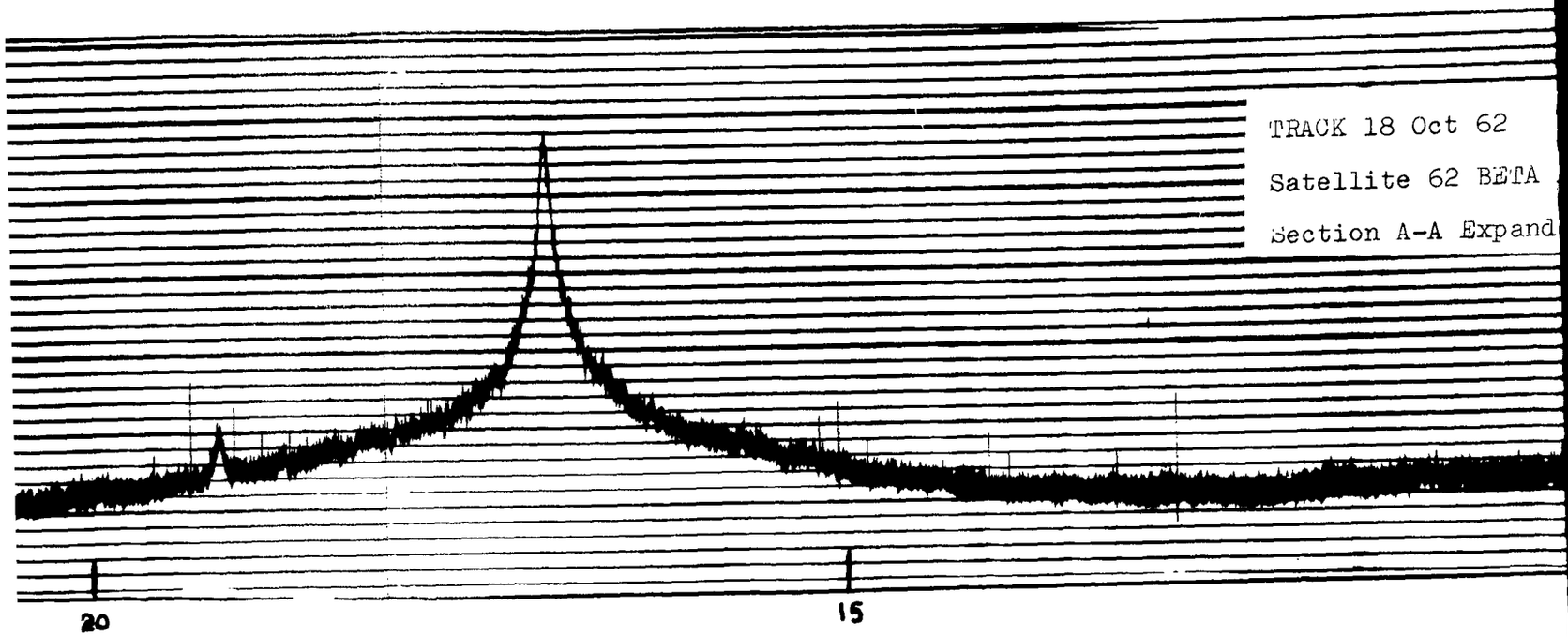
TRACK 18 Oct 62
Satellite 62 BETA
Section A-A Expand
20
15

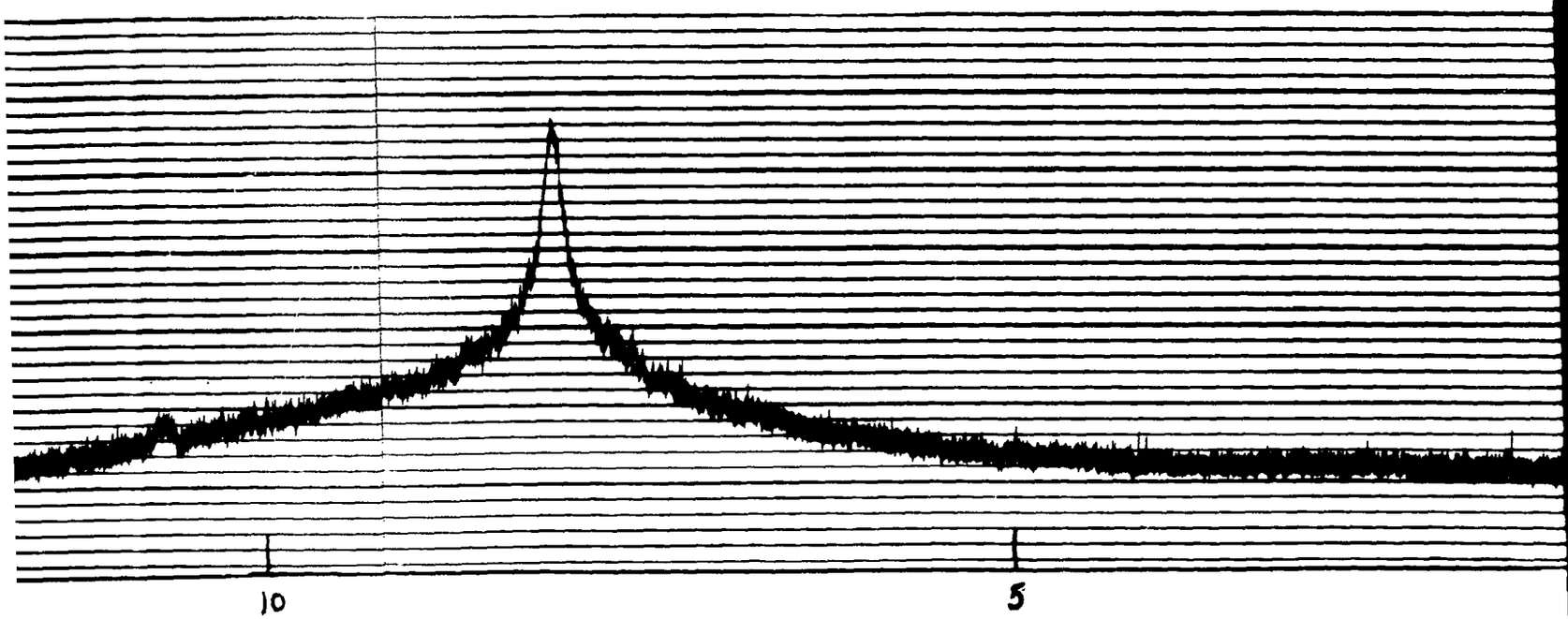
10
5

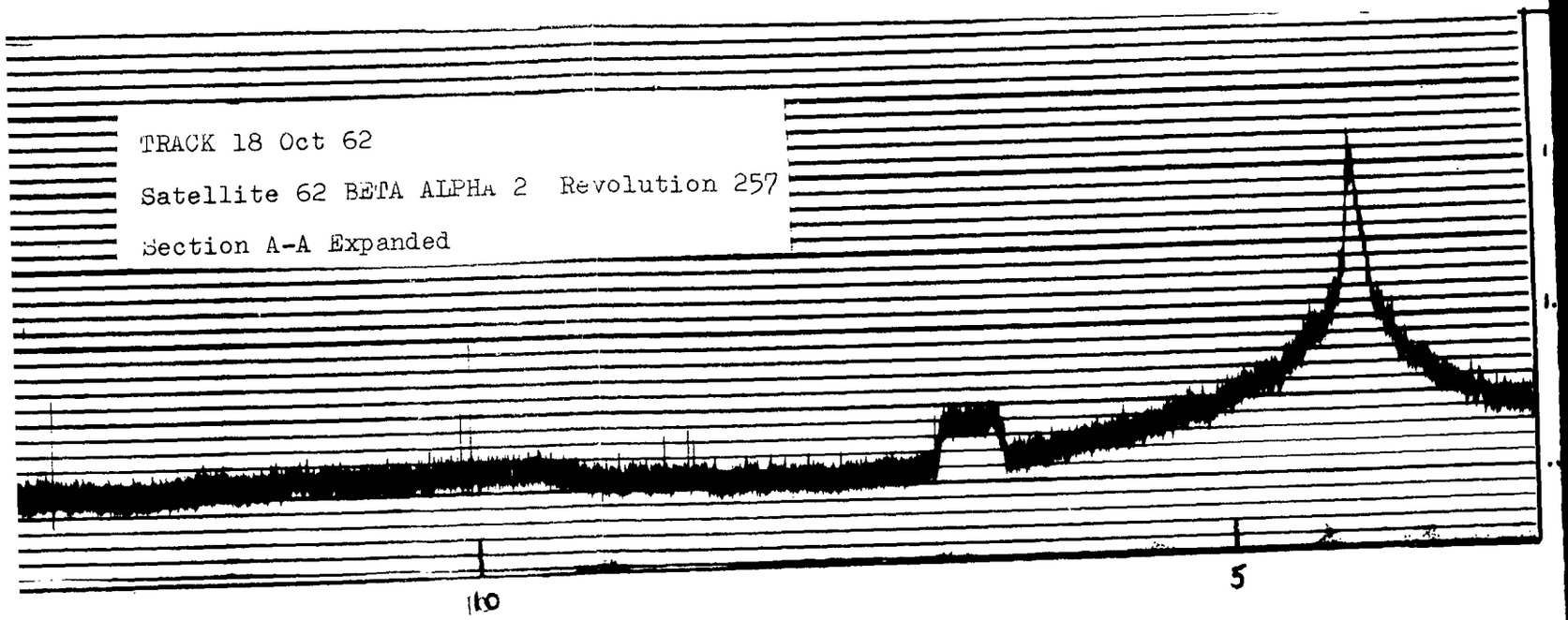
TRACK 18 Oct 62
Satellite 62 BETA ALPHA 2 Revolution 257
Section A-A Expanded
110
5

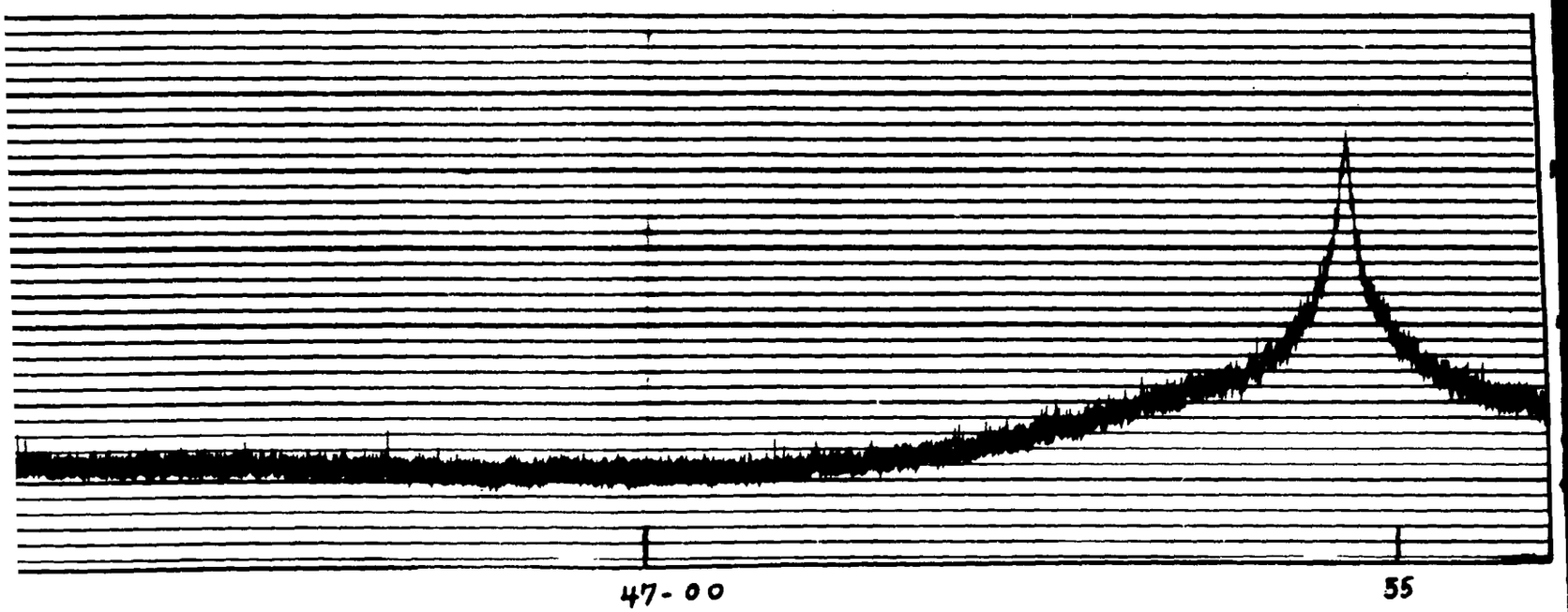
47-00
55

4

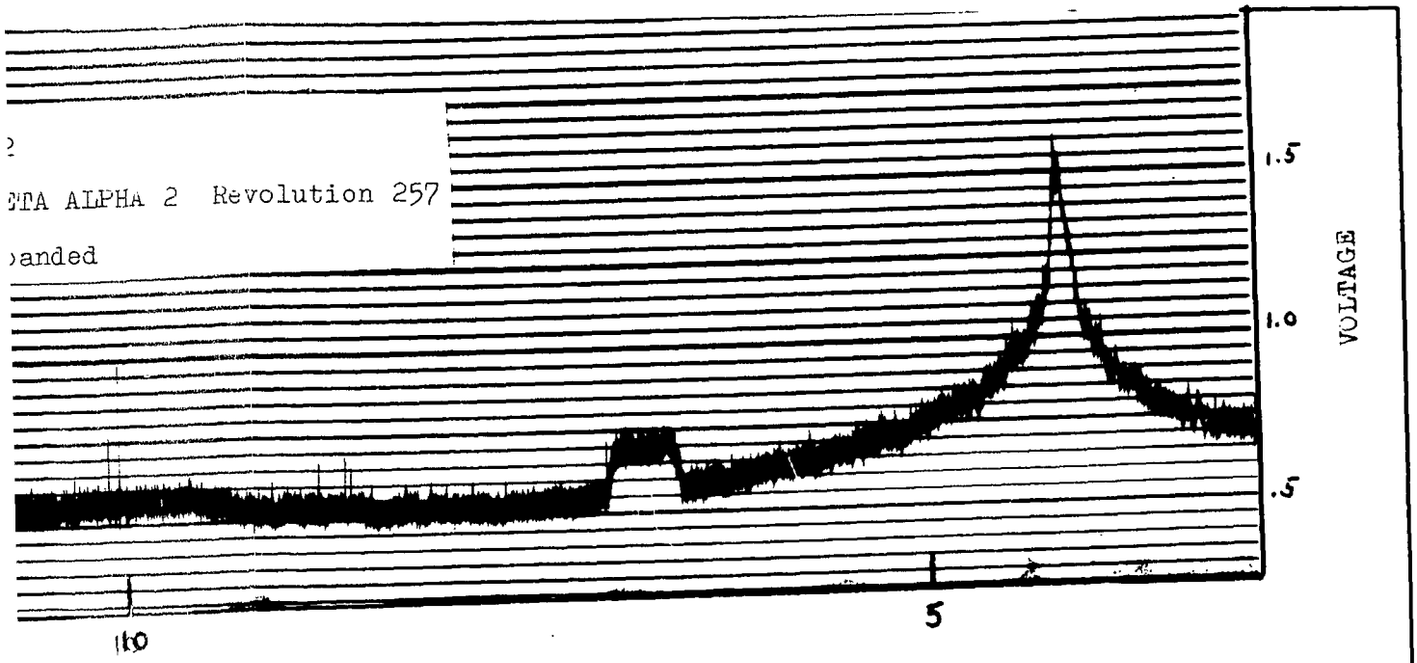
2
ETA ALPHA 2 Revolution 257
banded
1.5
1.0
.5
VOLTAGE
5


1.5
1.0
.5
VOLTAGE
47-00
55

Table VII

Tracking Data Satellite 62 Beta Alpha 2

Revolution 270

SGWADCTV 241 62B-ALPHA2 SAT. NO. 426 ELEM. 2

STARTED AT REVOLUTION NO. 156 VISUAL PASSES

REV NO.	ZEBRA TIME DAY	HR	MIN	ELEV ANG.	AZIM ANG.	RANGE KM	SUNS ELEV	ILLUMINATION
270	292	00	31.00	2.1	353.3	3542	-19.6	18.2
270	292	00	32.01	5.8	354.7	3177	-19.8	16.59
270	292	00	33.01	10.1	356.4	2815	-20.0	14.8
270	292	00	34.01	15.1	358.7	2460	-20.1	13.2
270	292	00	35.01	21.1	1.7	2117	-20.3	11.69
270	292	00	36.02	28.6	6.3	1795	-20.5	10.0
270	292	00	37.02	38.3	13.7	1509	-20.7	8.5
270	292	00	38.02	49.9	27.8	1284	-20.9	7.1
270	292	00	39.02	60.2	57.7	1159	-21.1	5.8
270	292	00	40.02	59.4	101.4	1168	-21.3	4.5
270	292	00	41.02	48.4	128.8	1307	-21.5	3.4
270	292	00	42.03	36.9	141.7	1541	-21.7	2.3
270	292	00	43.03	27.5	148.6	1835	-21.9	1.3
270	292	00	44.03	20.1	152.9	2163	-22.1	0.4
270	292	00	45.03	14.2	155.8	2512	-22.3	-0.3
270	292	00	46.03	9.2	157.8	2873	-22.4	-1.0
270	292	00	47.03	.0	159.4	3240	-22.6	-1.5
270	292	00	48.03	1.3	160.7	3612	-22.8	-1.9

GA/Phys/63-13

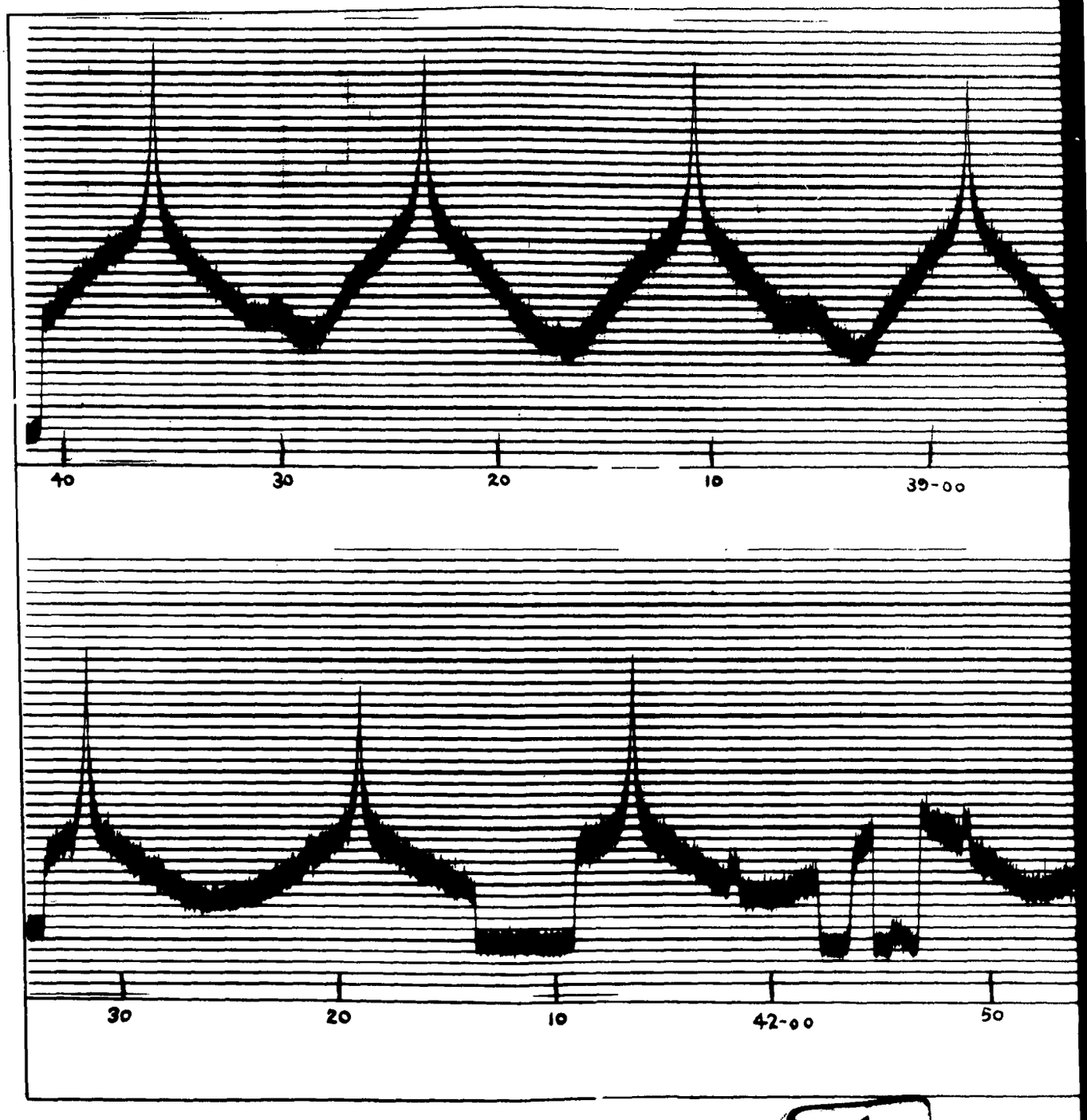

1

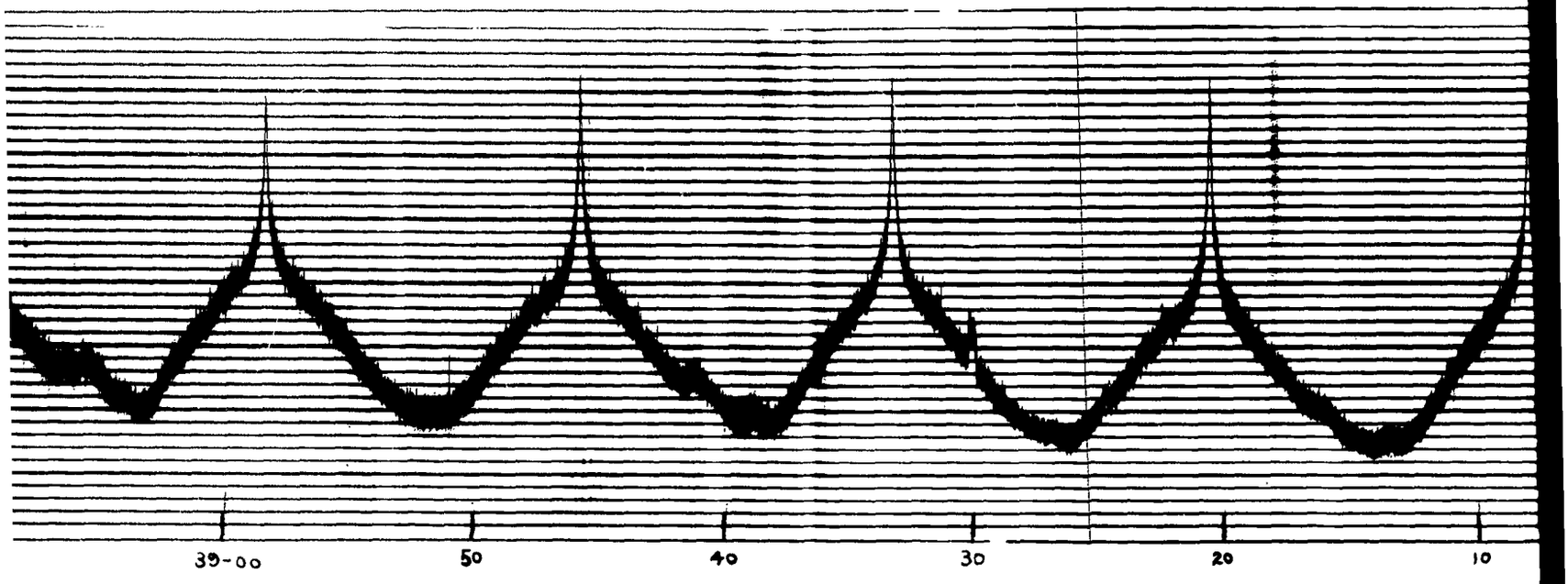

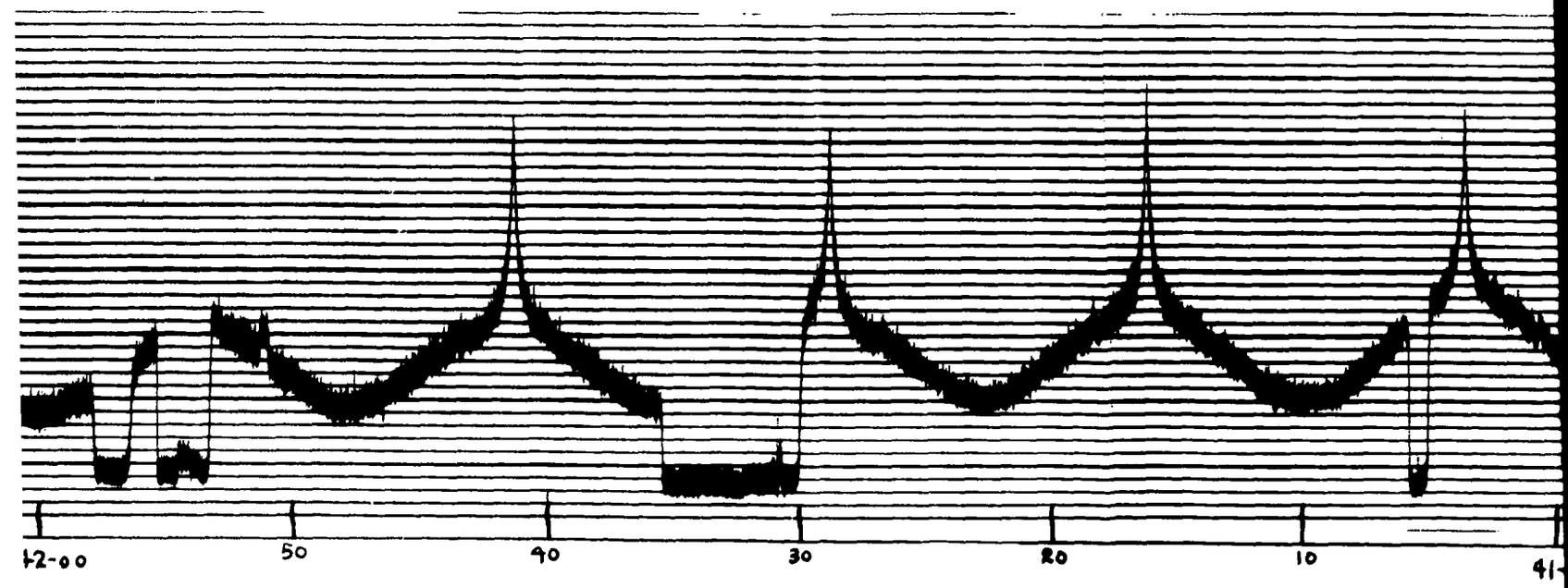

2

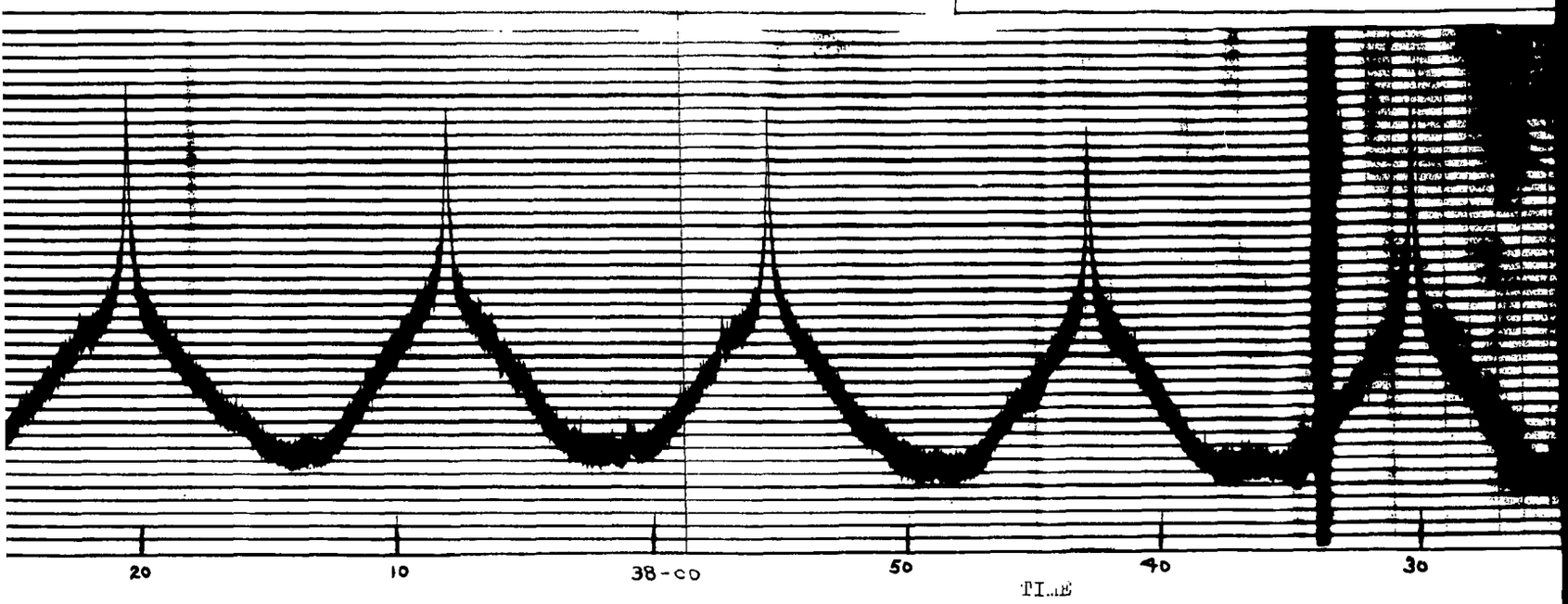

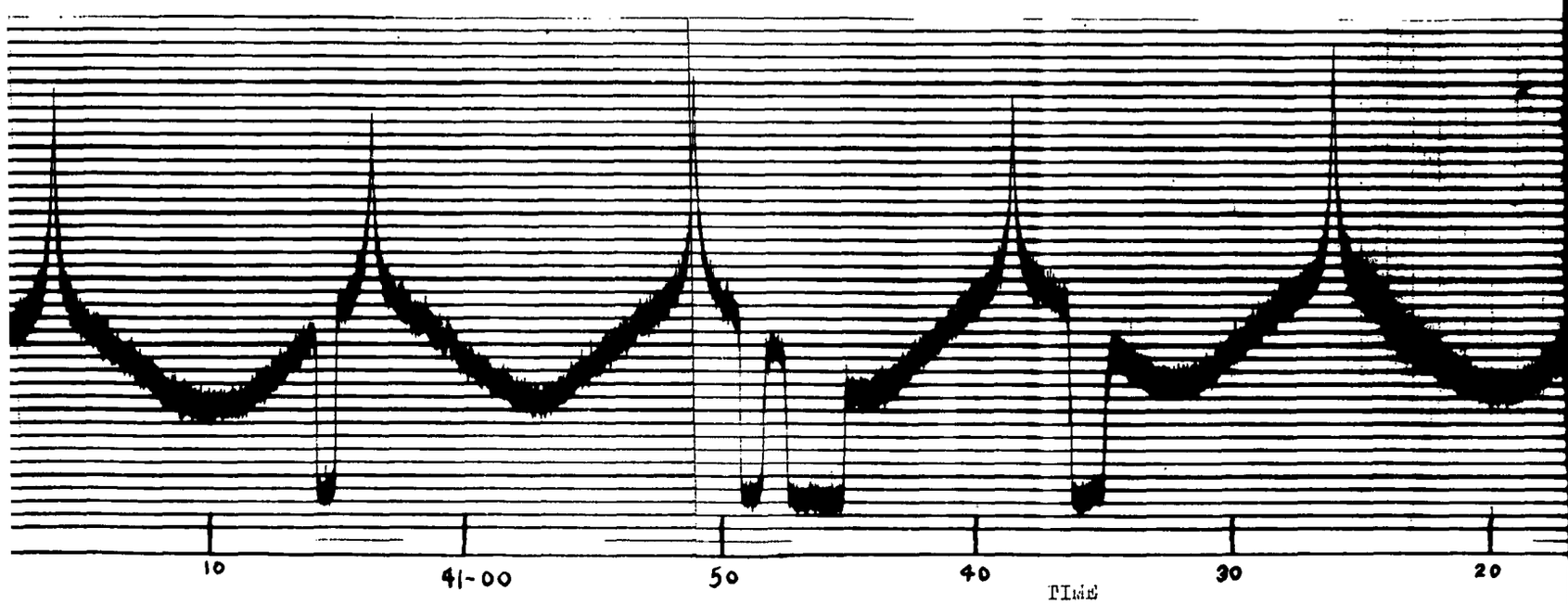

3

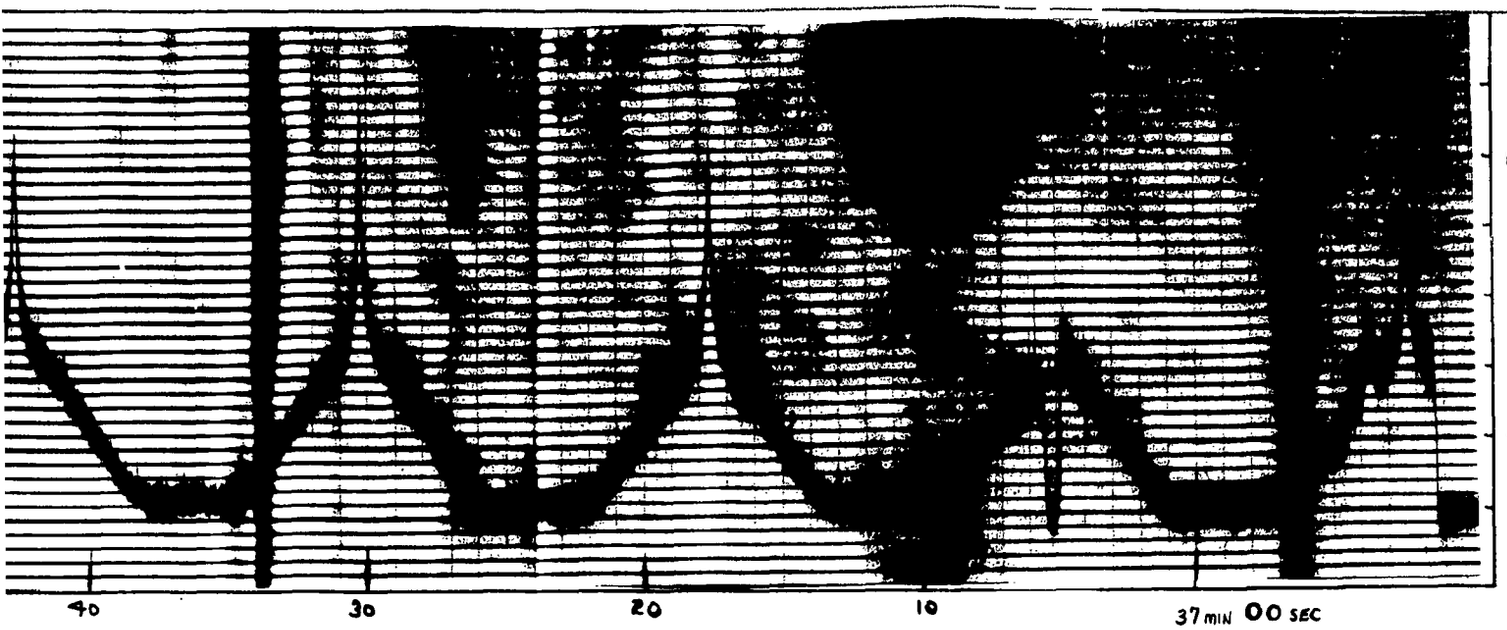
1.5
1.0
.5
VOLTAGE
40
30
20
10
37 MIN 00 SEC

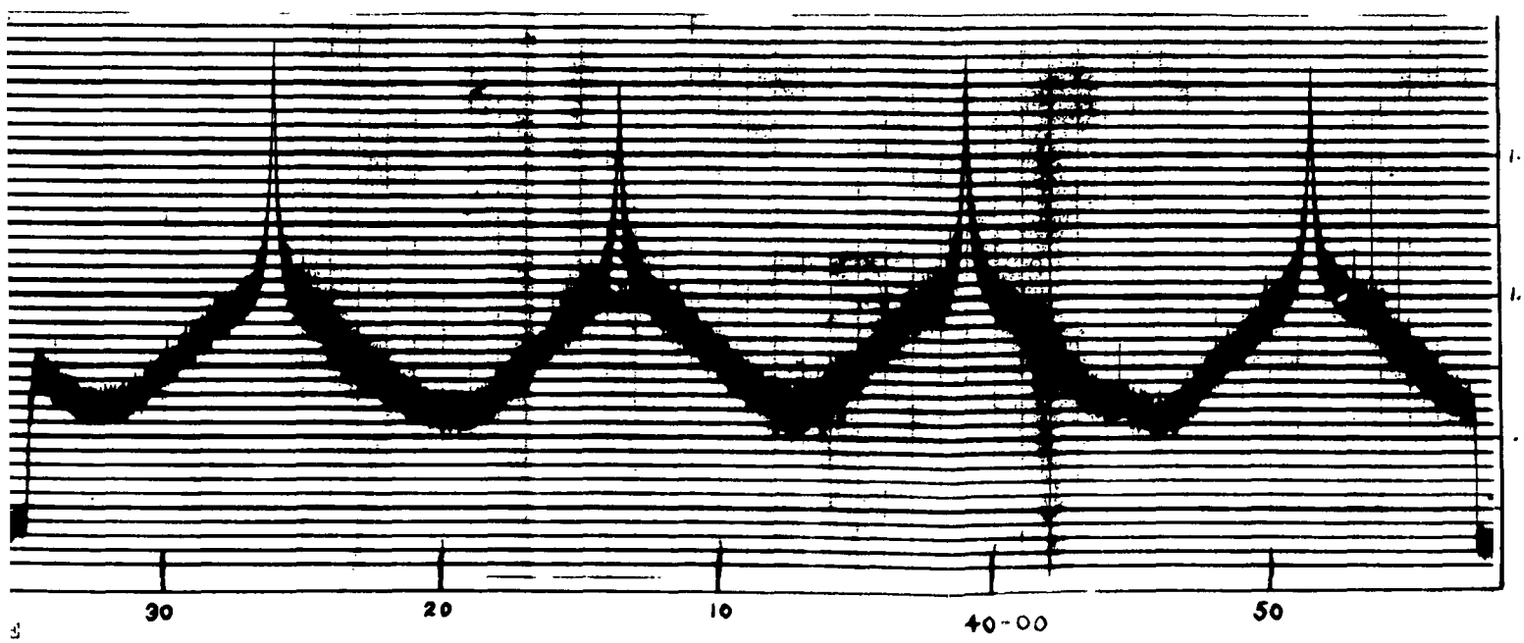
1.5
1.0
.5
VOLTAGE
30
20
10
40-00
50

4

TRACK 19 Oct 62

Satellite 62 BETA ALPHA 2

AGENA B Rocket Body

Revolution 270

Time 00hr - 36min - 51sec

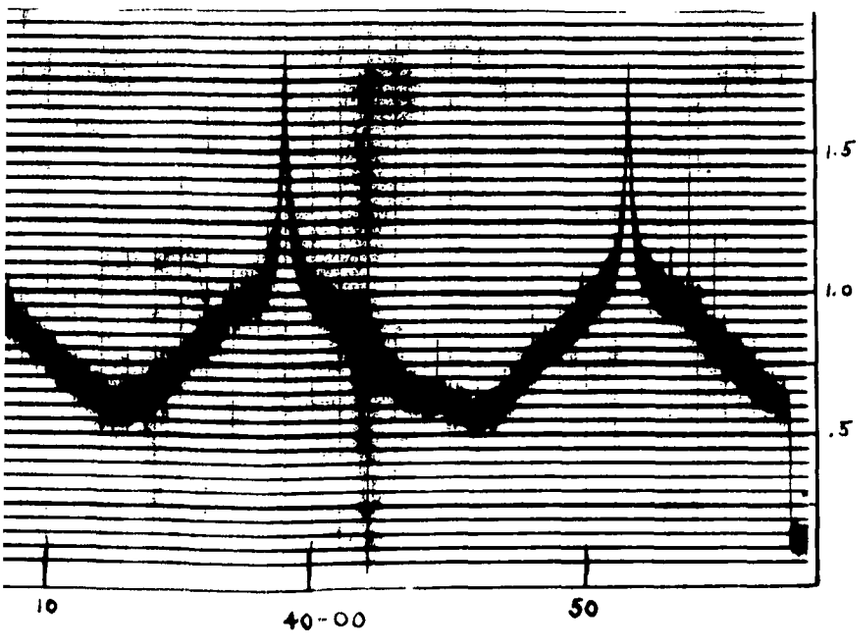

5

Table VIII

Tracking Data Satellite 62 Beta Alpha 2
Revolution 2674

DAYTON OHIO SGWA 241 62B-ALPHA2 SAT. NO. 426

REV NO.	ZEBRA TIME DAY	HR	MIN.	ELEV ANG.	AZIM ANG.	RANGE KM.	SUNS ELEV	ILLUMI NATION
2674	103	2	22.62	.8	342.5	3672	-24.0	30.8
2674	103	2	23.62	4.3	340.9	3307	-24.2	28.4
2674	103	2	24.62	8.3	338.7	2948	-24.3	25.9
2674	103	2	25.62	12.8	335.8	2596	-24.5	23.4
2674	103	2	26.62	18.0	331.8	2260	-24.7	21.0
2674	103	2	27.62	24.3	326.0	1946	-24.8	18.6
2674	103	2	28.62	31.6	317.1	1671	-25.0	16.1
2674	103	2	29.62	39.5	302.9	1457	-25.1	13.8
2674	103	2	30.62	45.5	280.8	1334	-25.3	11.4
2674	103	2	31.62	45.6	253.8	1329	-25.4	9.1
2674	103	2	32.62	39.7	231.3	1443	-25.6	6.8
2674	103	2	33.62	31.7	216.7	1651	-25.7	4.6
2674	103	2	34.62	24.2	207.5	1923	-25.9	2.4
2674	103	2	35.62	17.9	201.6	2234	-26.0	.3

Table IX

Tracking Data, Satellite 62 Beta Alpha 2
Revolution 2687

DAYTON OHIO SGWA 241 62B-ALPHA2 SAT. NO. 426

REV NO.	ZEBRA TIME DAY	HR	MIN.	ELEV ANG.	AZIM ANG.	RANGE KM.	SUNS ELEV	ILLUMI NATION
2687	104	1	13.62	2.9	353.9	3445	-12.3	32.1
2687	104	1	14.62	6.8	355.5	3080	-12.4	29.7
2687	104	1	15.62	11.1	357.6	2718	-12.6	27.3
2687	104	1	16.62	16.3	.2	2365	-12.8	24.9
2687	104	1	17.62	22.6	3.9	2027	-13.0	22.5
2687	104	1	18.62	30.4	9.4	1713	-13.1	20.1
2687	104	1	19.62	40.3	18.7	1441	-13.3	17.8
2687	104	1	20.62	51.5	36.6	1241	-13.5	15.4
2687	104	1	21.62	58.8	70.7	1153	-13.7	13.1
2687	104	1	22.62	54.3	109.0	1200	-13.8	10.8
2687	104	1	23.62	43.2	130.8	1370	-14.0	8.6
2687	104	1	24.62	32.6	141.8	1624	-14.2	6.4
2687	104	1	25.62	24.1	148.1	1928	-14.4	4.3
2687	104	1	26.62	17.4	152.1	2262	-14.5	2.2

GA/Phys/63-13

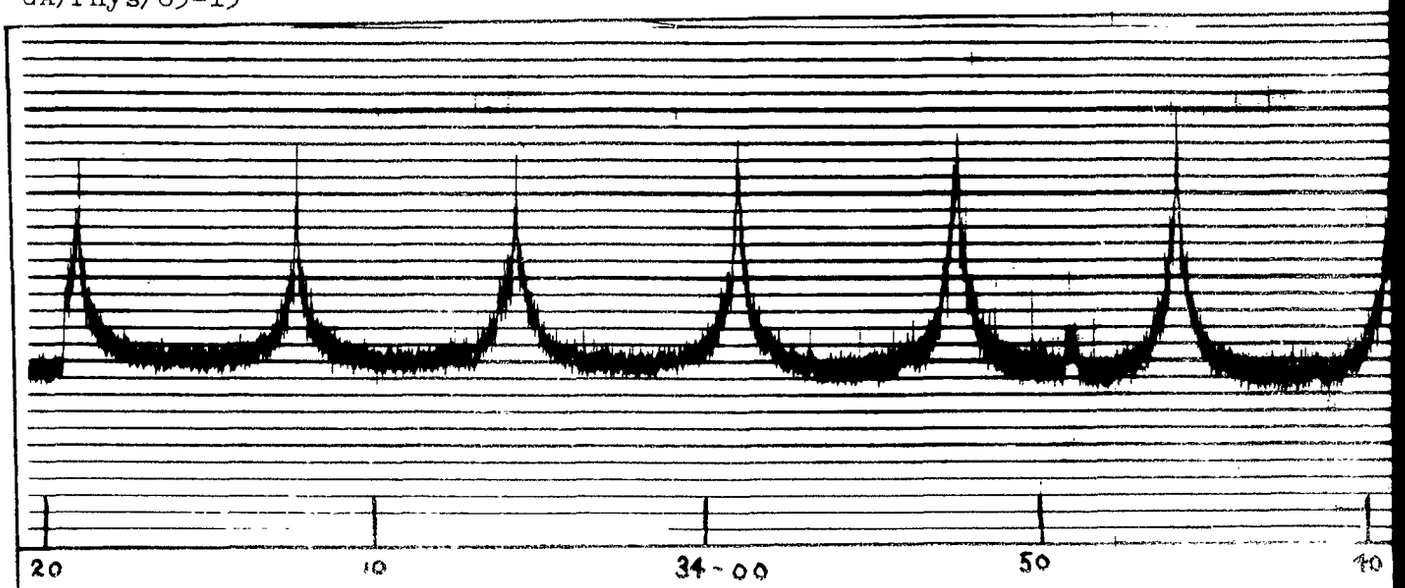

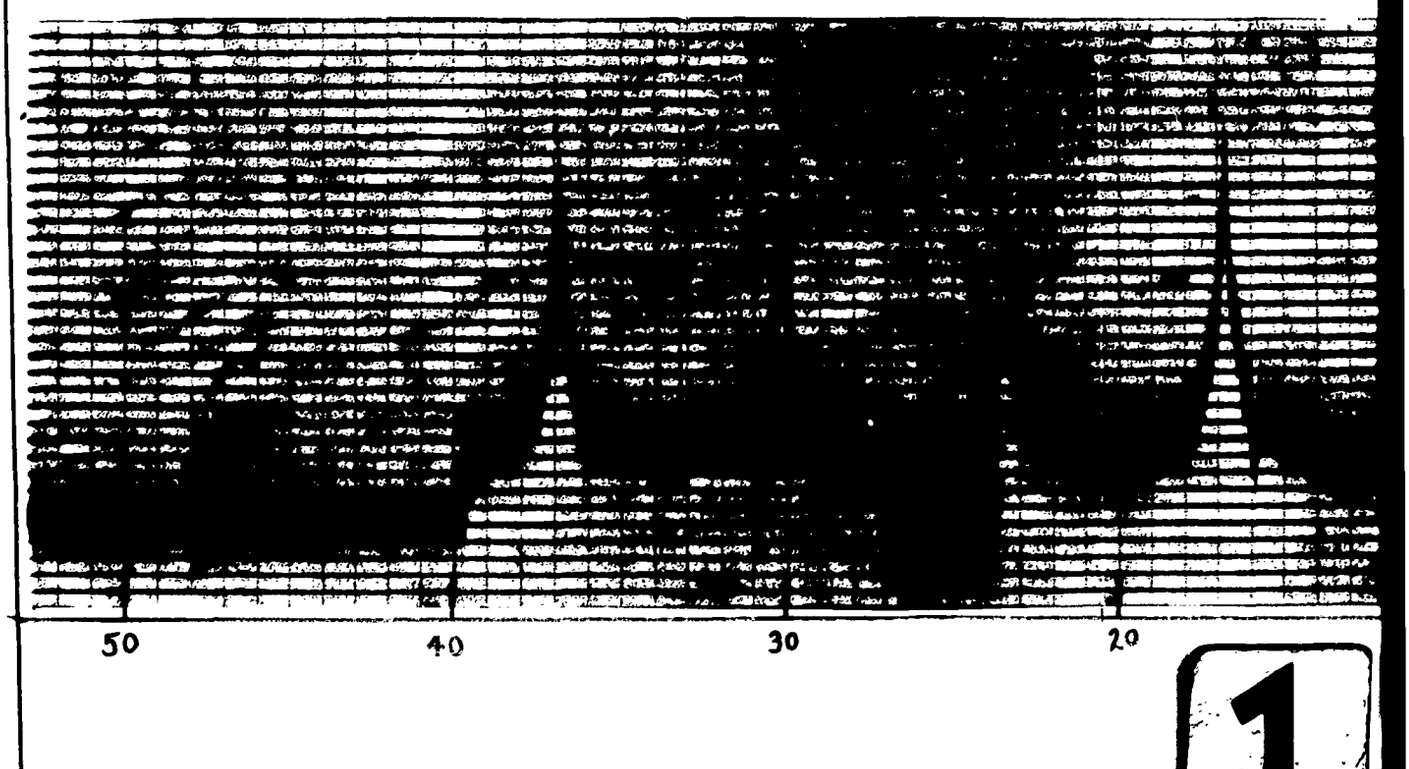

1

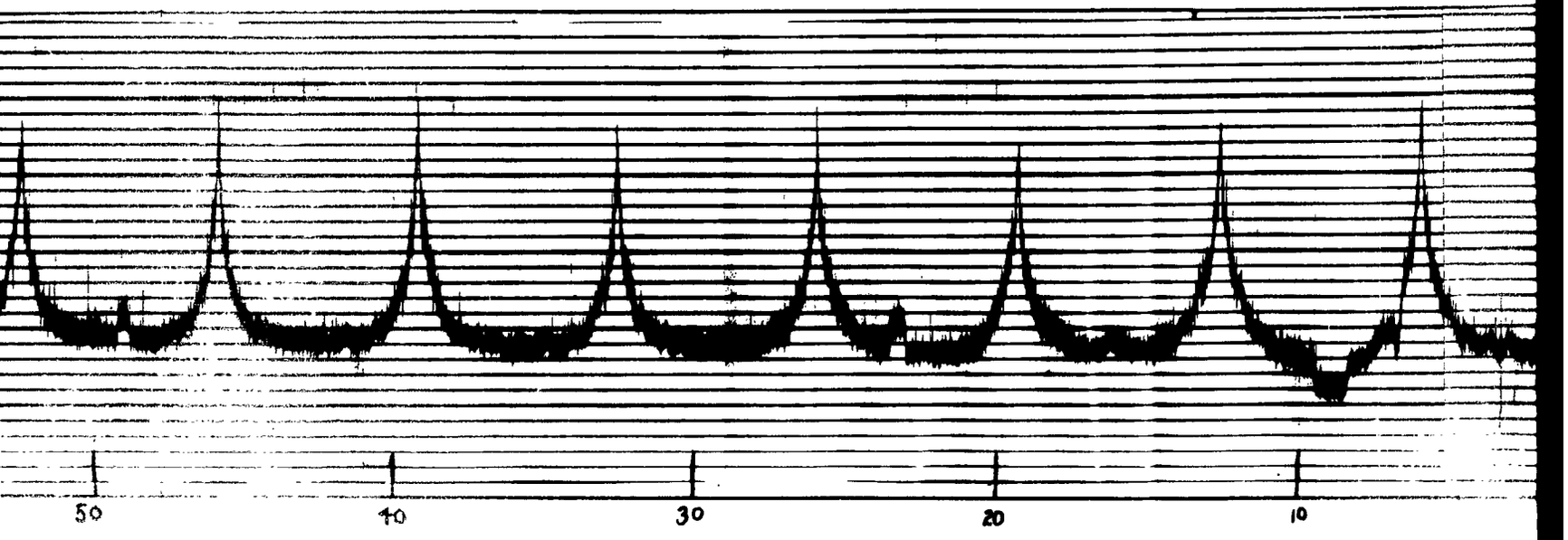

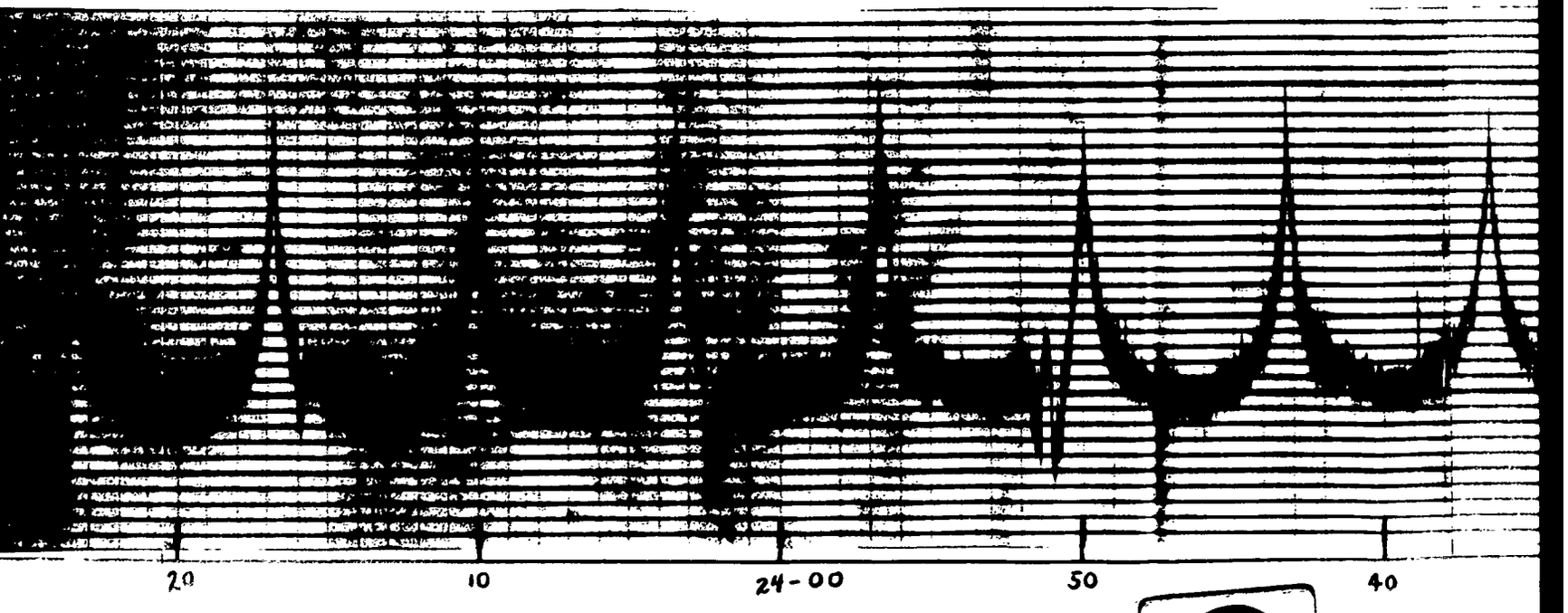

2

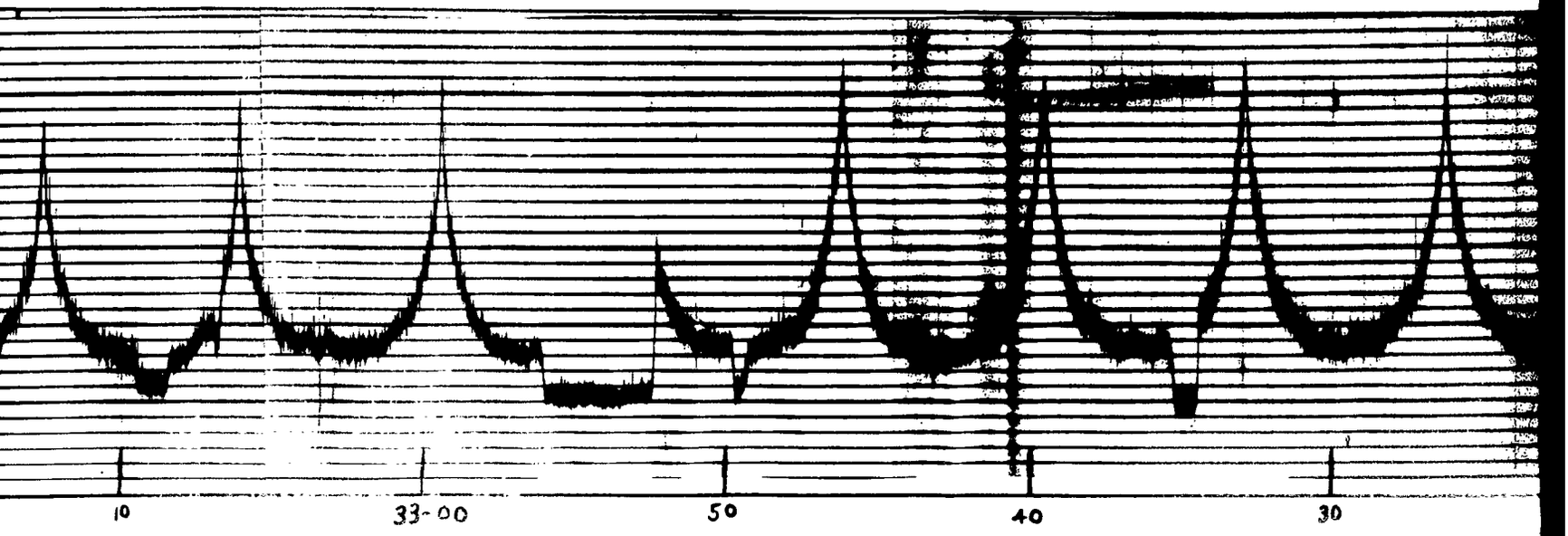
10
33-00
50
40
30

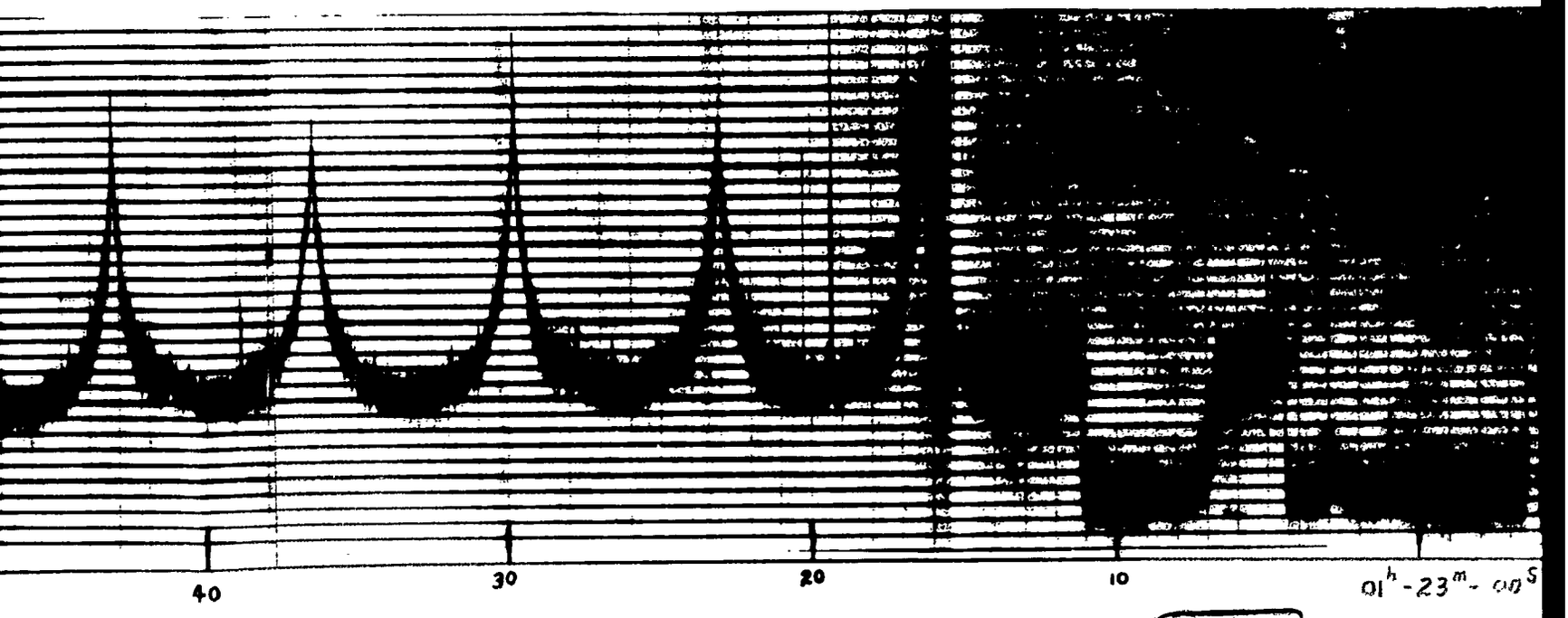
40
30
20
10
01h-23m-00s

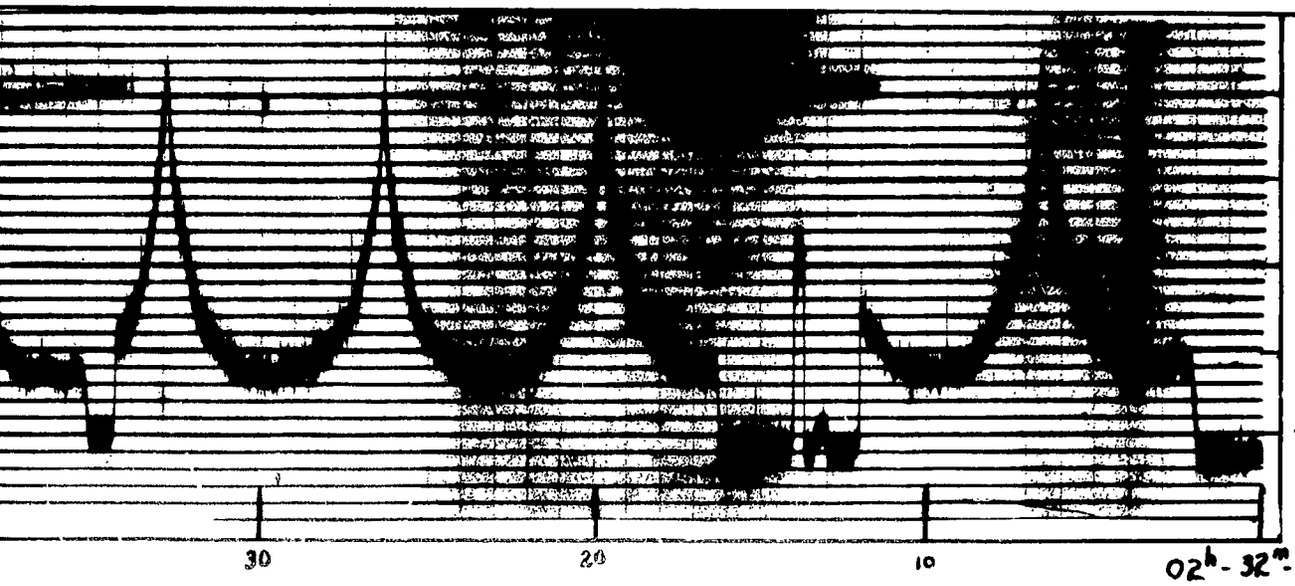

TRACK 13 April 63

BETA ALPHA 2 Revolutio

Time 02hr - 32min - 00s

1.0

.5

VOLTAGE

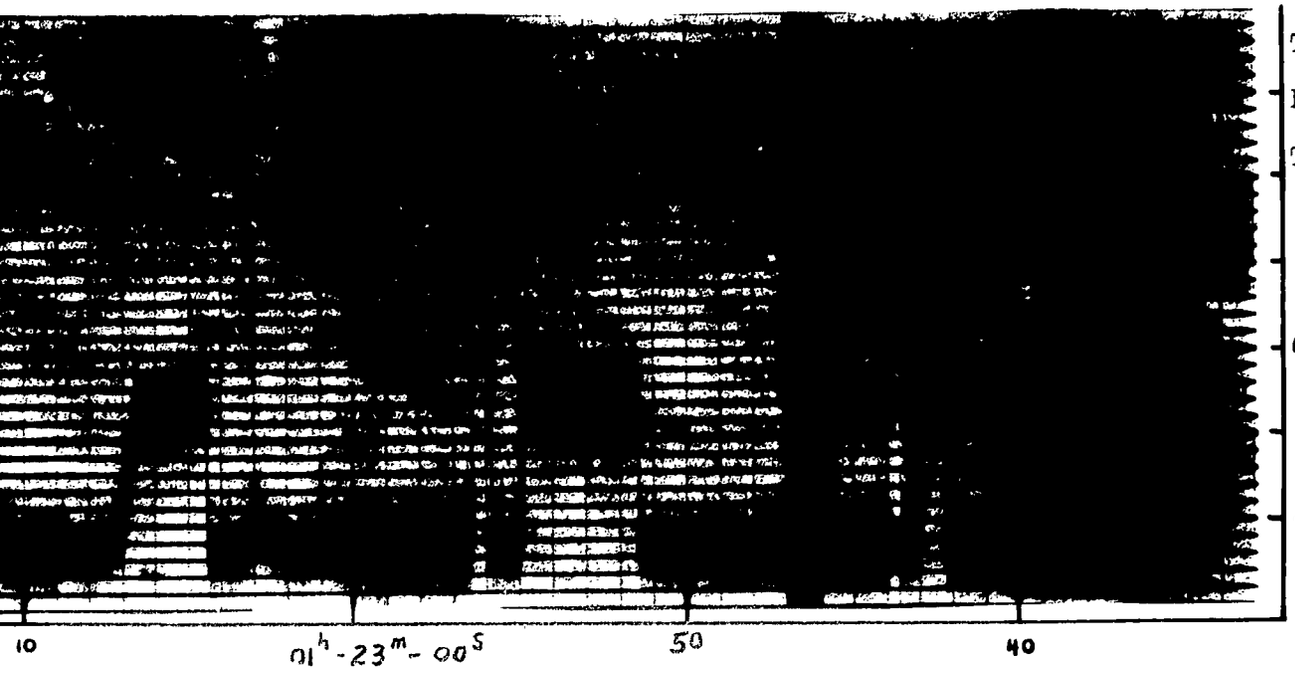

TRACK 14 April 63

BETA ALPHA 2 Revolutio

Time 01hr - 23min - 36s

1.0

.50

VOLTAGE

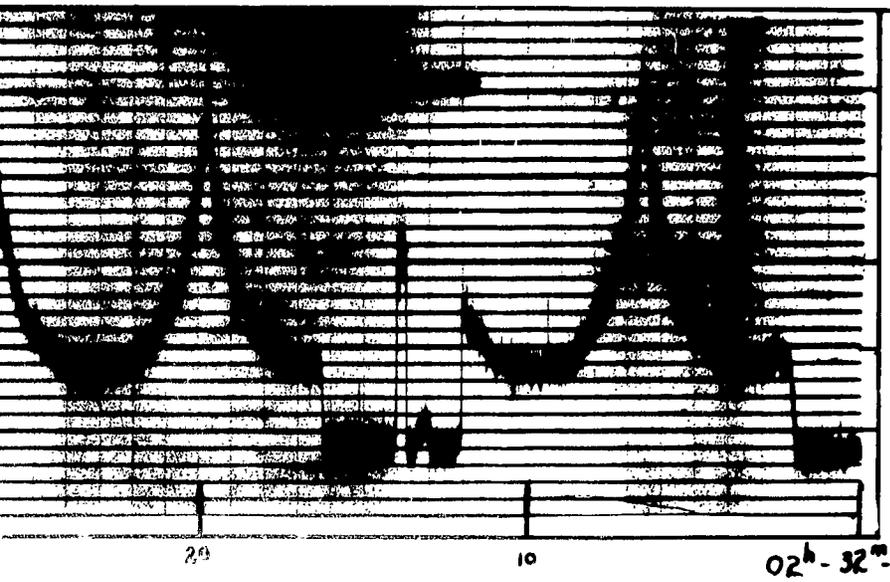

TRACK 13 April 63

BETA ALPHA 2 Revolution 2674

Time 02hr - 32min - 00sec

1.0

.5

VOLTAGE

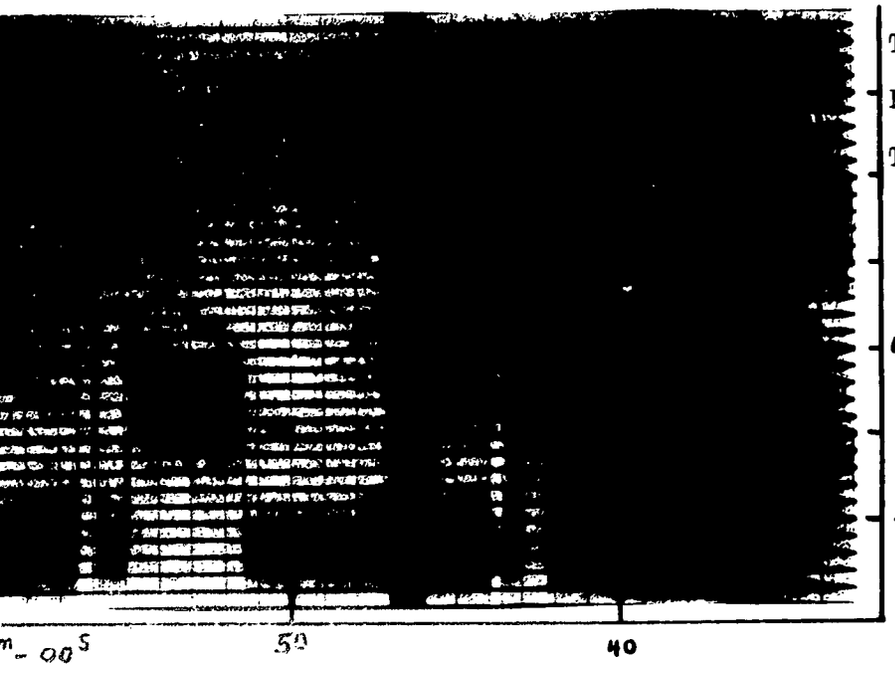

TRACK 14 April 63

BETA ALPHA 2 Revolution 2687

Time 01hr - 23min - 36sec

1.0

.50

VOLTAGE

Table X

Tracking Data, Satellite 62 Beta Alpha 2
Revolution 2701

DAYTON OHIO SGWA 241 62B-ALPHA2 SAT. NO. 426

REV NO.	ZEBRA TIME DAY	HR	MIN.	ELEV ANG.	AZIM ANG.	RANGE KM.	SUNS ELEV	ILLUMI NATION
2701	105	1	50.62	2.7	345.1	3464	-18.4	32.2
2701	105	1	51.62	6.6	344.2	3092	-18.6	29.8
2701	105	1	52.62	11.0	342.9	2725	-18.7	27.5
2701	105	1	53.62	16.2	341.0	2365	-18.9	25.2
2701	105	1	54.62	22.7	338.3	2019	-19.1	22.9
2701	105	1	55.62	30.3	333.9	1696	-19.2	20.5
2701	105	1	56.62	41.4	326.0	1415	-19.4	18.3
2701	105	1	57.62	54.1	309.3	1206	-19.6	16.0
2701	105	1	58.62	63.2	271.6	1111	-19.7	13.8
2701	105	1	59.62	57.7	227.3	1159	-19.9	11.6
2701	105	2	.62	44.9	205.7	1335	-20.1	9.4
2701	105	2	1.62	33.4	195.9	1597	20.2	7.3
2701	105	2	2.62	24.5	190.7	1909	-20.4	5.2
2701	105	2	3.62	17.5	187.5	2249	-20.5	3.2
2701	105	2	4.62	11.9	185.3	2605	-20.7	1.3

GA/Phys/63-13

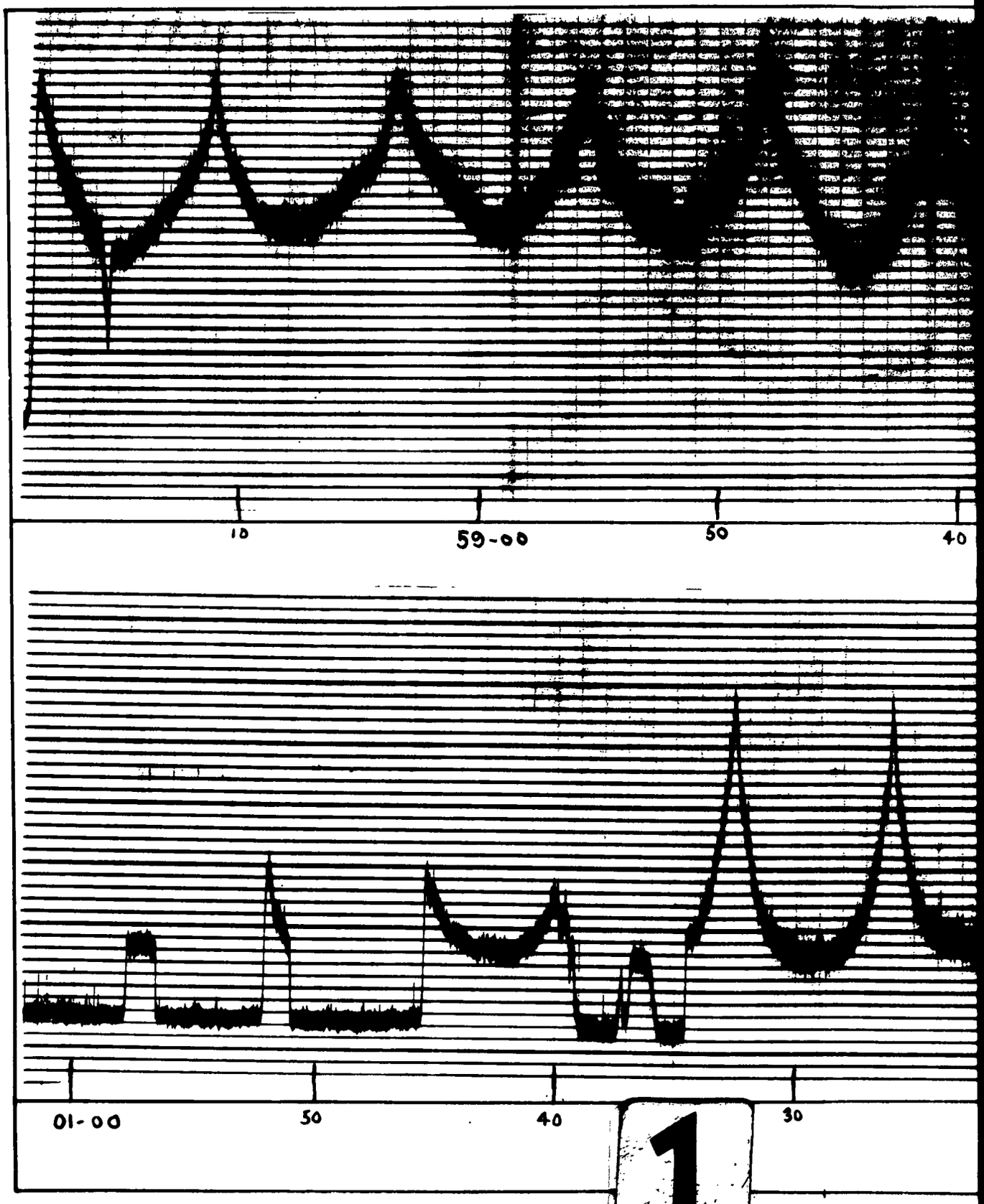

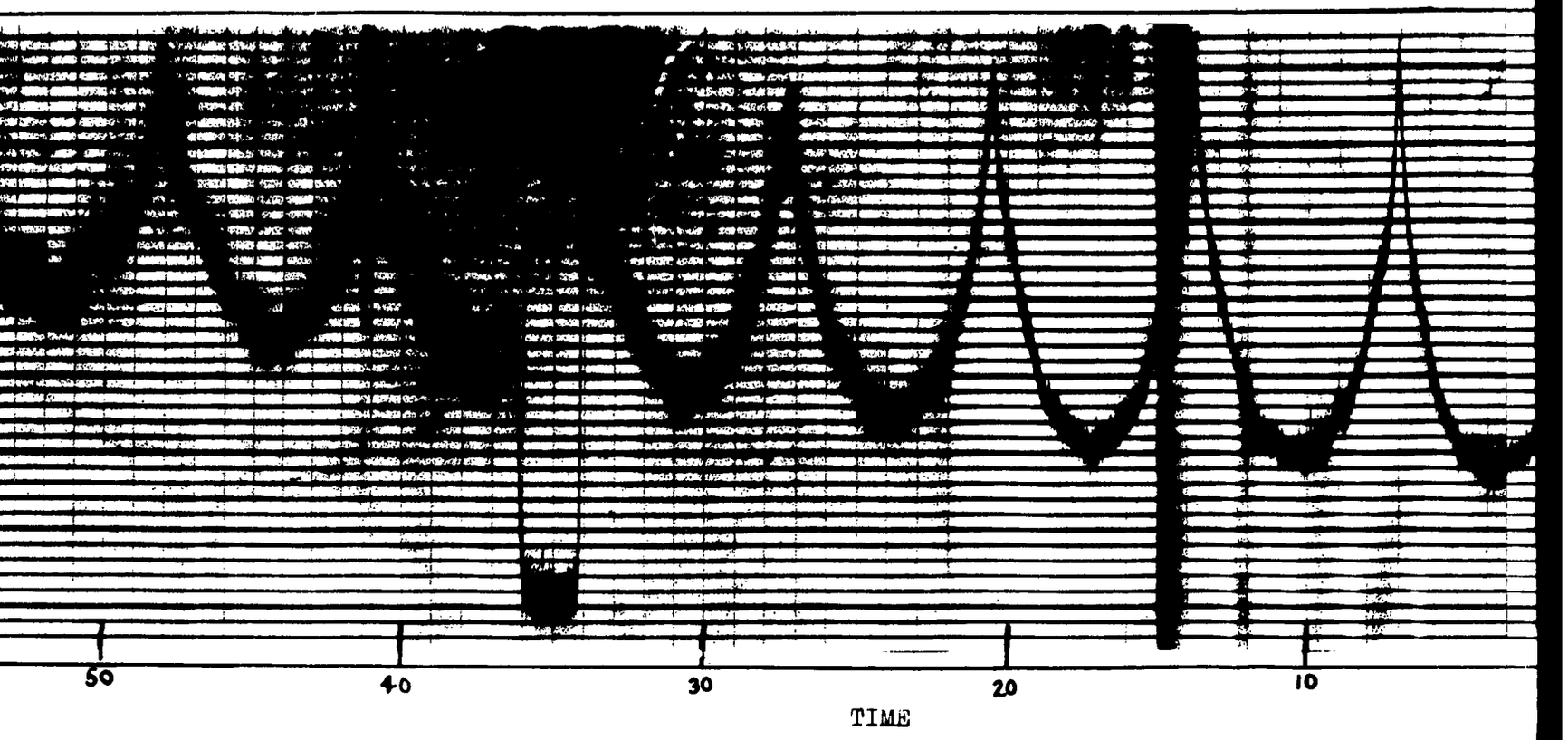

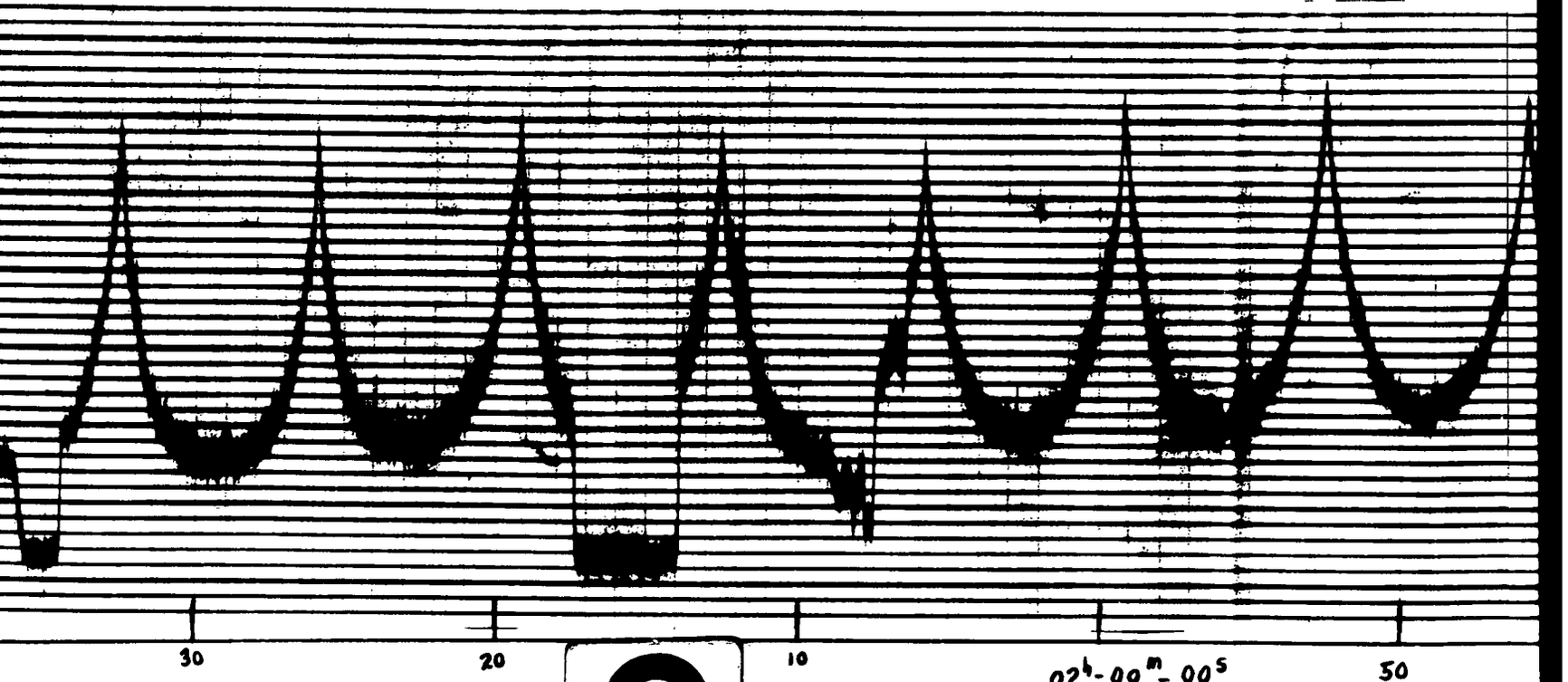

2

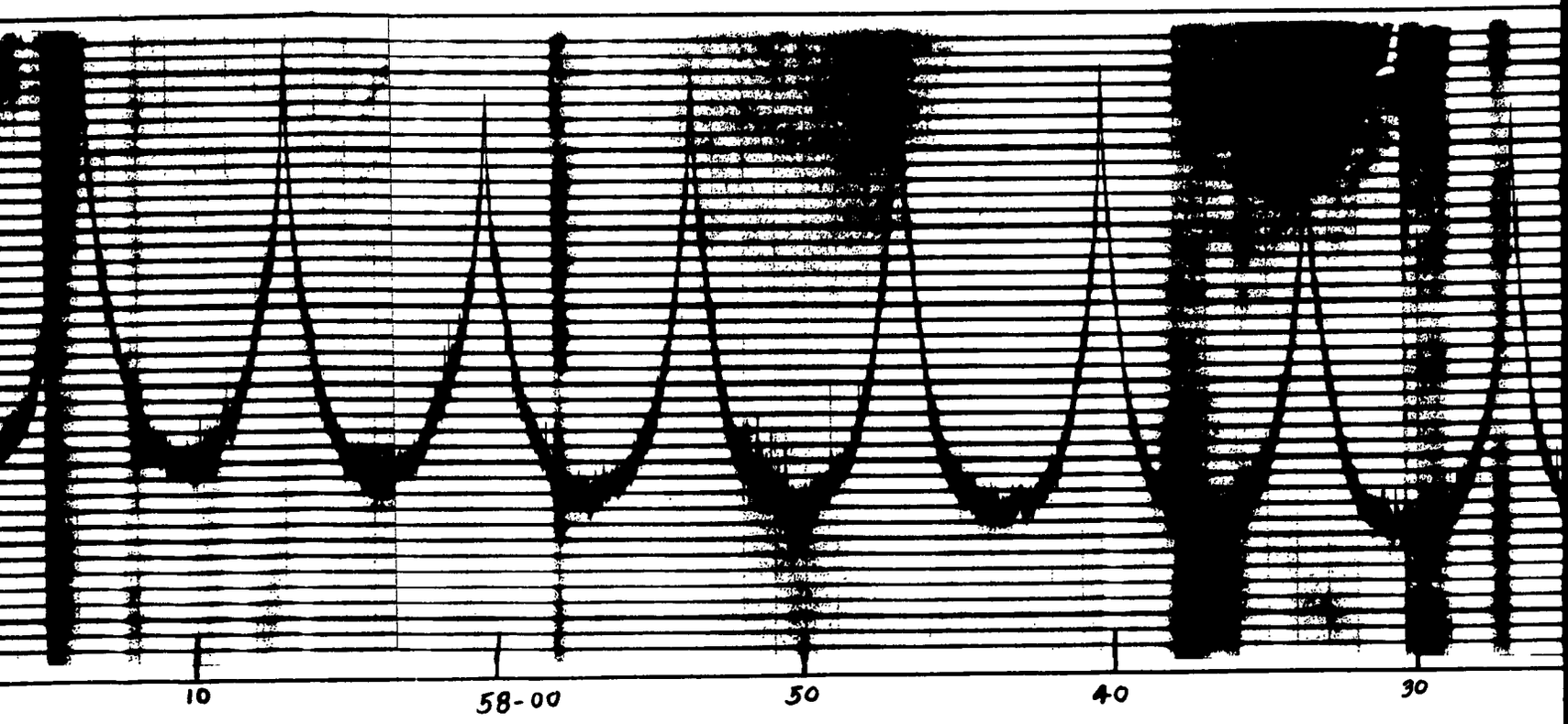

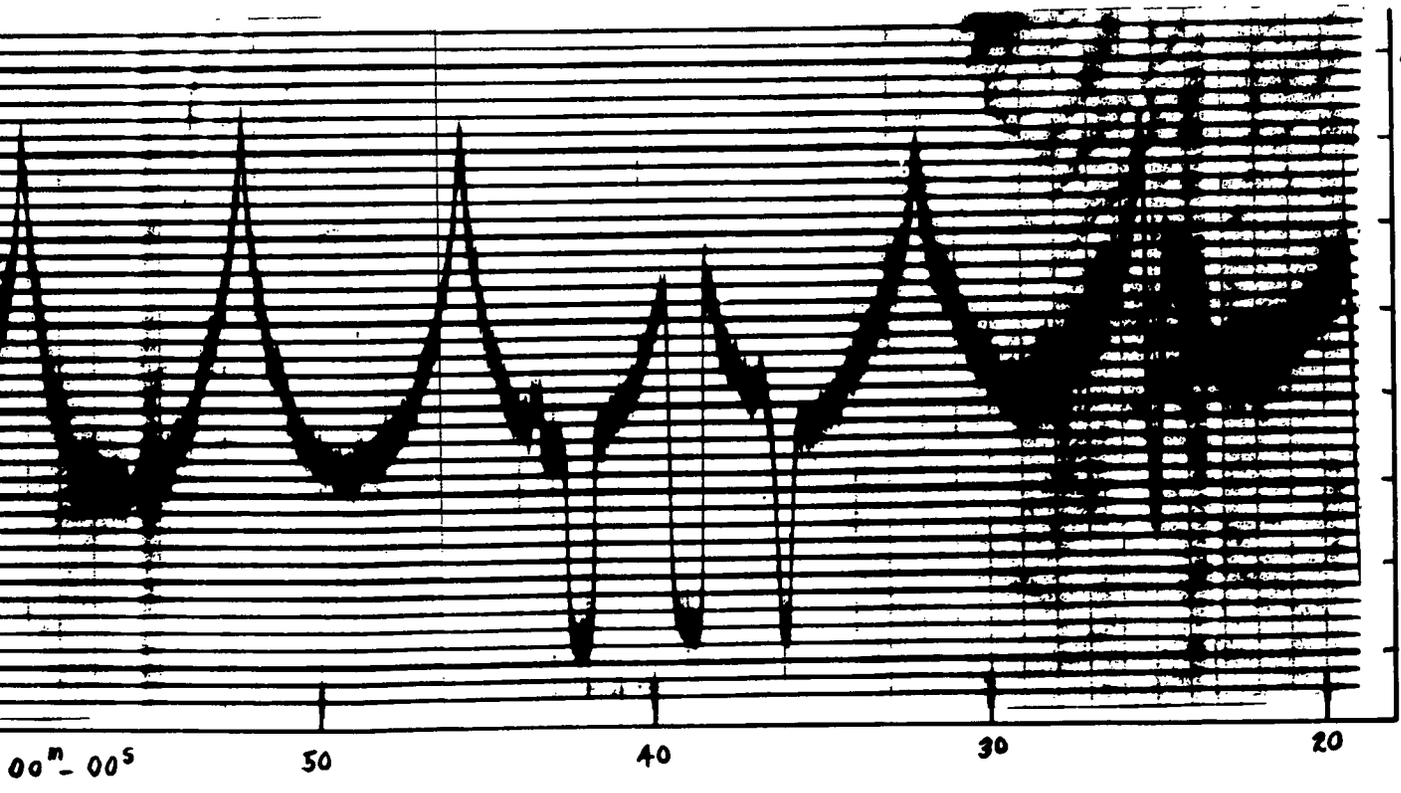

3

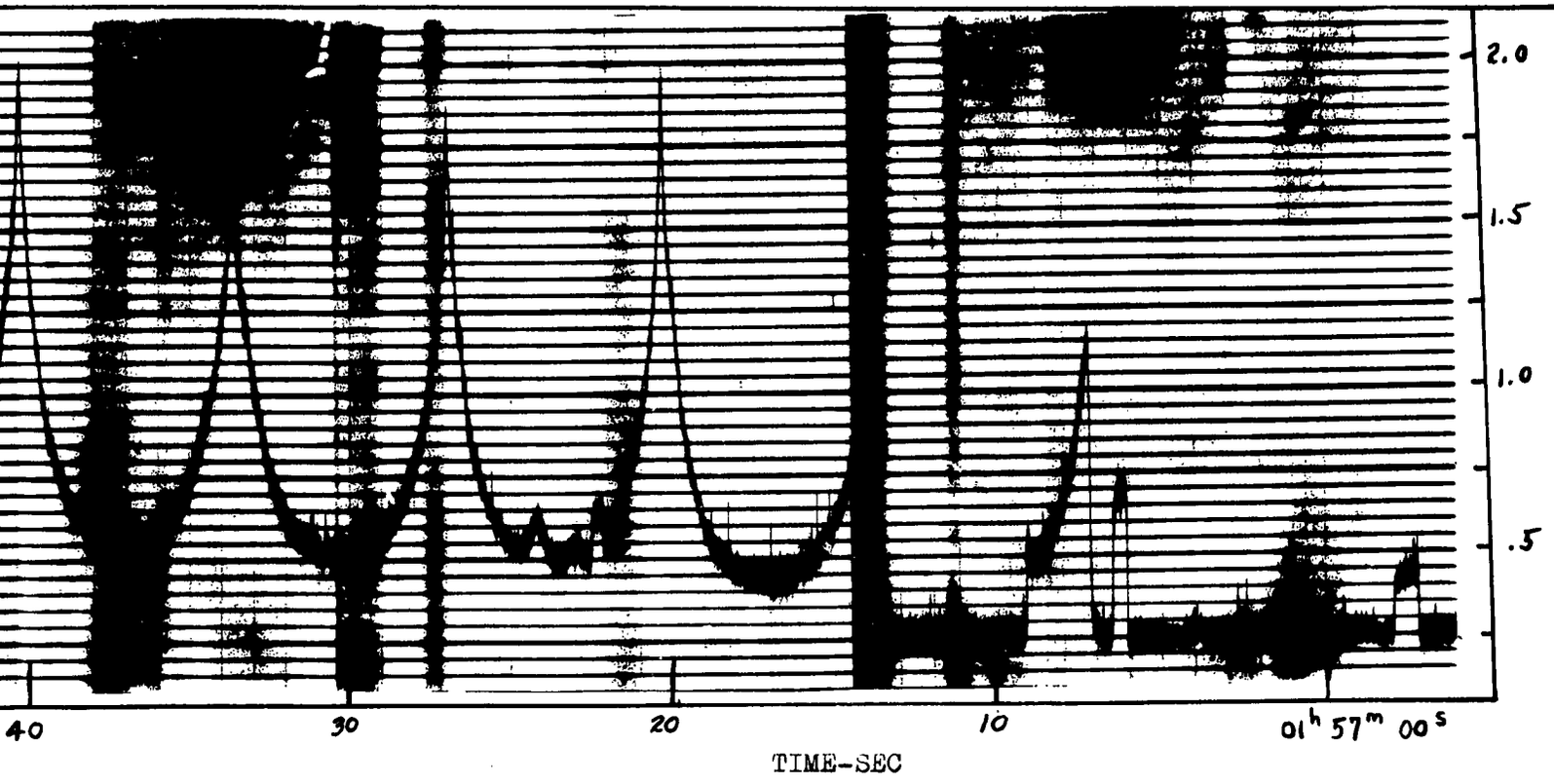

TIME-SEC

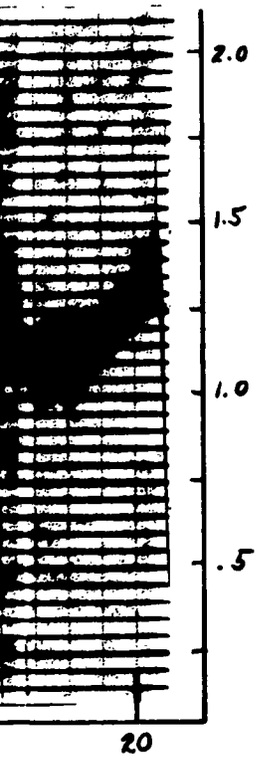

VOLTAGE

TRACK 15 APRIL 63

Satellite 62 BETA ALPHA 2 (62492)

Revolution 2701 Day 105

Time 01hr - 56min - 56sec

4

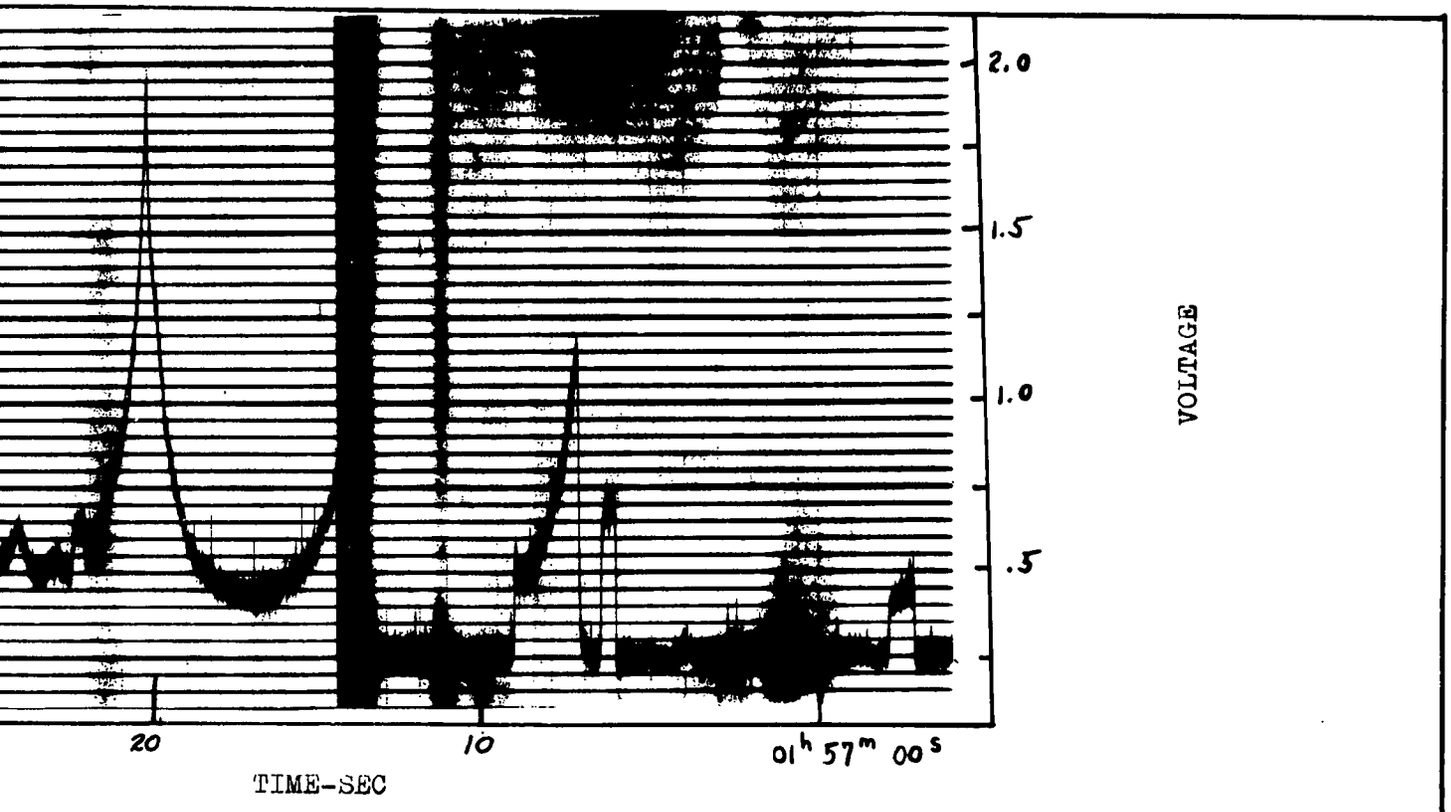

TRACK 15 APRIL 63

Satellite 62 BETA ALPHA 2 (62492)

Revolution 2701 Day 105

Time 01hr - 56min - 56sec

5

Table XI

Tracking Data, Satellite 62 Beta Alpha 2

Revolution 3537

DAYTON OHIO SGWA 241 62B-ALPHA2 SAT. NO. 426 ELEM 9

COMPUTATIONS STARTED AT REVOLUTION NO. 3484 VISUAL PASSES

REV NO.	ZEBRA TIME DAY	HR	MIN.	ELEV ANG.	AZIM ANG.	RANGE KM.	RATE KM/SEC	R.A. DEG.	DEC DEG	SUNS ELEV	ILLUMI NATION
3537	166	7	1.95	56.6	246.4	1164	-2.0	251.404	21.503	-23.9	2.6
3537	166	7	2.95	62.1	289.0	1113	.3	247.157	43.122	-23.8	6.1
3537	166	7	3.95	53.6	326.4	1203	2.5	237.390	63.584	-23.8	9.5
3537	166	7	4.95	41.3	344.0	1408	4.1	206.940	77.811	-23.7	12.9
3537	166	7	5.95	30.8	352.6	1685	5.0	140.920	79.204	-23.6	16.3
3537	166	7	6.95	22.7	357.7	2004	5.5	112.625	72.743	-23.5	19.8
3537	166	7	7.95	16.3	.9	2346	5.8	103.318	66.427	-23.5	23.2
3537	166	7	8.95	11.0	3.3	2703	6.0	99.134	61.065	-23.4	26.6
3537	166	7	9.95	6.6	5.1	3067	6.1	96.887	56.490	-23.3	30.1

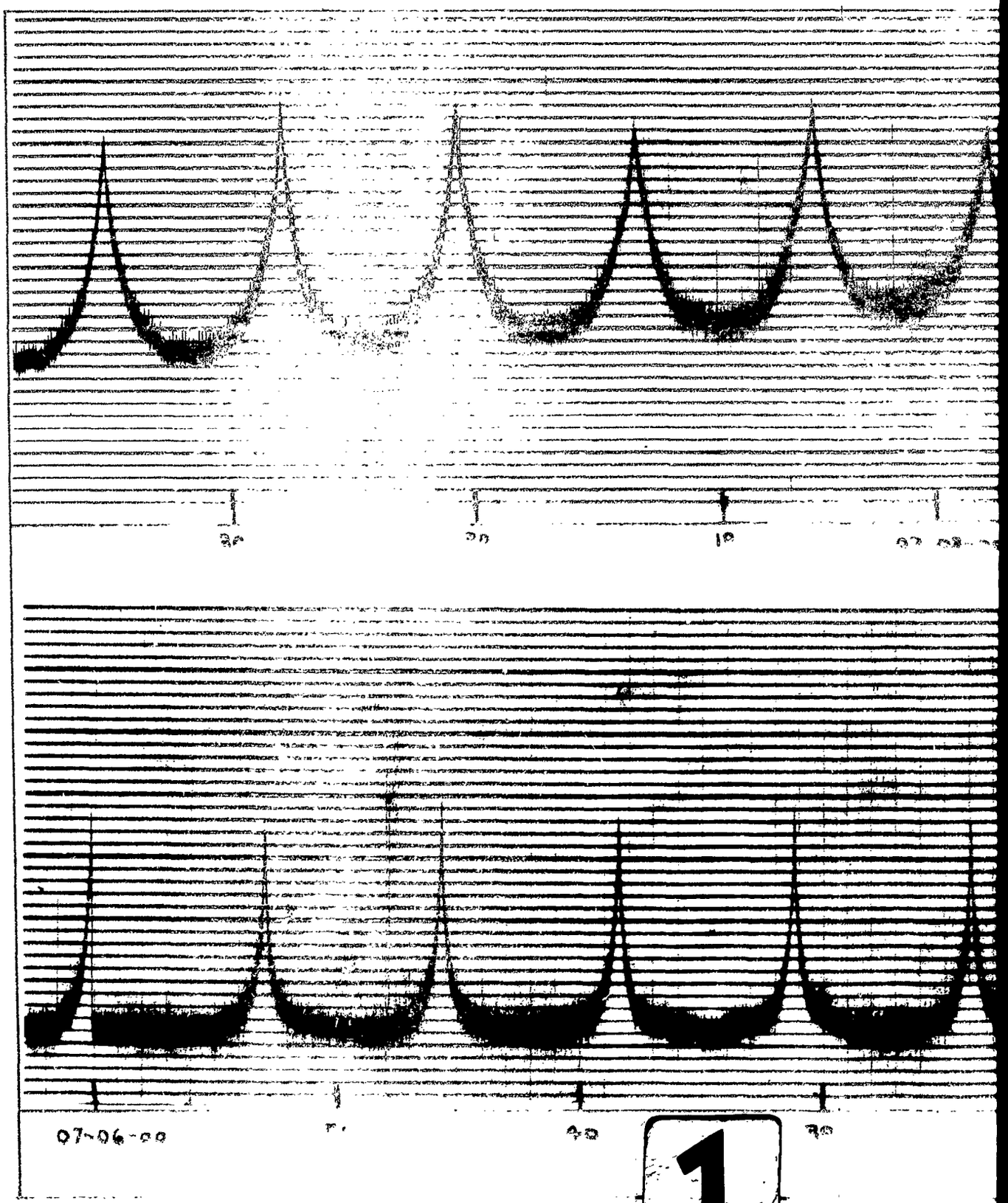

1

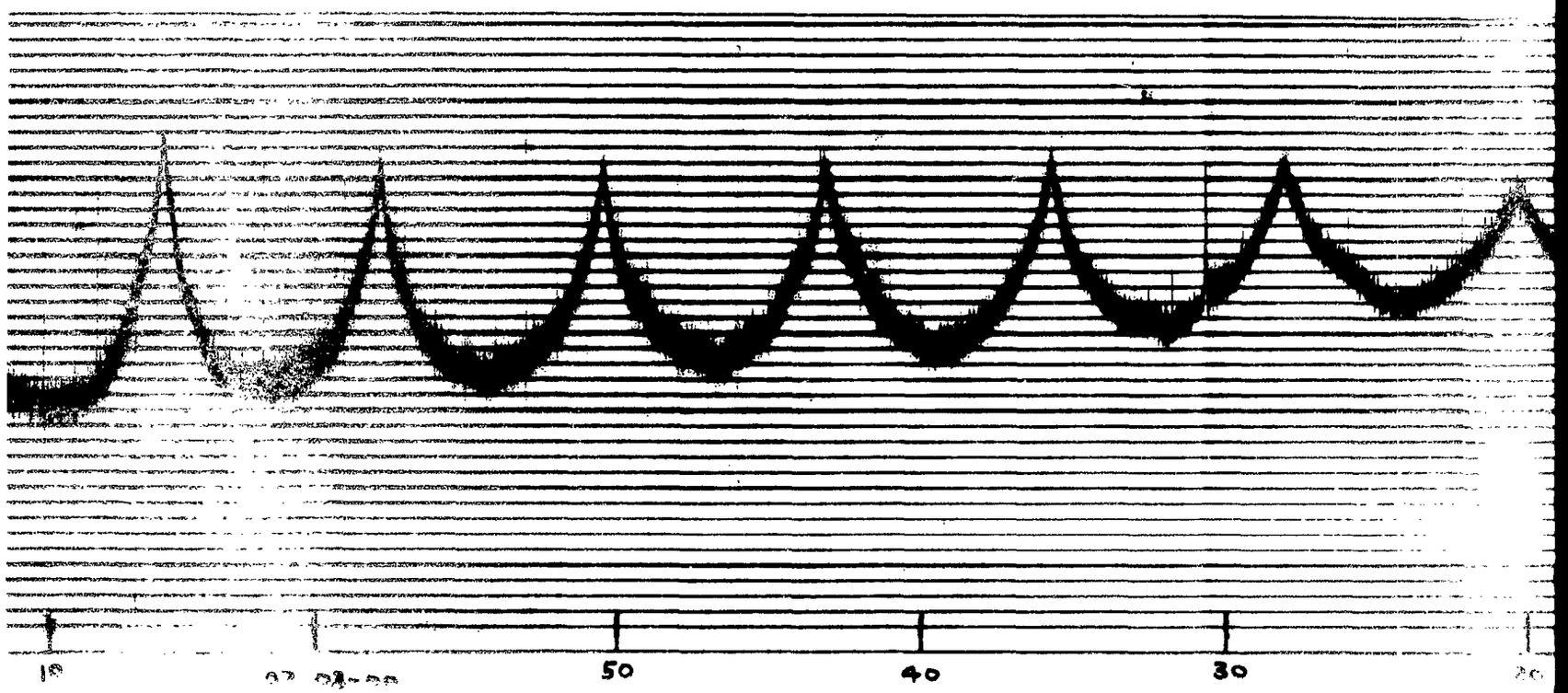

TIME - SEC

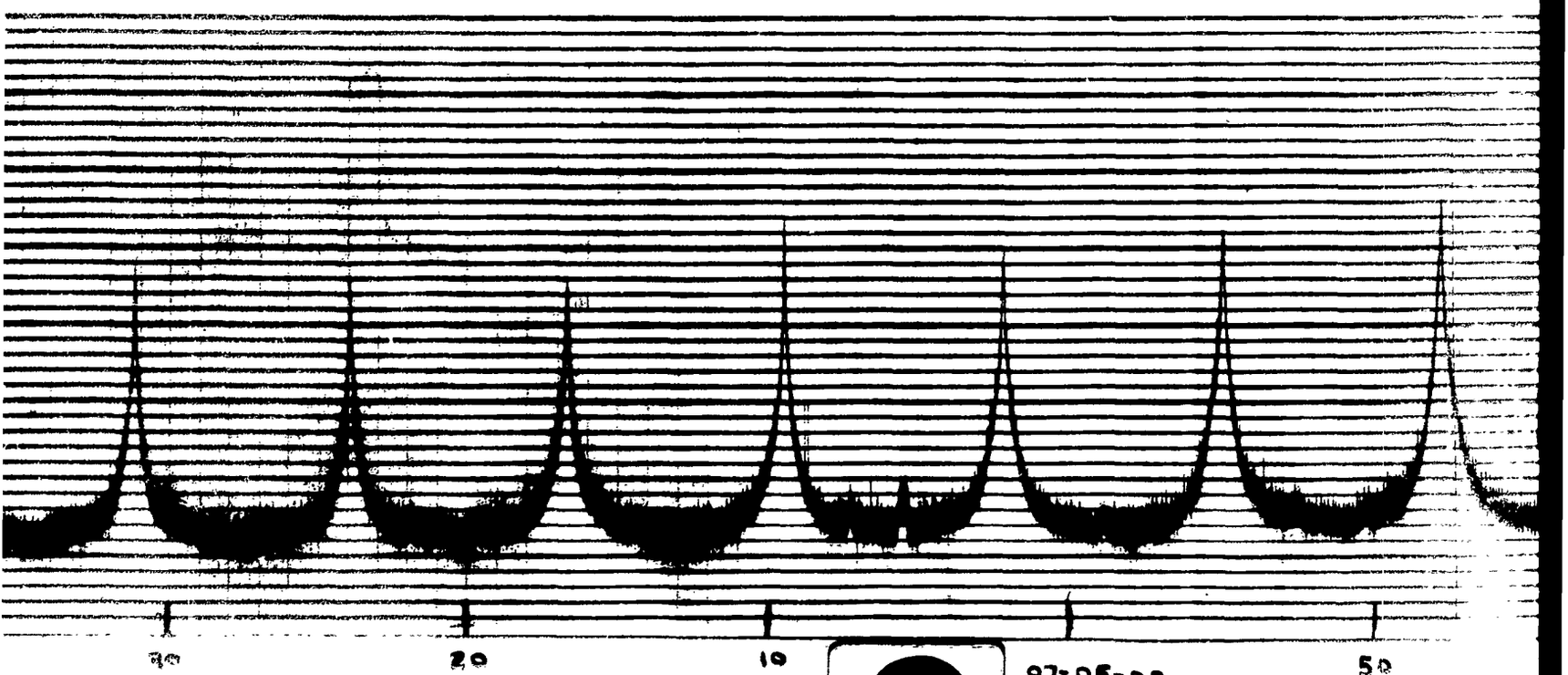

2

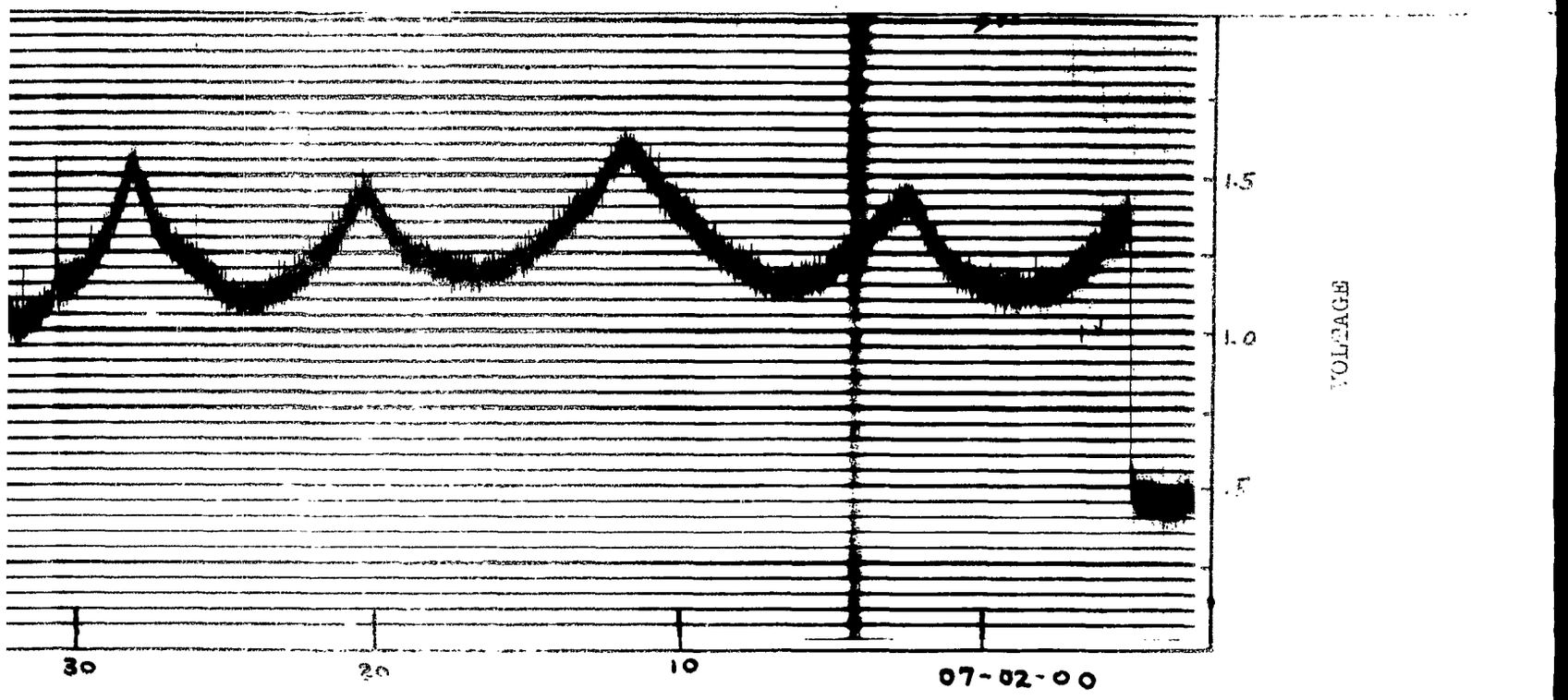
1.5
1.0
.5
VOLTAGE
30
20
10
07-02-00

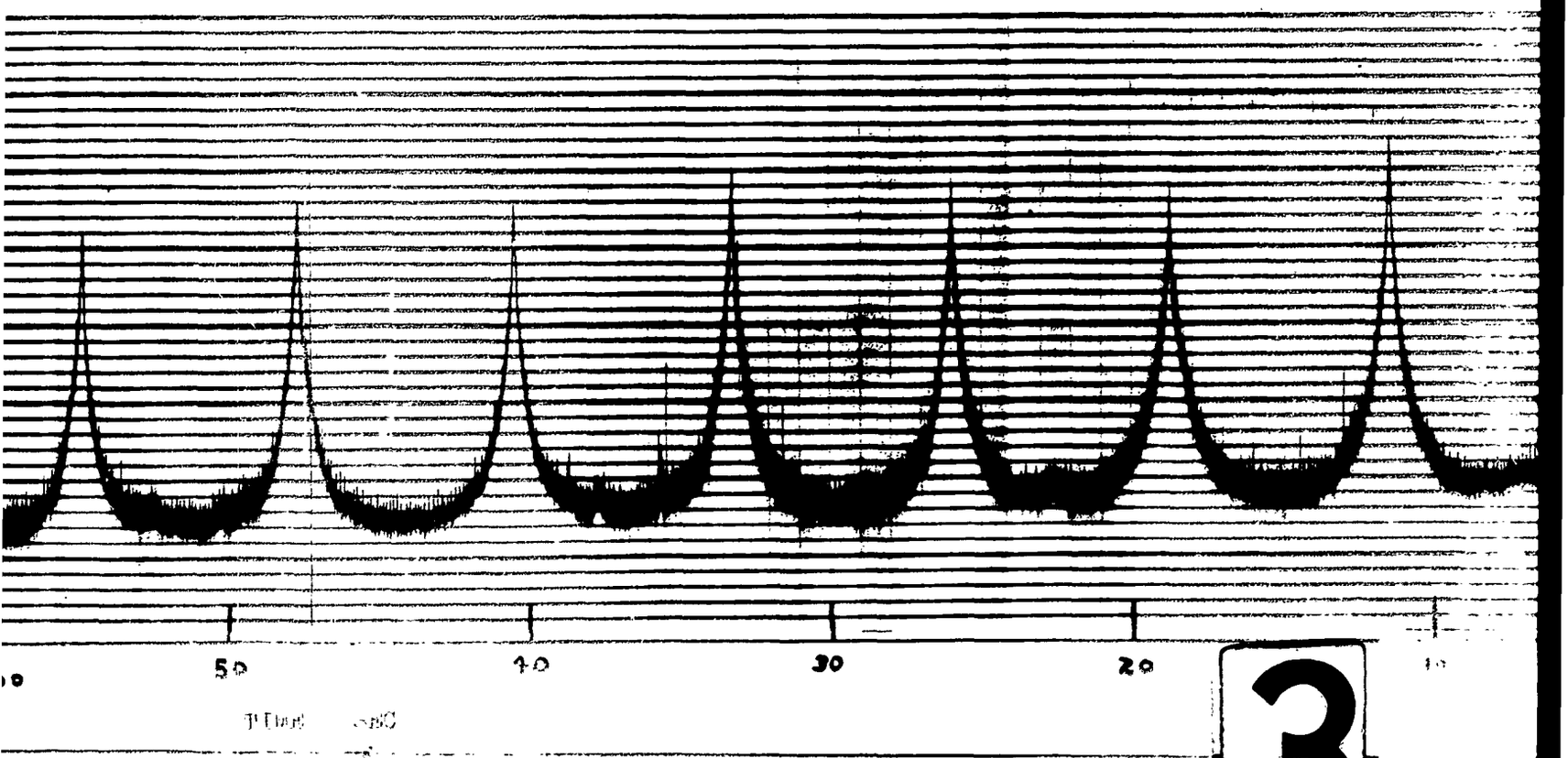
50
40
30
20
3

[illegible] June 63

[illegible] 62 BETA ALPHA 2

[illegible] Rocket Body

[illegible] 3537

[illegible] 01min - 58sec

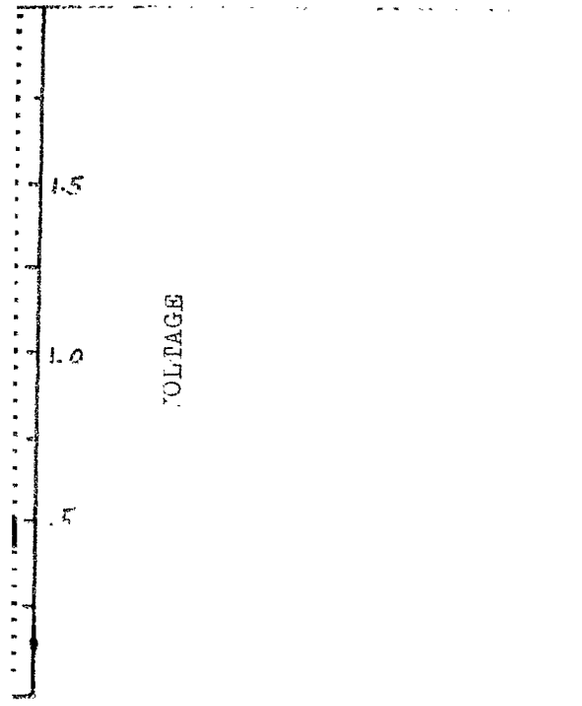

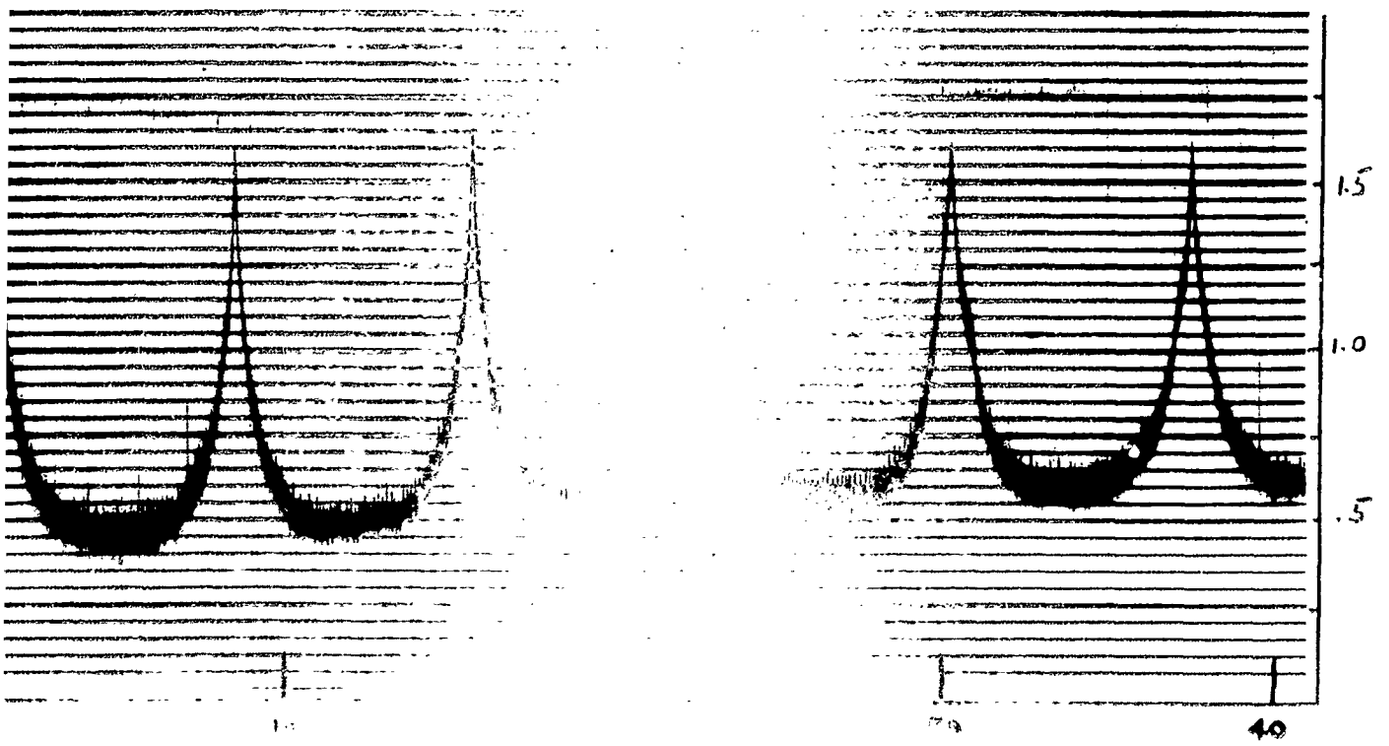

4

Table XII
Orbital and Tracking Data
Satellite 63-10B

Source	Launch	Nodal Period	Inclination	Apogee Km	Perigee Km
USSR	13 Apr	90.9	48.92	408	241

REV NO.	ZEBRA TIME DAY	HR	MIN.	ELEV ANG.	AZIM ANG.	RANGE KM.	SUNS ELEV	ILLUMI NATION
312	123	8	21.84	47.8	344.5	613	-22.2	.4
312	123	8	22.84	33.3	29.7	733	-22.1	3.9
312	123	8	23.84	20.1	41.7	1395	-22.3	7.4
312	123	8	24.84	11.8	47.3	1461	-21.8	10.9
312	123	8	25.84	6.3	1.1	1348	-21.7	14.4
312	123	8	26.84	1.1	54.6	2244	-21.5	17.9

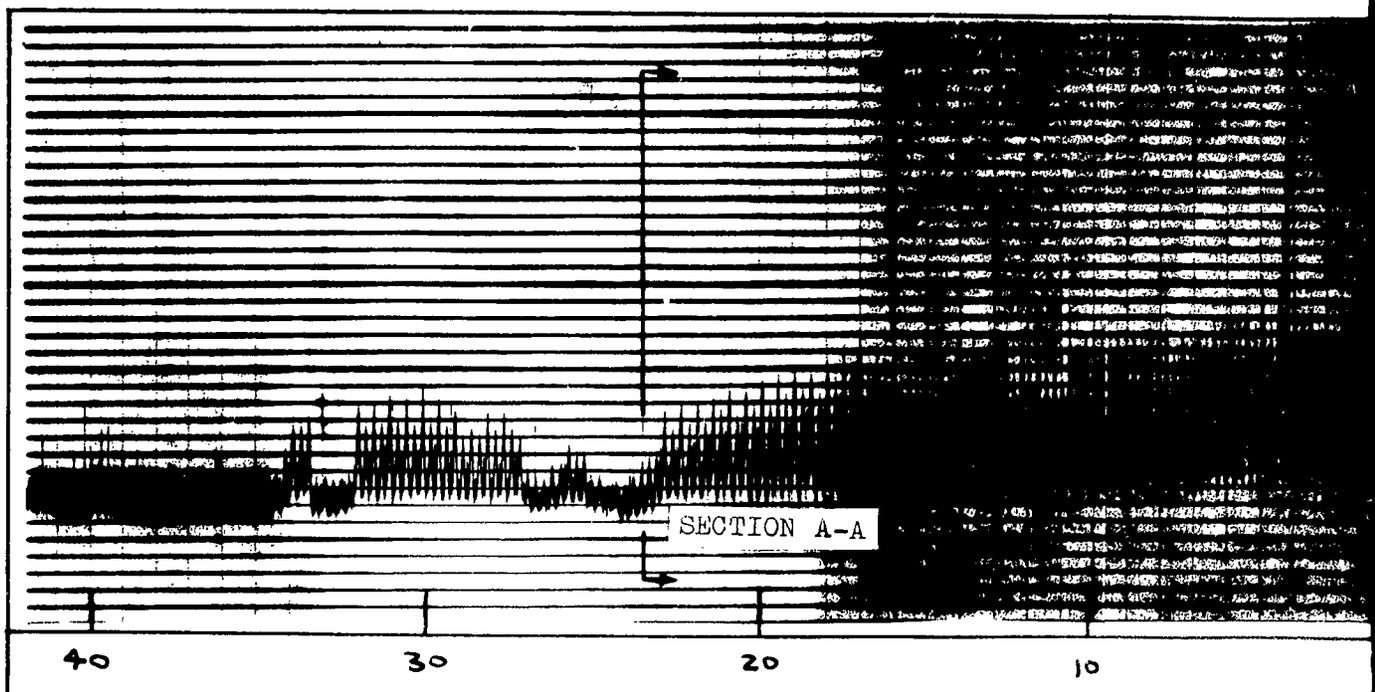

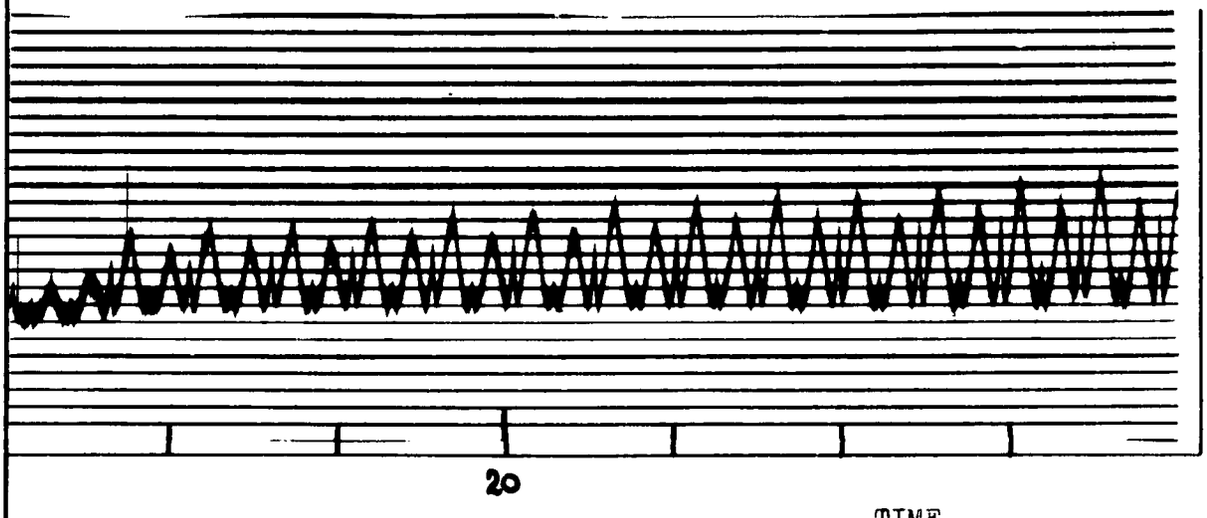

SECTION A-A EXPANDED

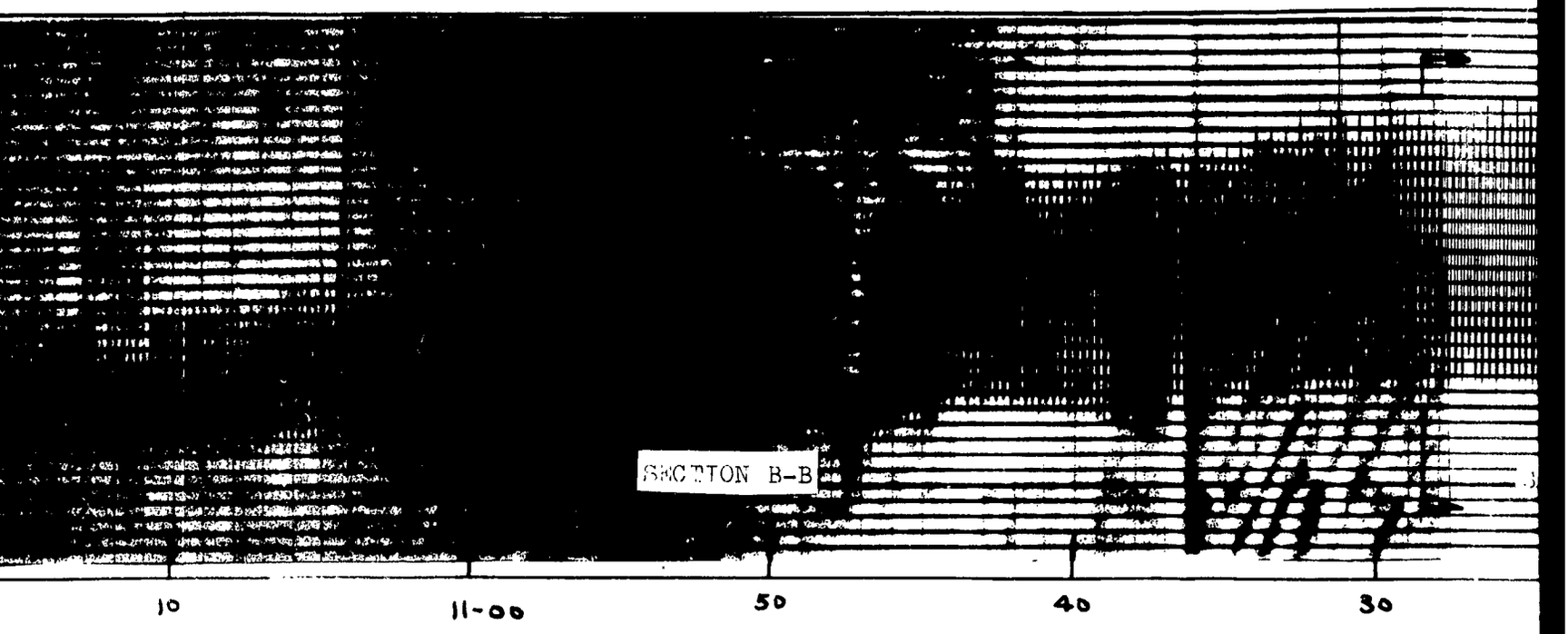

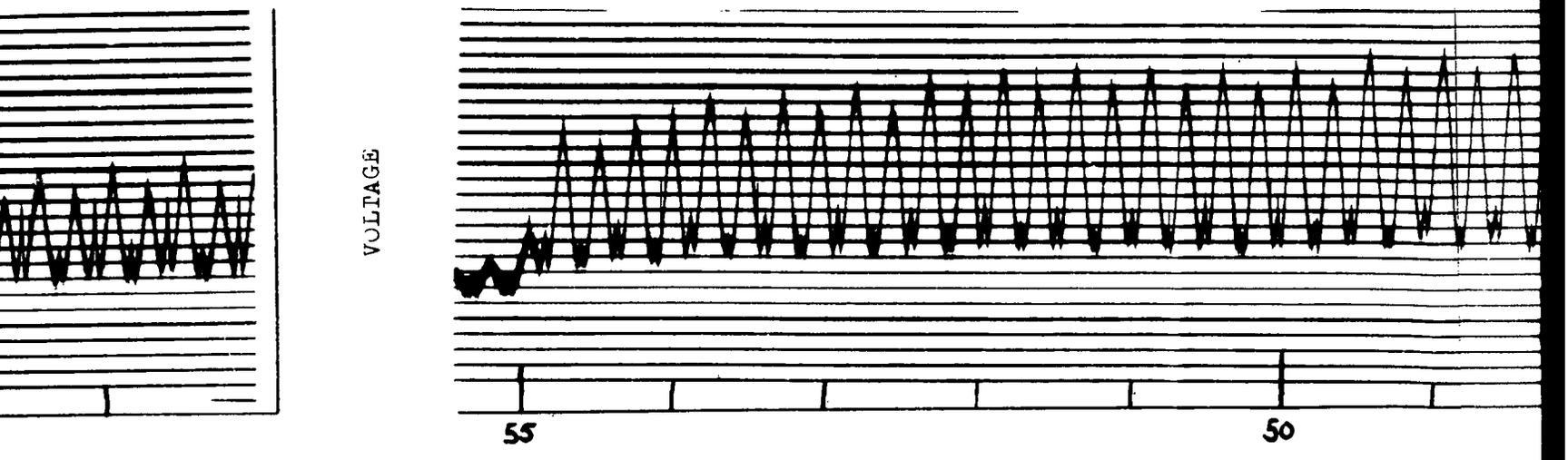

SECTION B-B EXPANDED

2

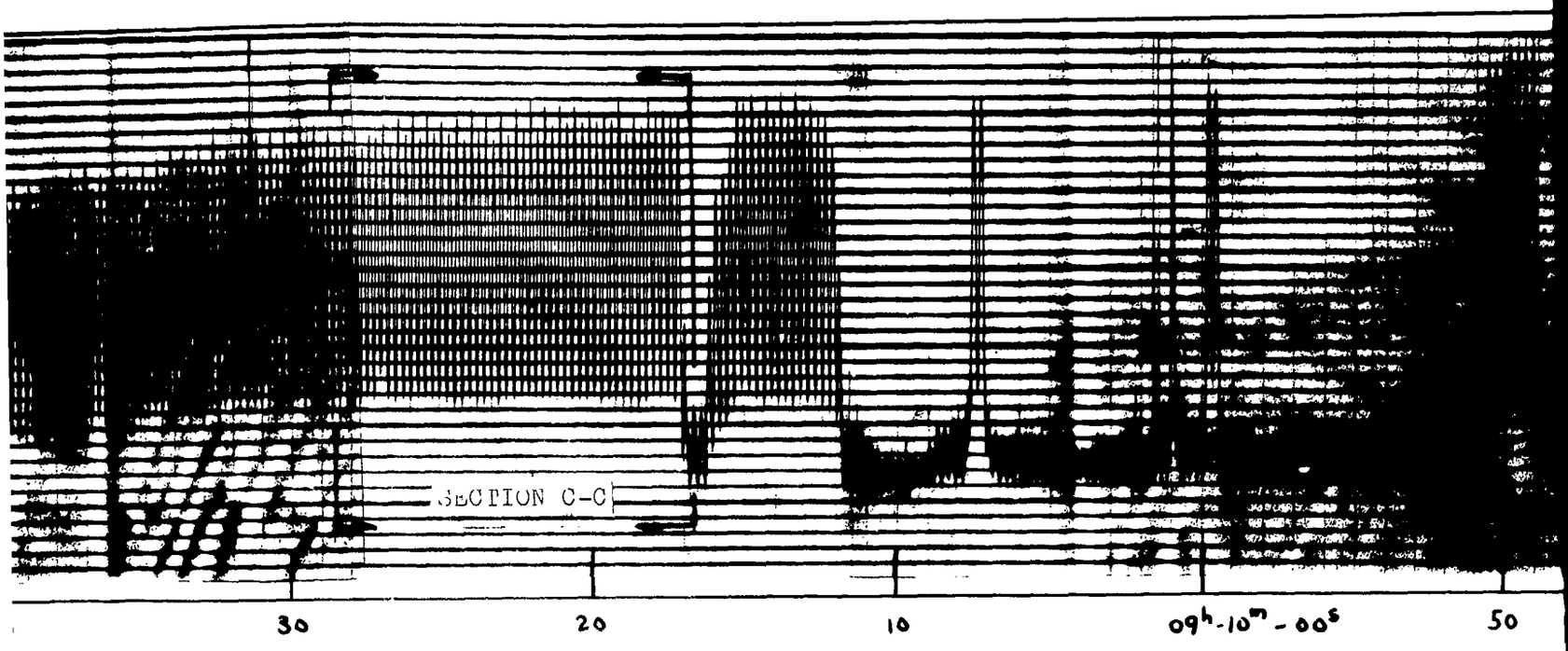

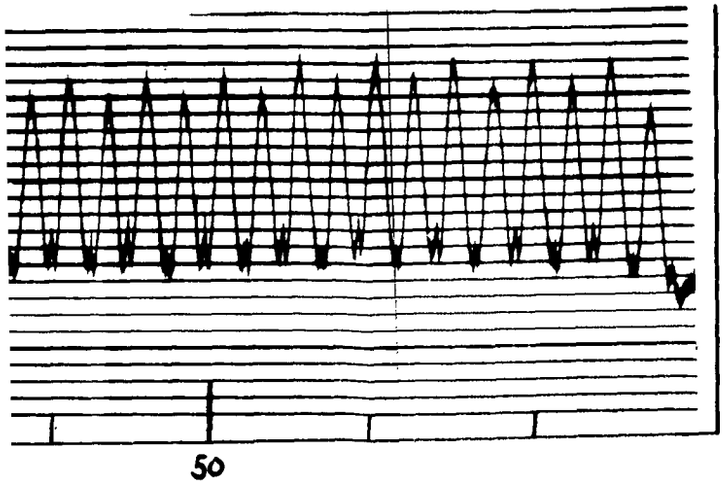

TIME

VOLTAGE

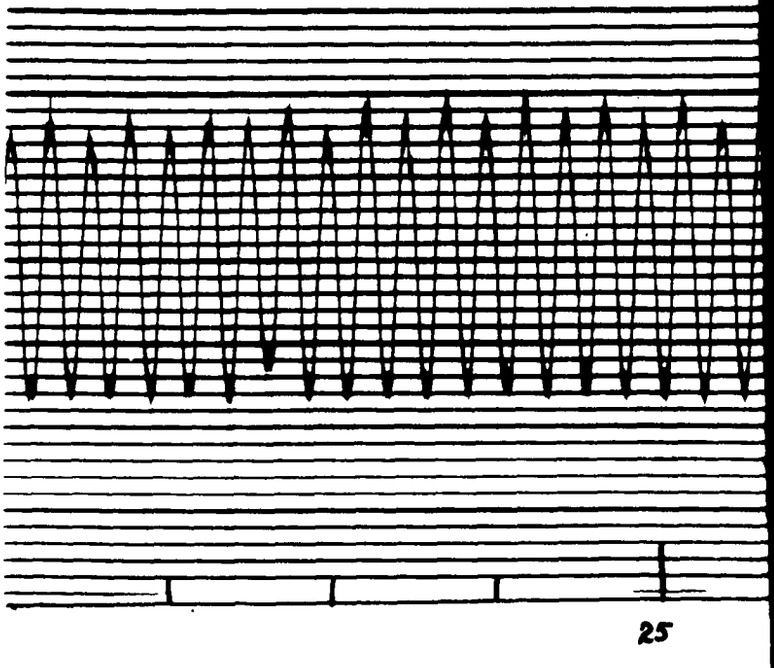

-B EXPANDED

3

TRACK 28 Apr

Satellite 63

Russian Rock

Time 09hr -0

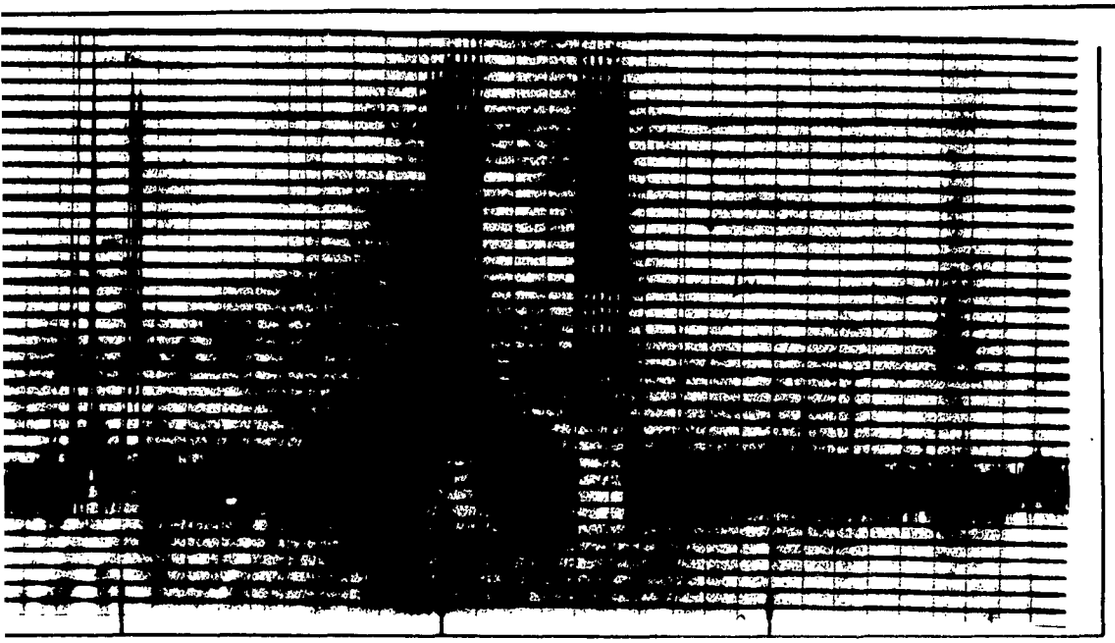

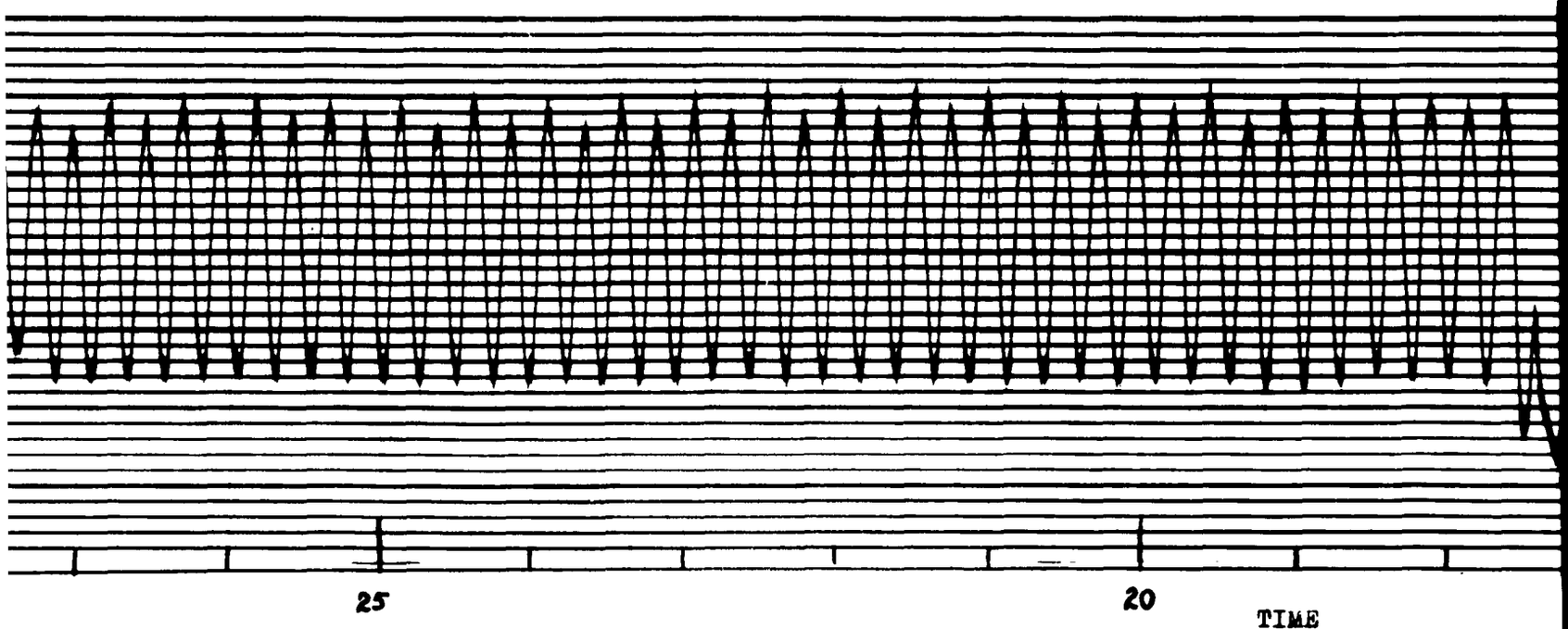

SECTION C-C EXPANDED

4

TRACK 28 April 63

Satellite 63-10B

Russian Rocket Body

Time 09hr -09min - 32sec

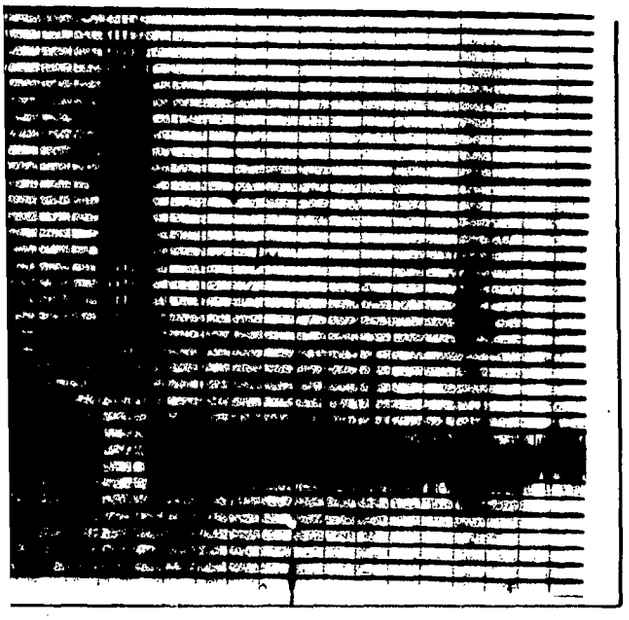

VOLTAGE

40

TIME

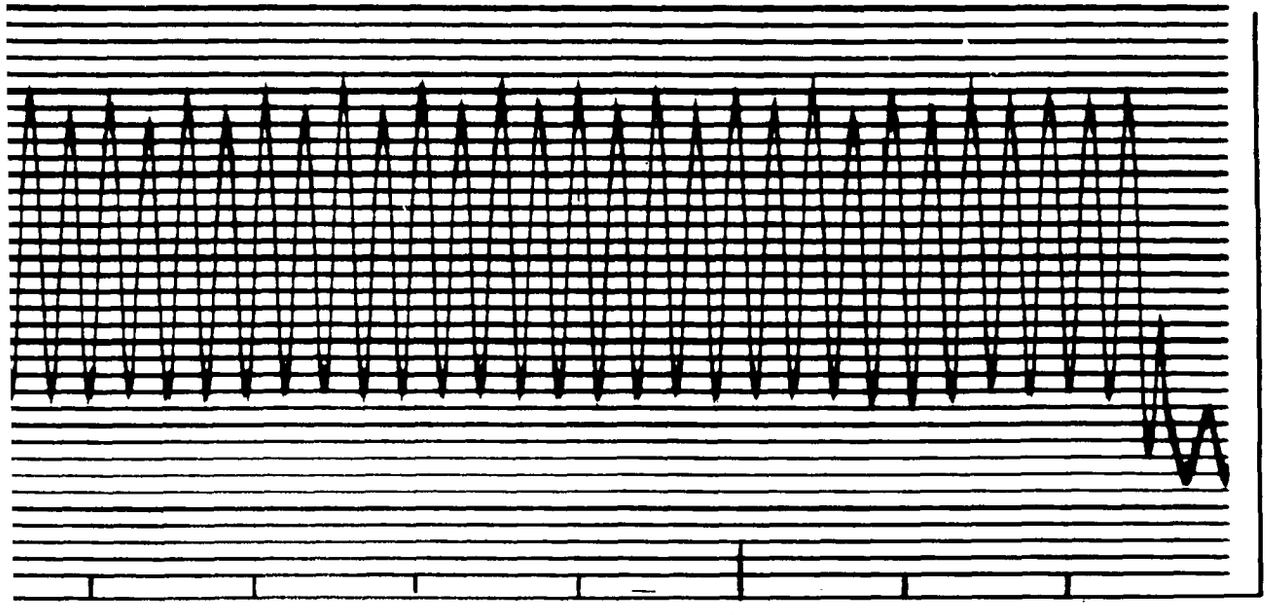

VOLTAGE

20

TIME

SECTION C-C EXPANDED

5

GA/Phys/63-13

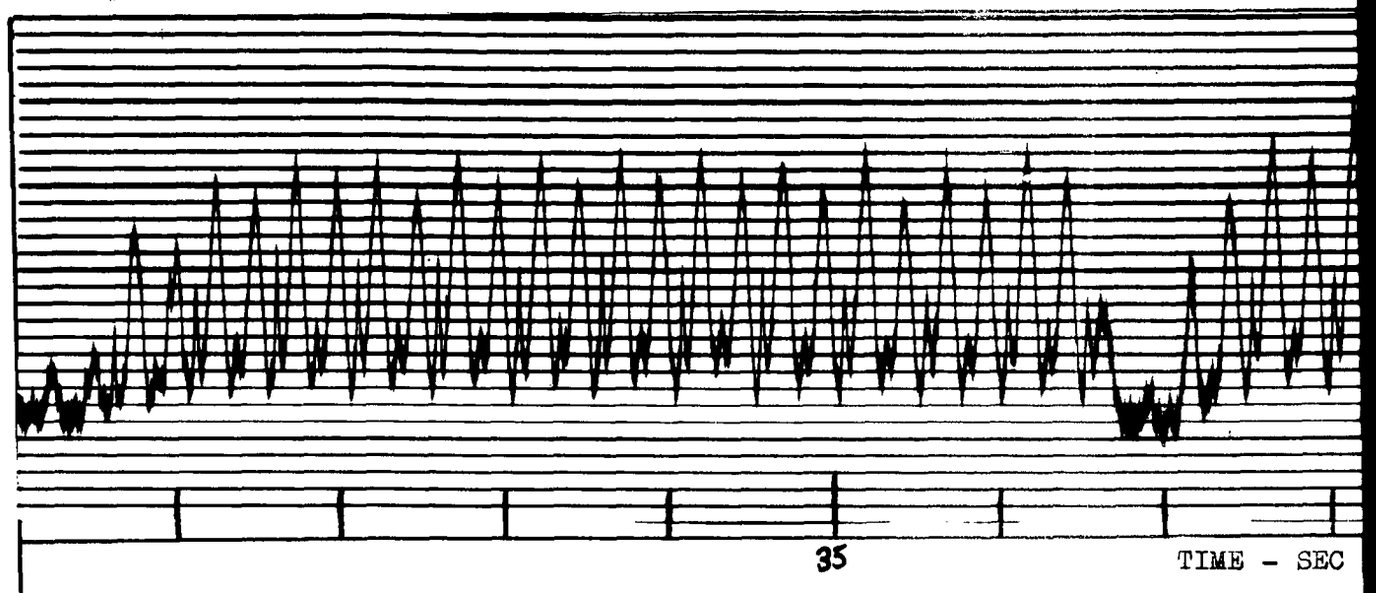

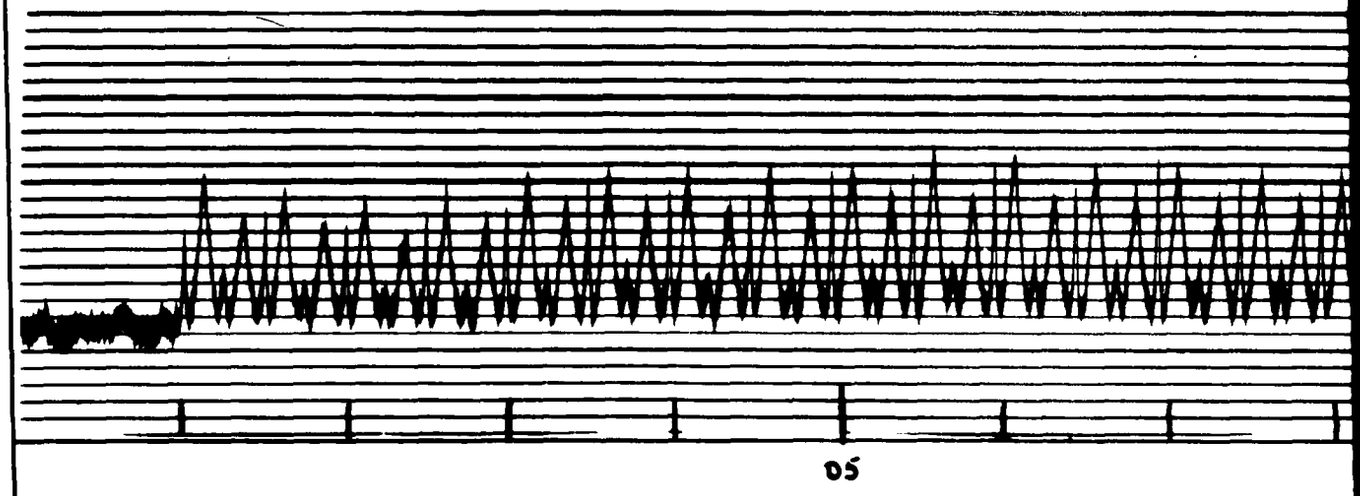

1

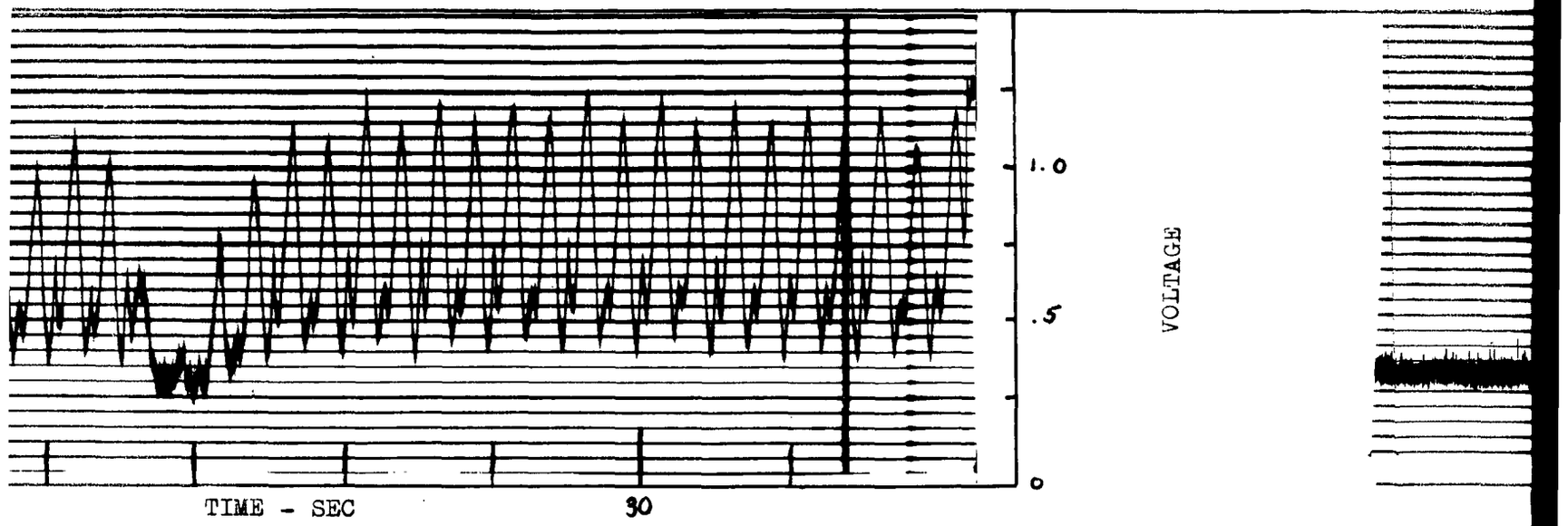

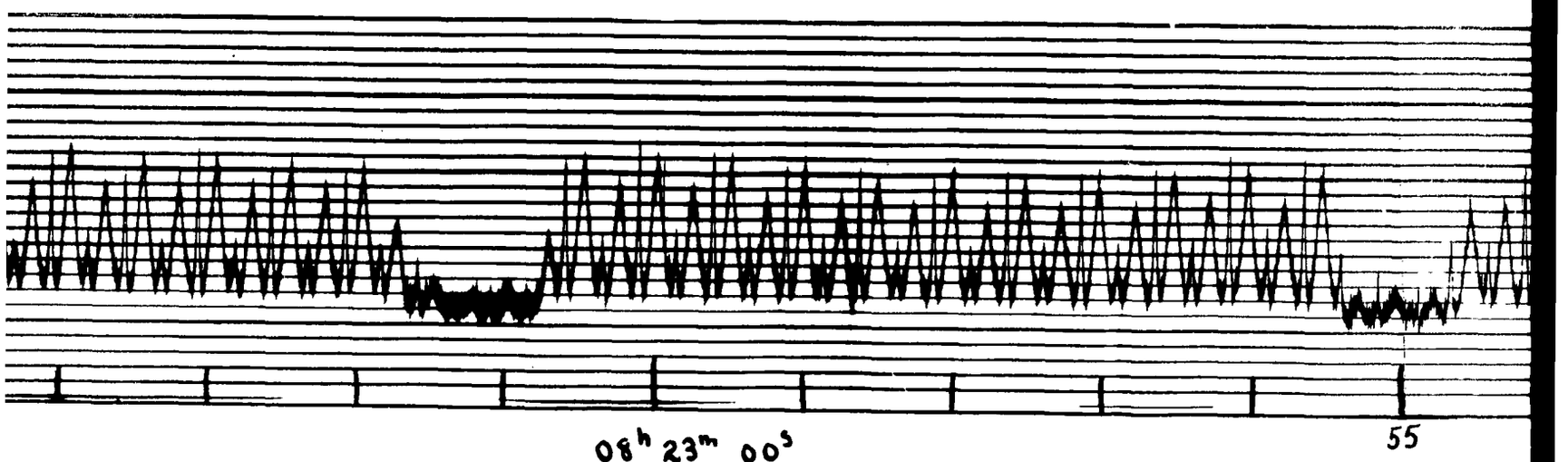

TRACK 3 May 63

Satellite 63 - 10B

Russian Rocket Body

Revolution 312

Time 08hr - 22min - 28sec

2

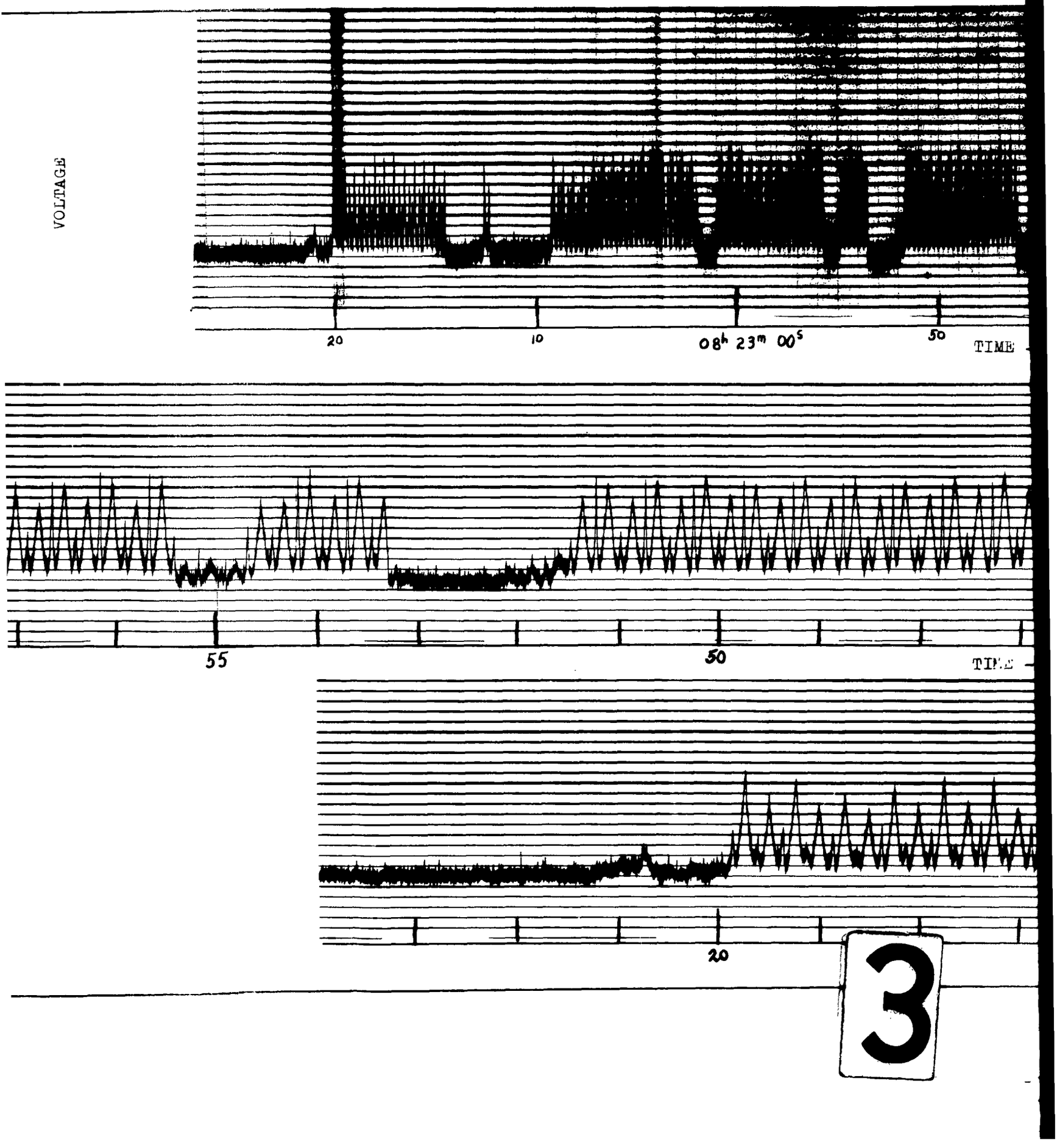

3

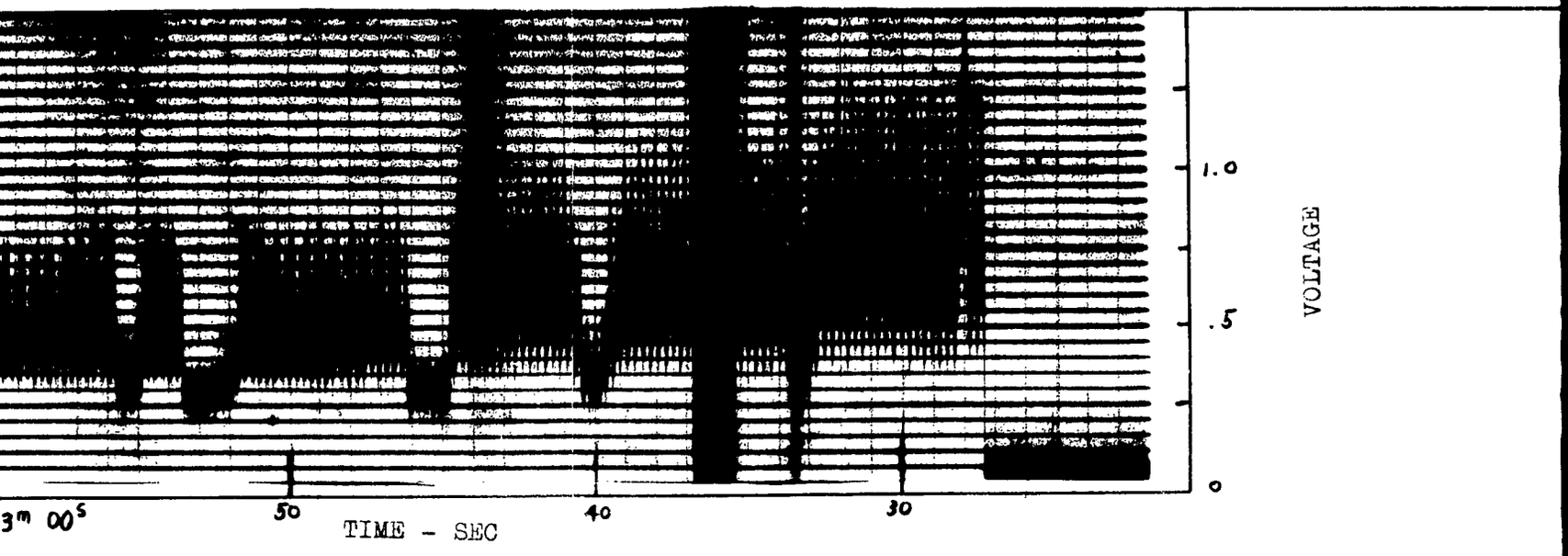
1.0
.5
0
VOLTAGE
3m 00s
50
40
30
TIME - SEC

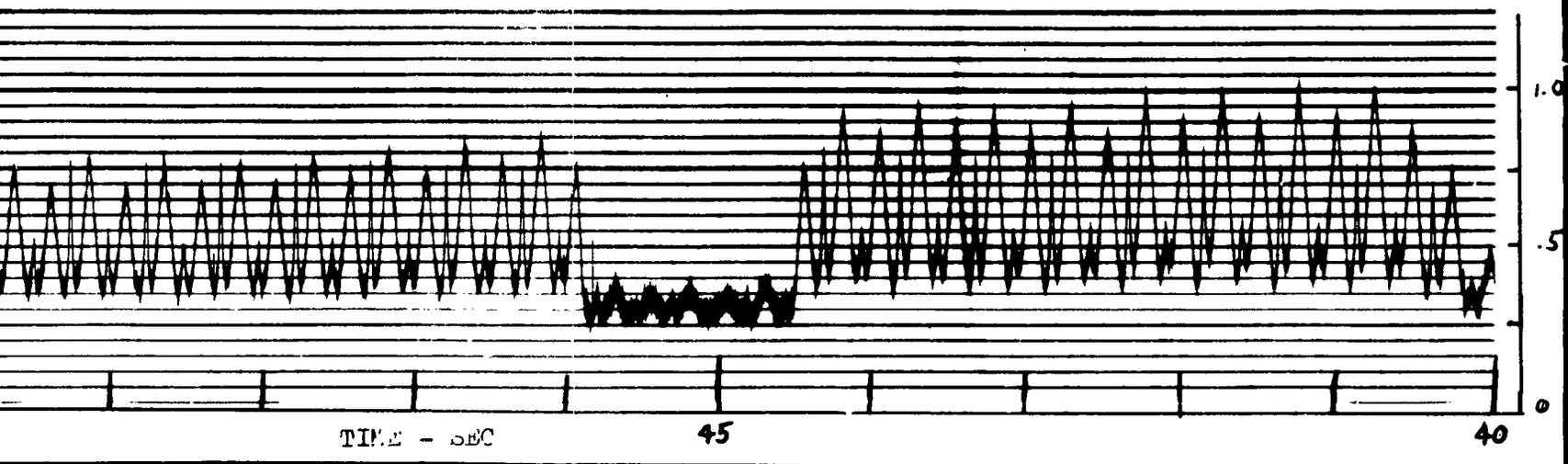
1.0
.5
0
TIME - SEC
45
40

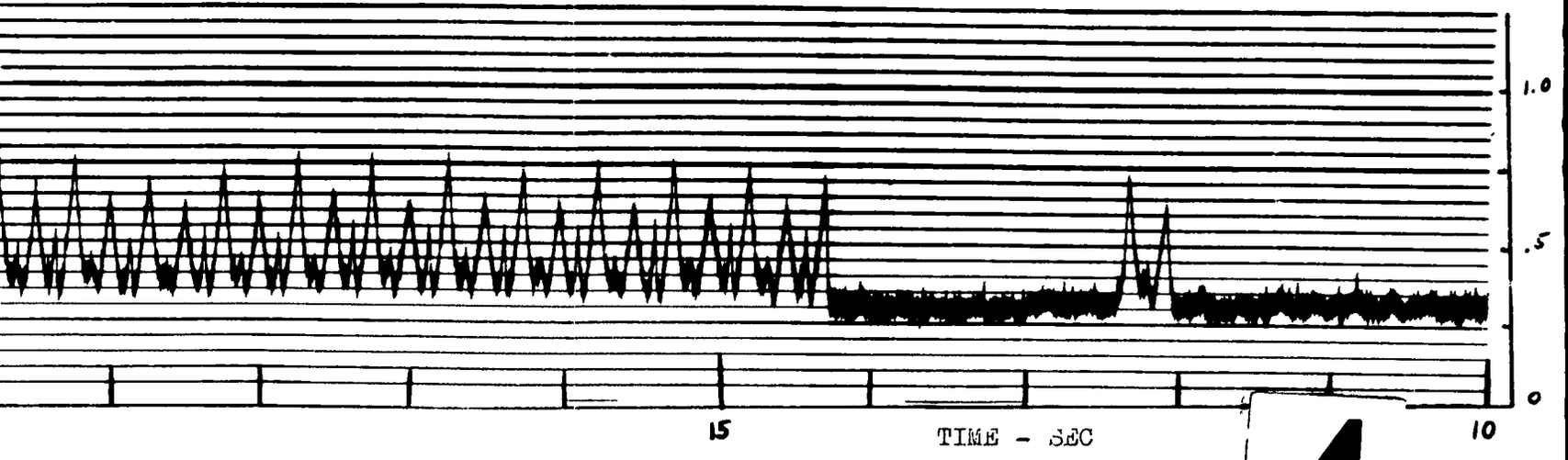
1.0
.5
0
15
TIME - SEC
10

4

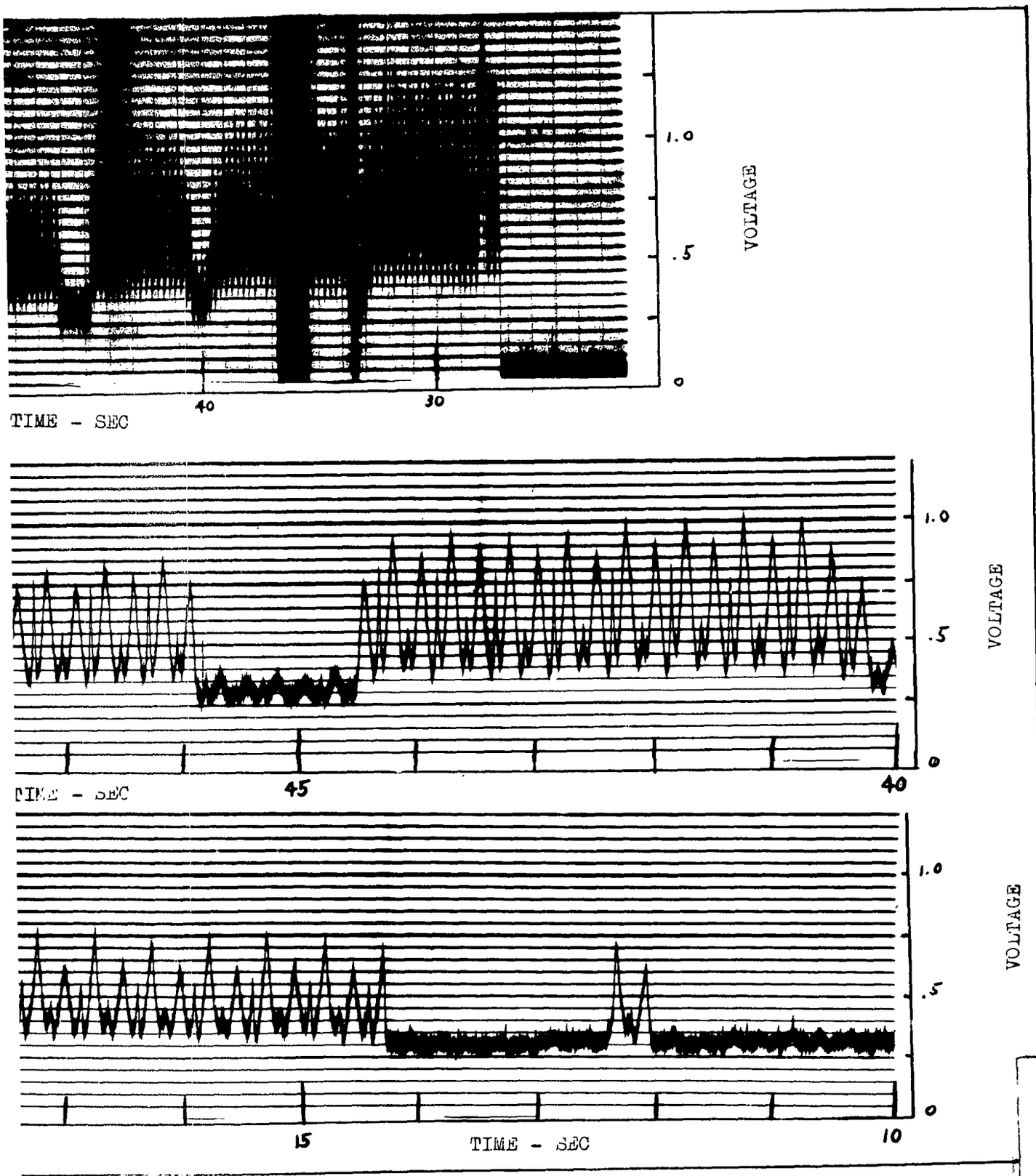
1.0
.5
0
VOLTAGE
40
30
TIME - SEC
1.0
.5
0
VOLTAGE
45
40
TIME - SEC
1.0
.5
0
VOLTAGE
15
TIME - SEC
10

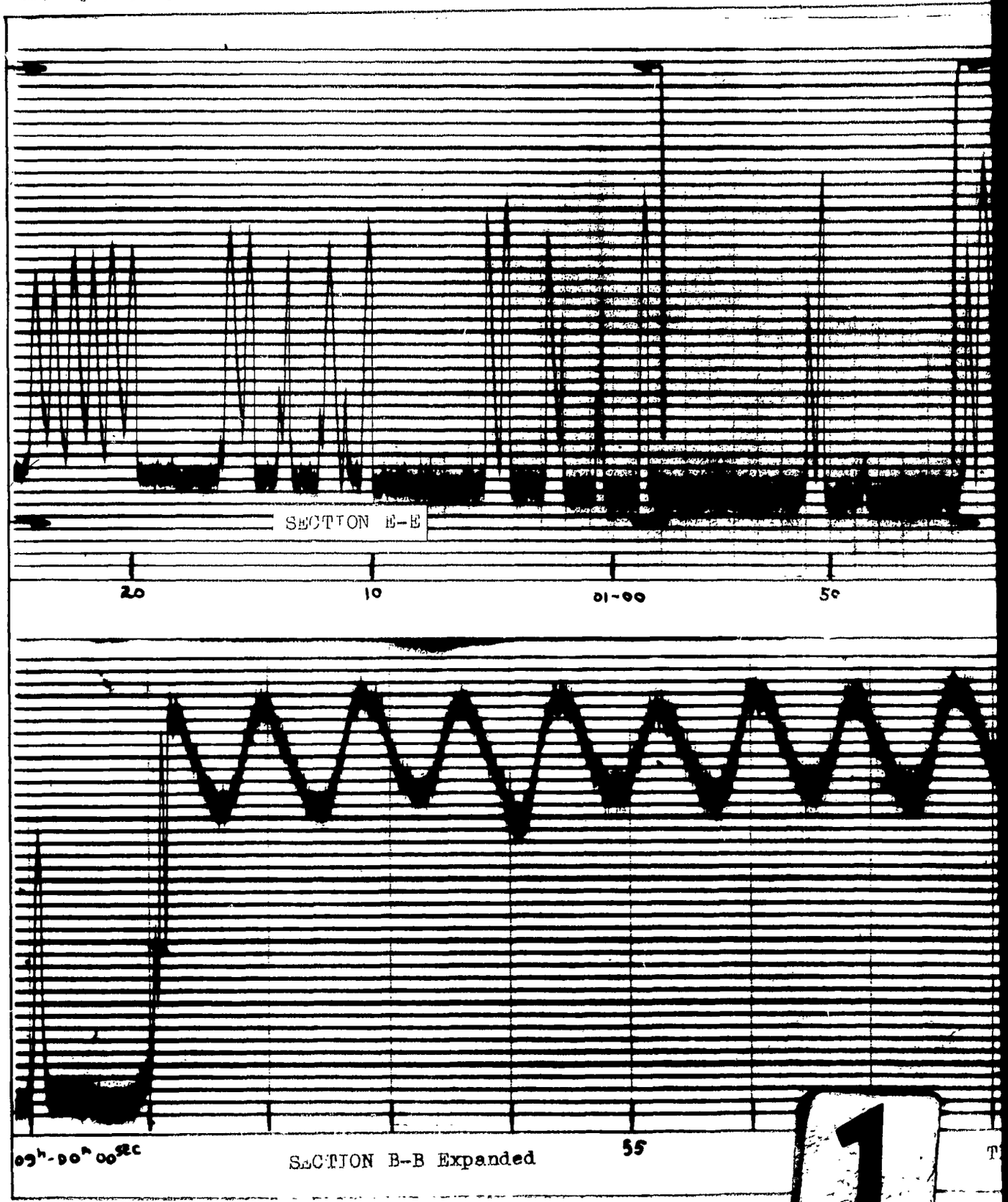
SECTION E-E
20
10
01-00
50
09h-00h 00sec
SECTION B-B Expanded
55
1

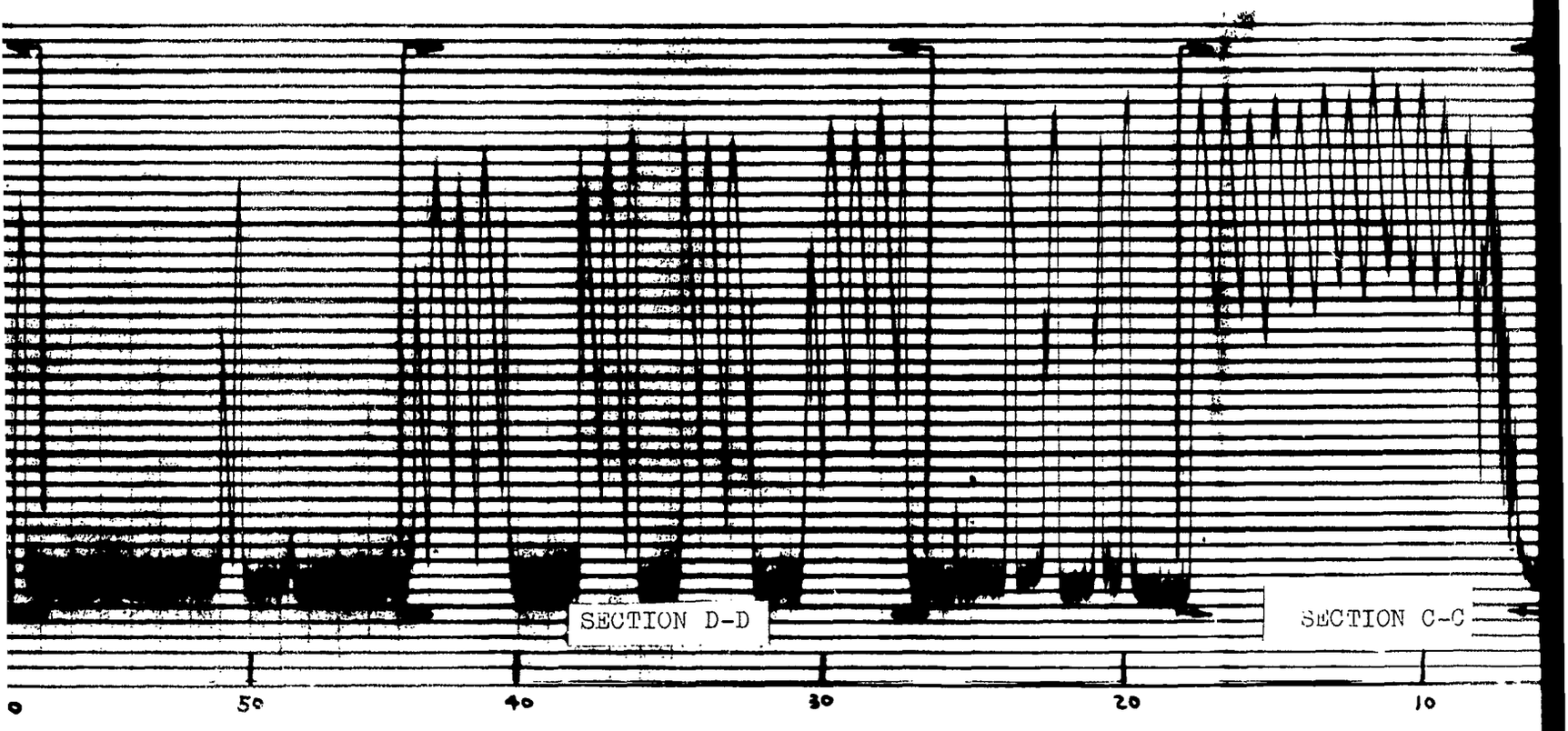
SECTION D-D
SECTION C-C
50
40
30
20
10

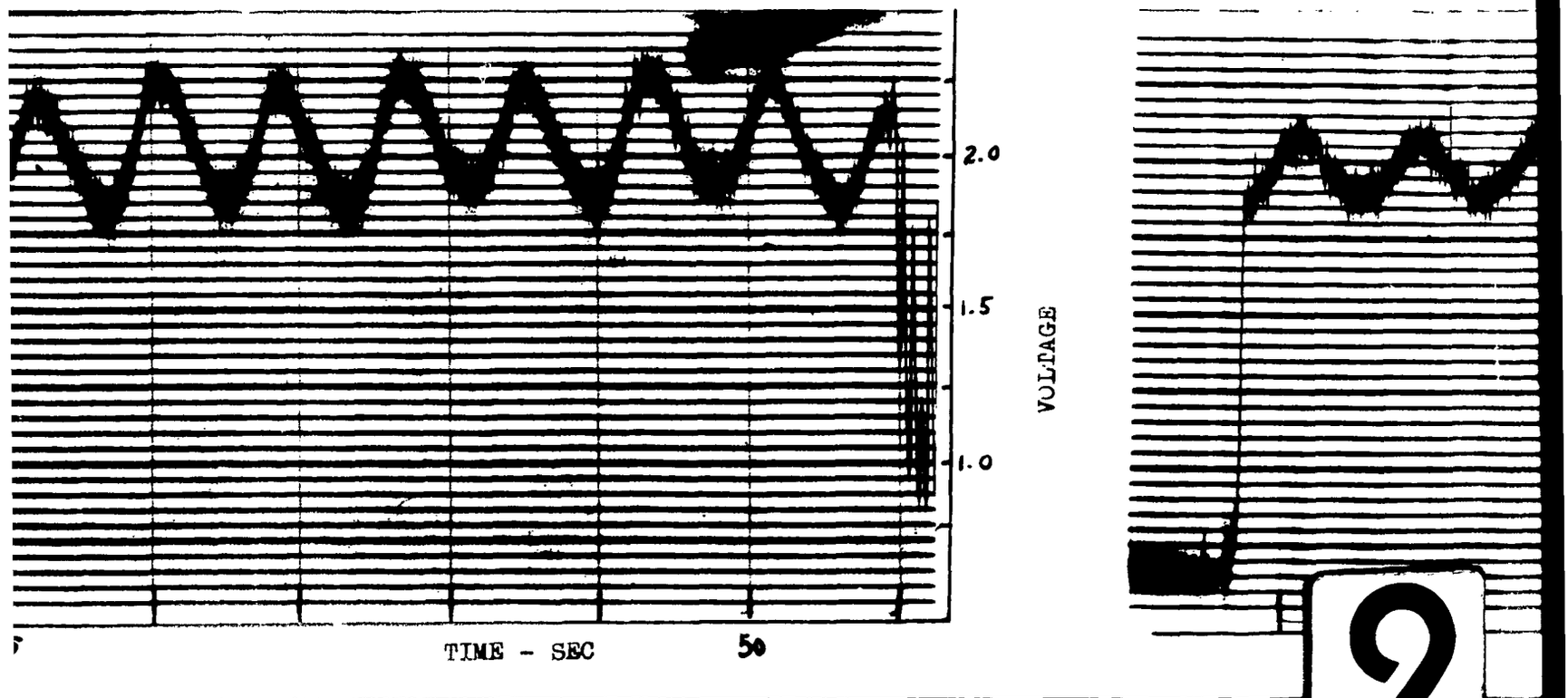
2.0
1.5
1.0
VOLTAGE
TIME - SEC
50

2

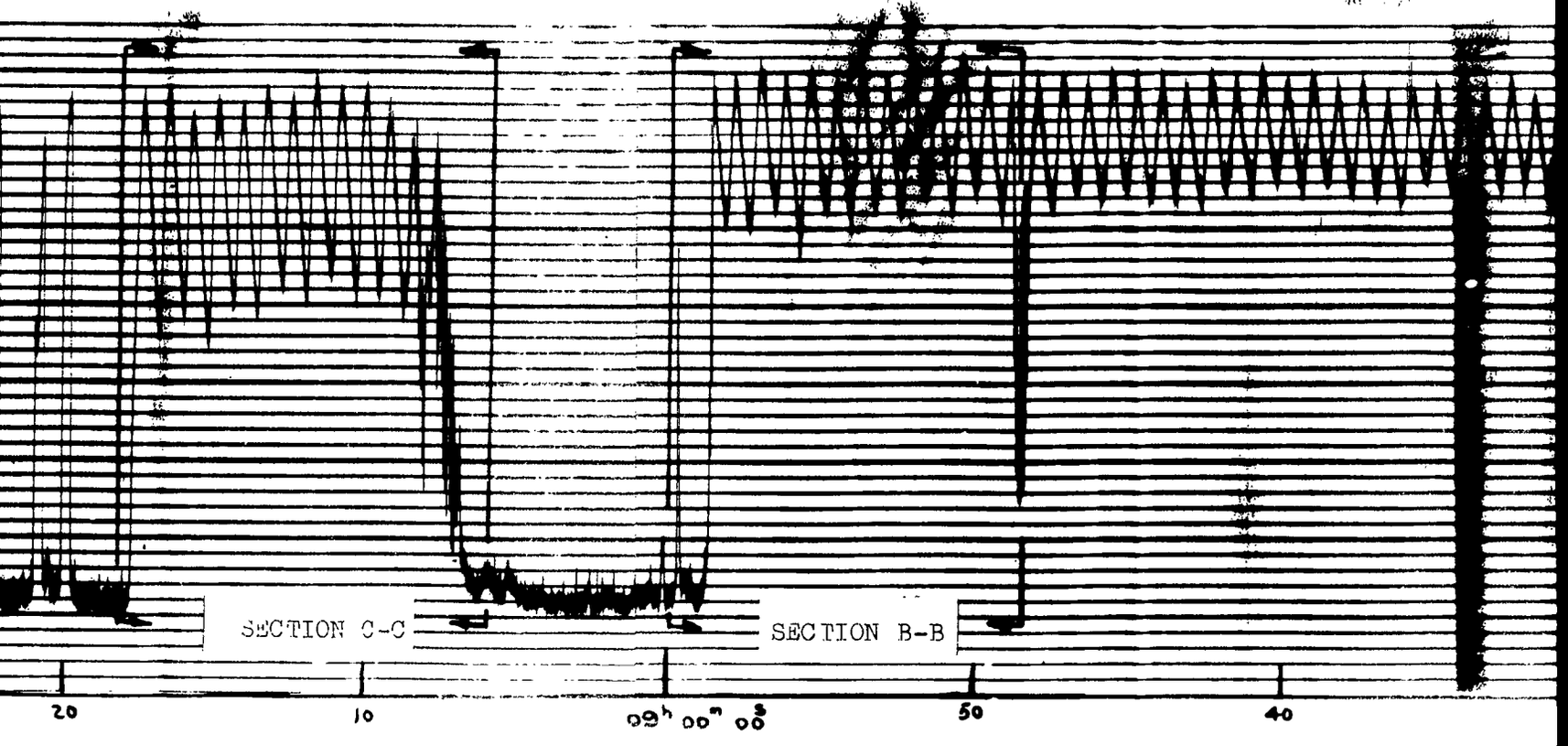
SECTION C-C
SECTION B-B
20
10
09h 00m 00s
50
40

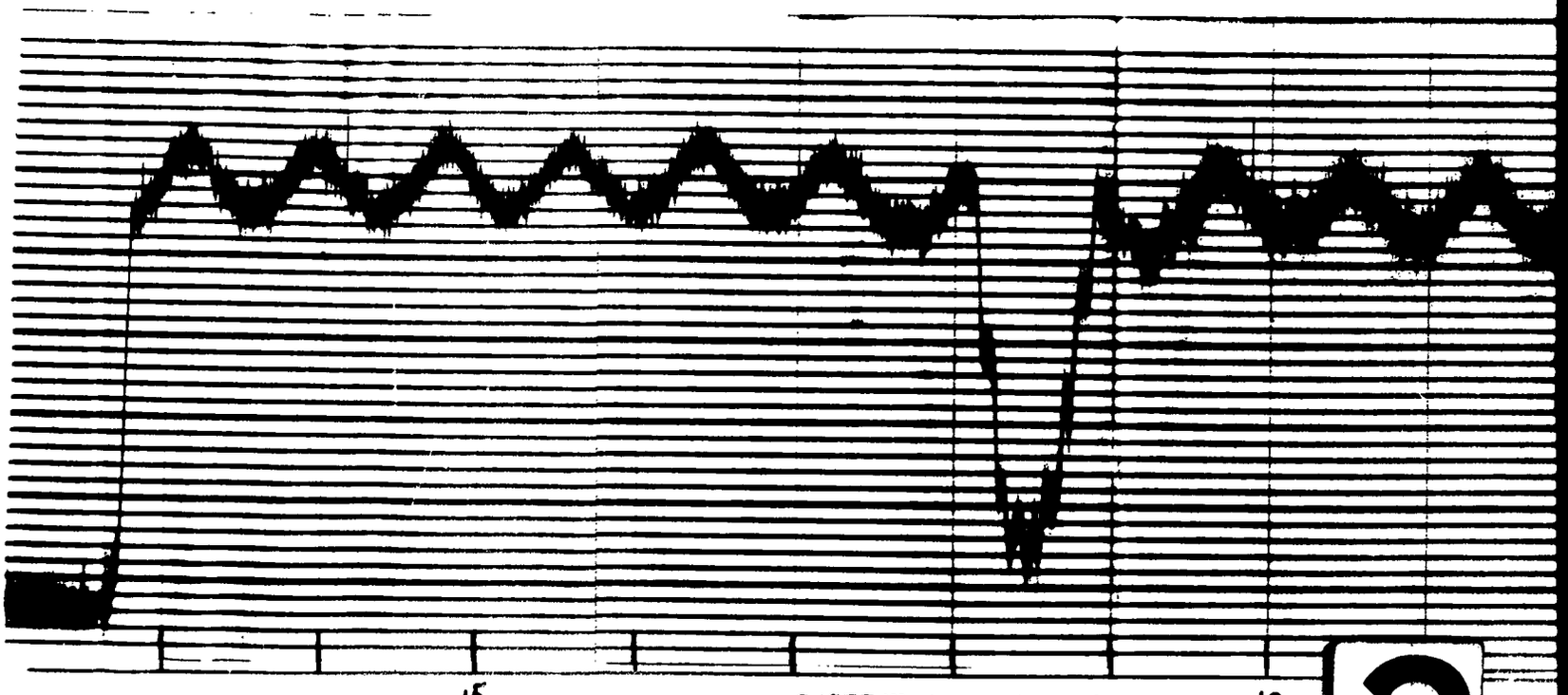
15
SECTION A-A Expanded
10

3

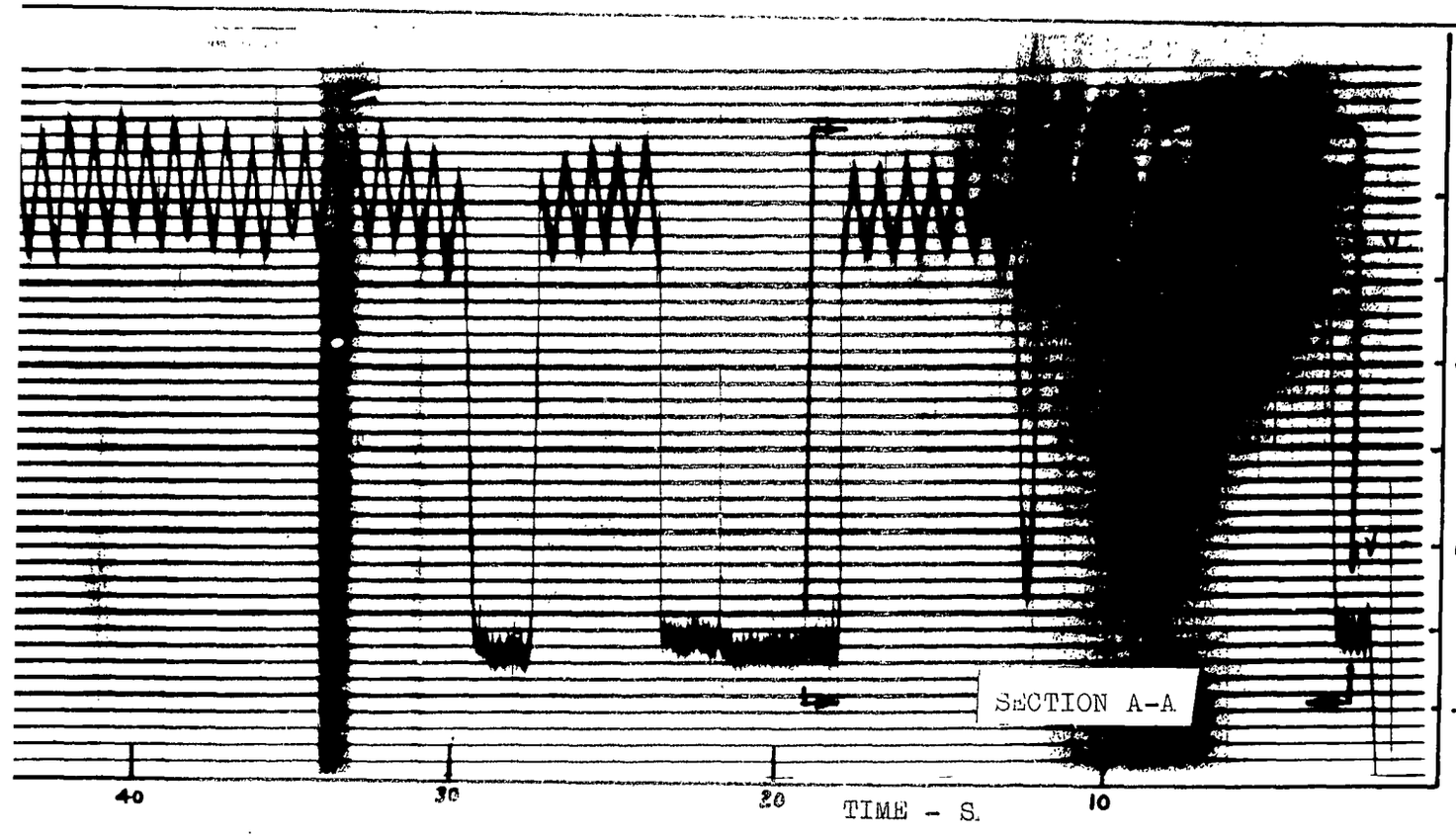
TRACK 7 May
Satellite 62
Russian Rock
Time 08hr -
1.5
1.0
.5
VOLTAGE
SECTION A-A
40
30
20
10
TIME - S.

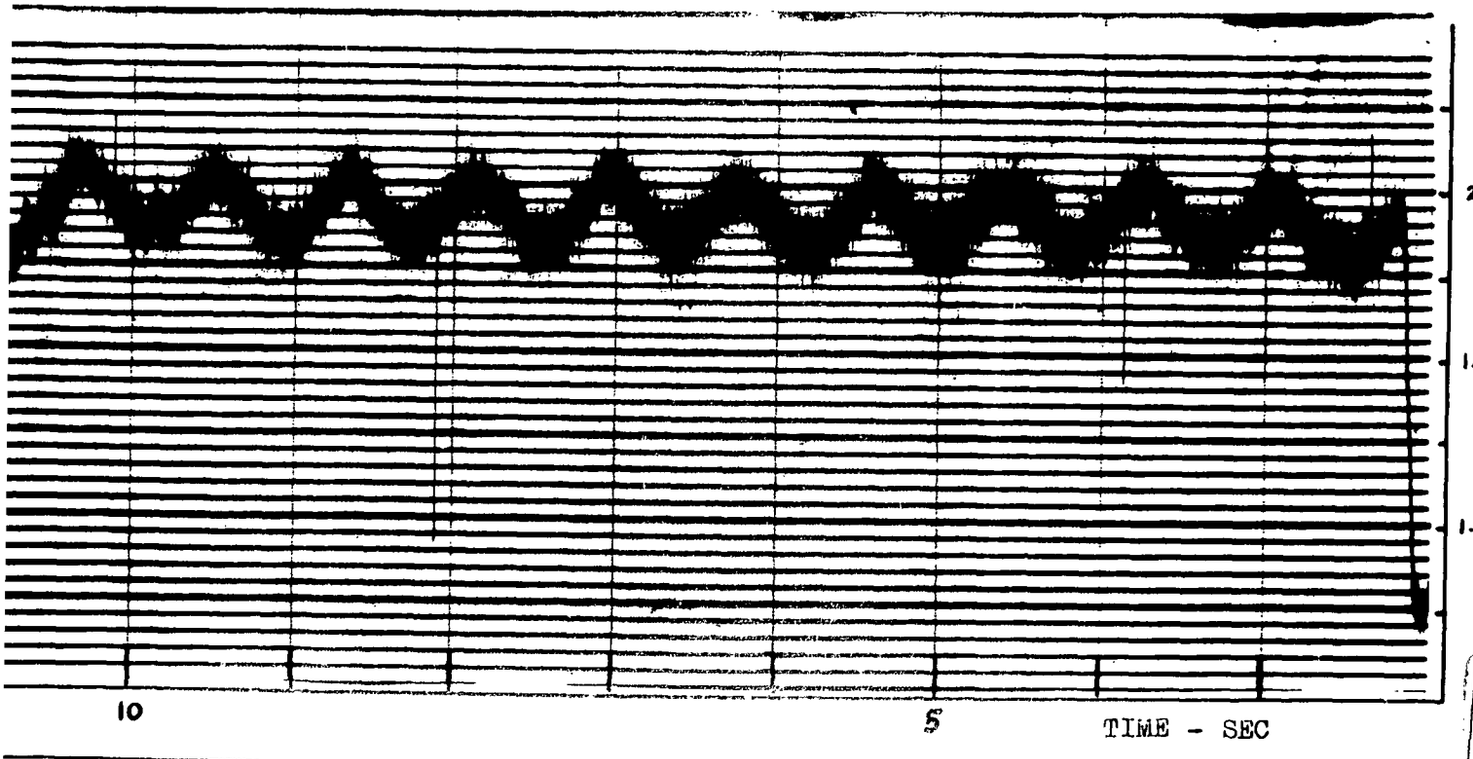
2.0
1.5
1.0
VOLTAGE
10
5
TIME - SEC

4

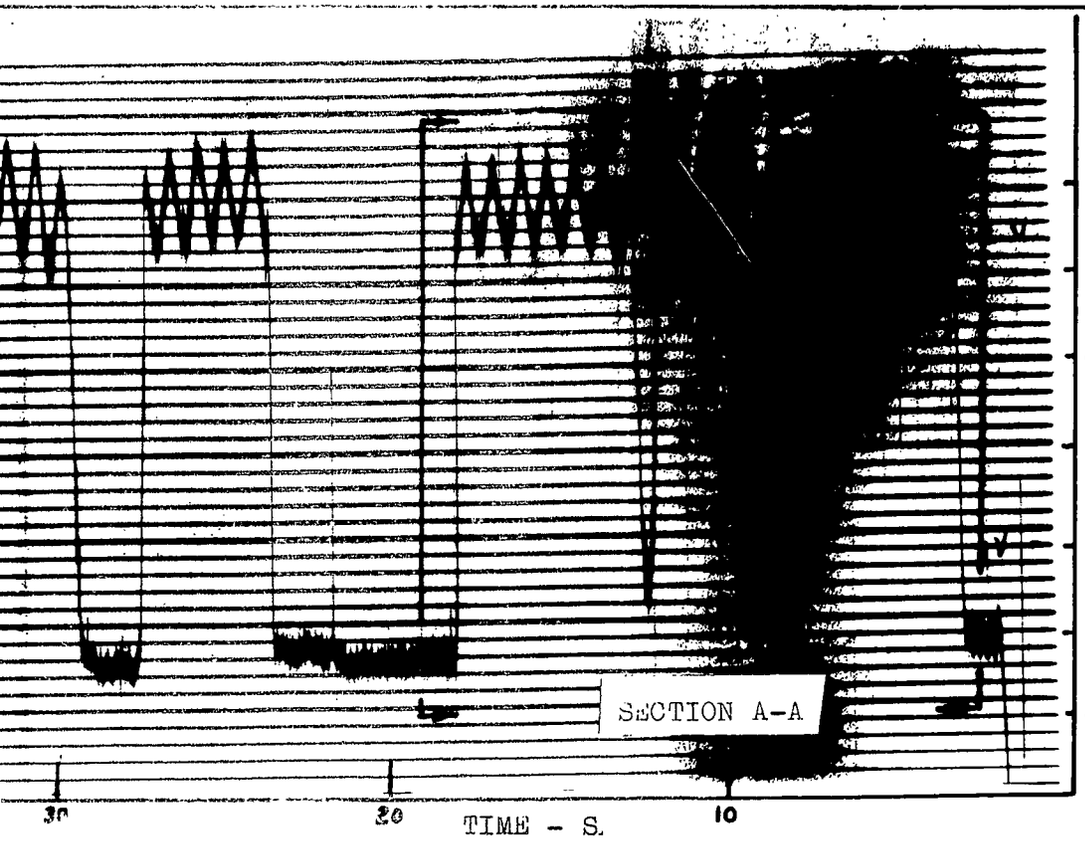

TRACK 7 May 63

Satellite 62 BETA THETA 2

Russian Rocket Body

Time 08hr - 59min - 02sec

1.5

1.0

.5

VOLTAGE

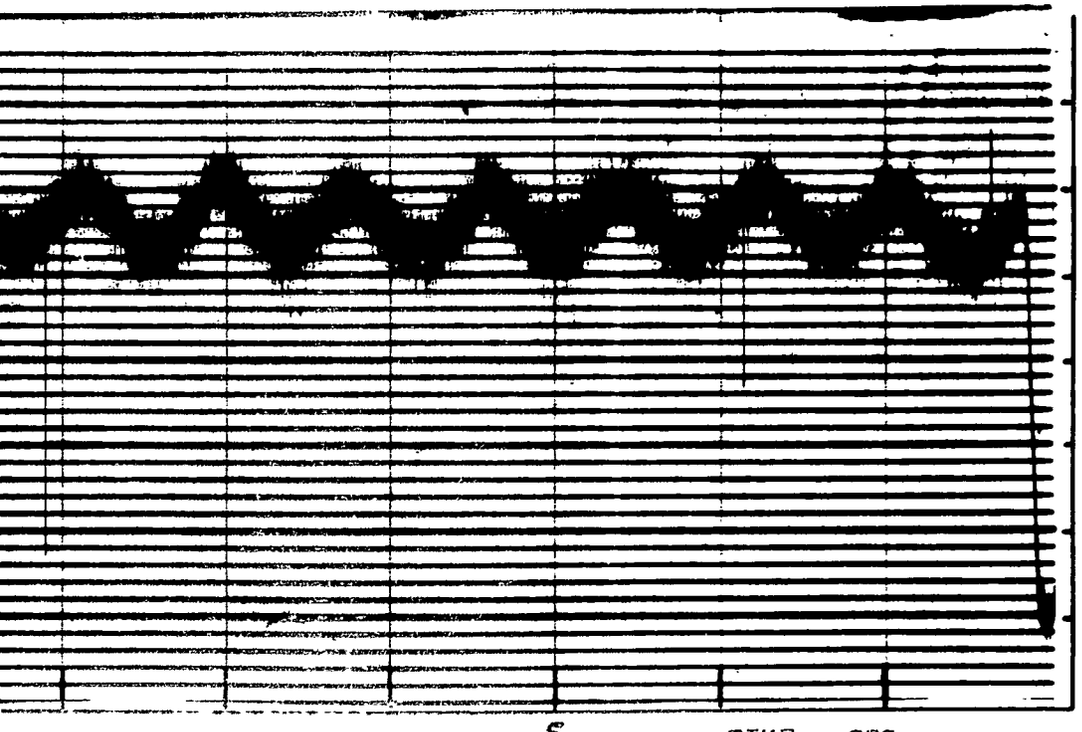

2.0

1.5

1.0

VOLTAGE

5

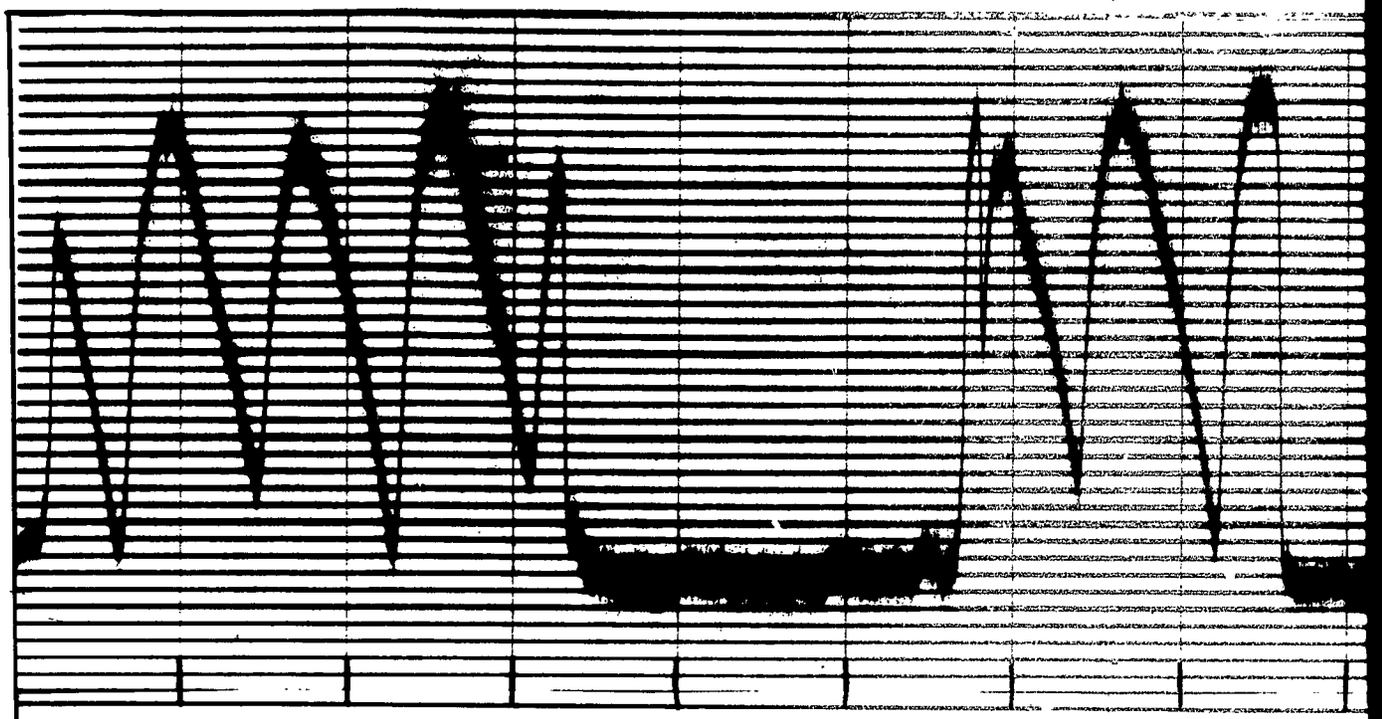

SECTI

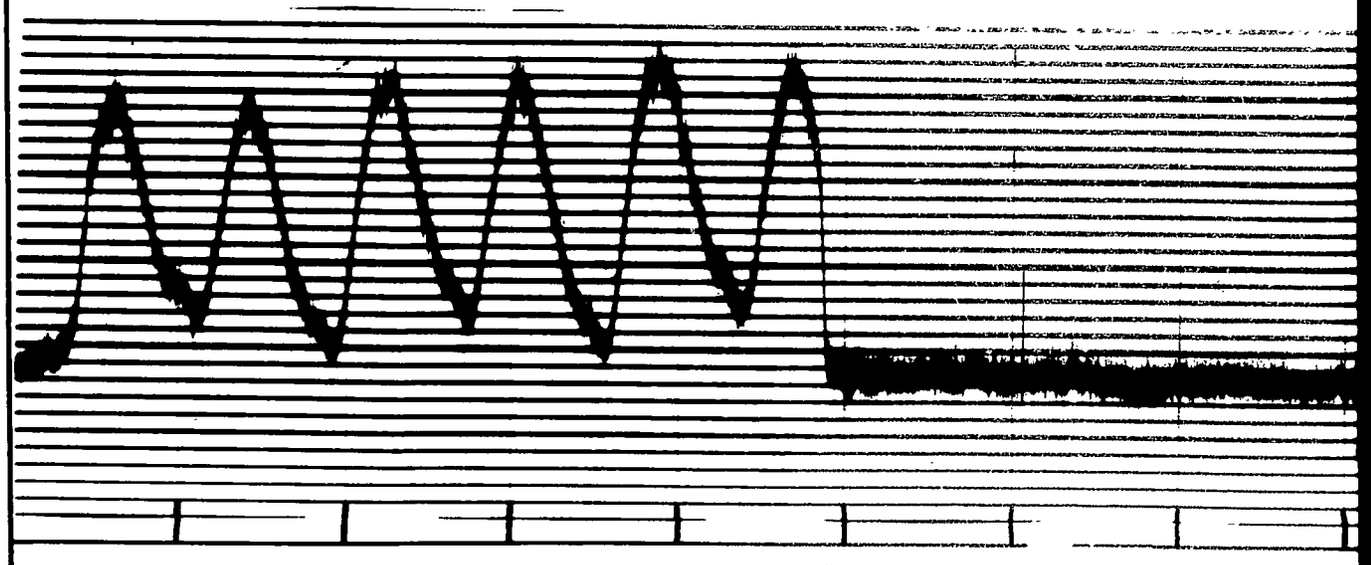

SECTION D-D Expanded

30

TIME -

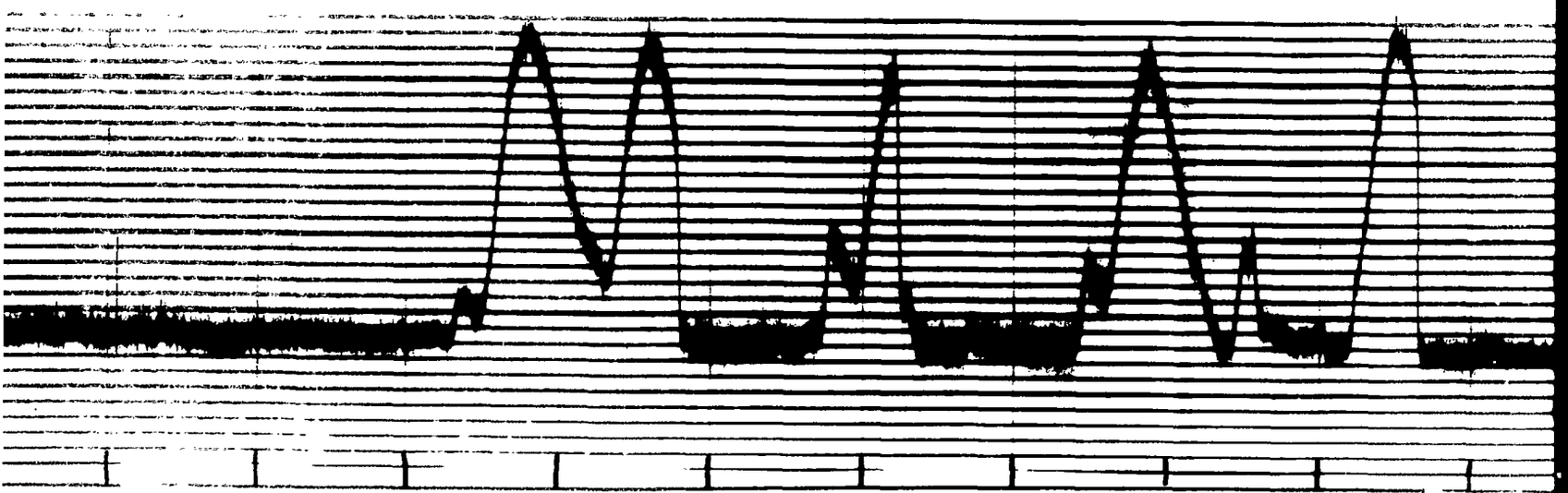

15

SECTION E-E Expanded

10

2

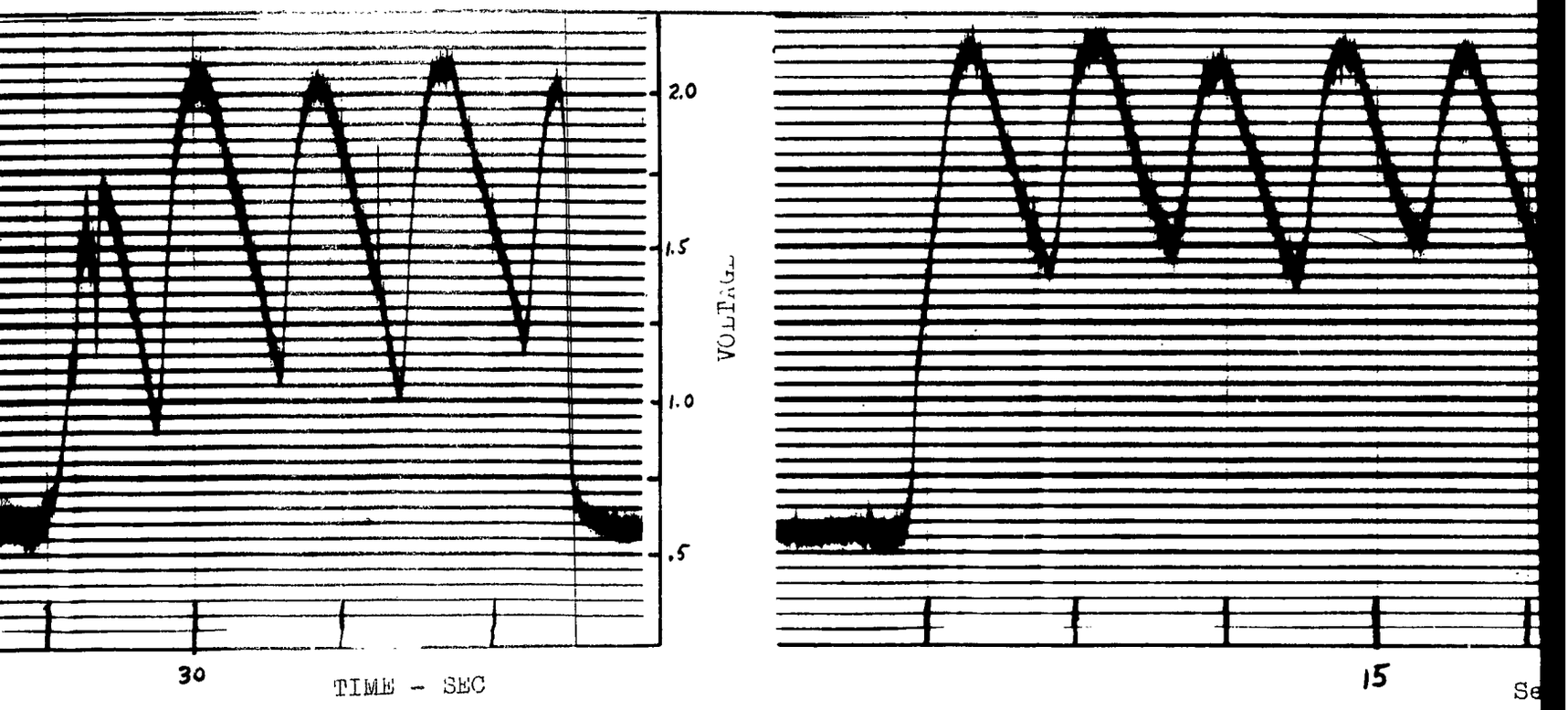

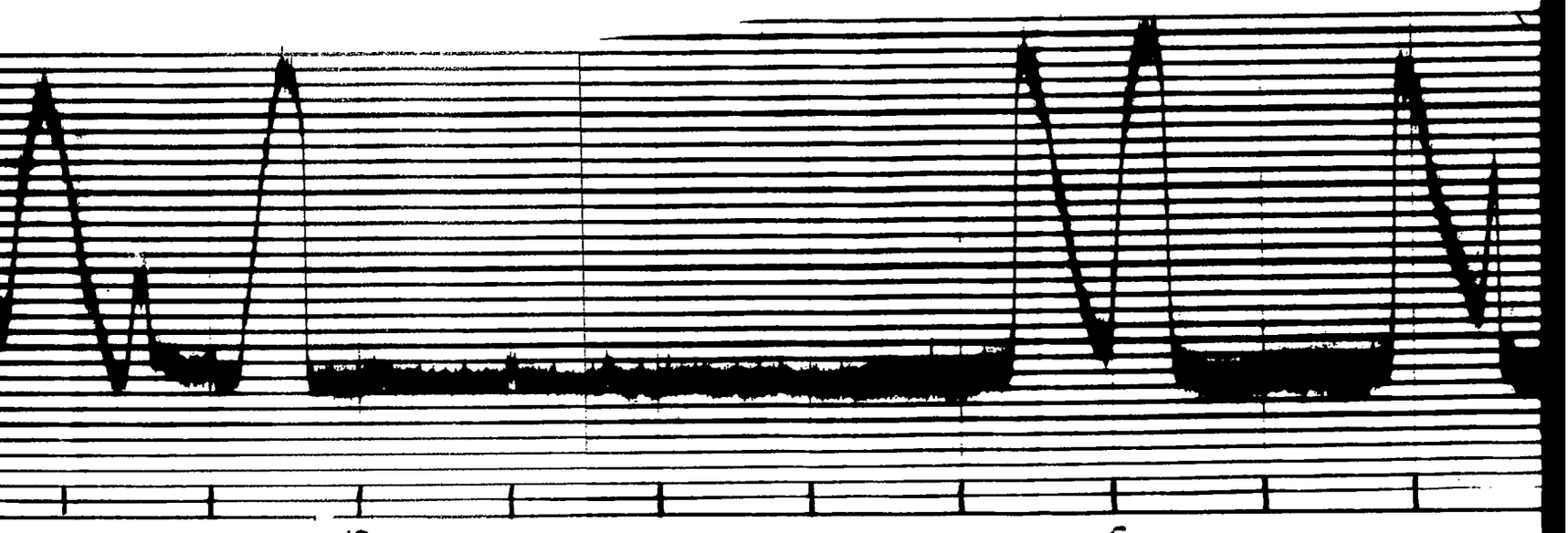

C-E Expanded

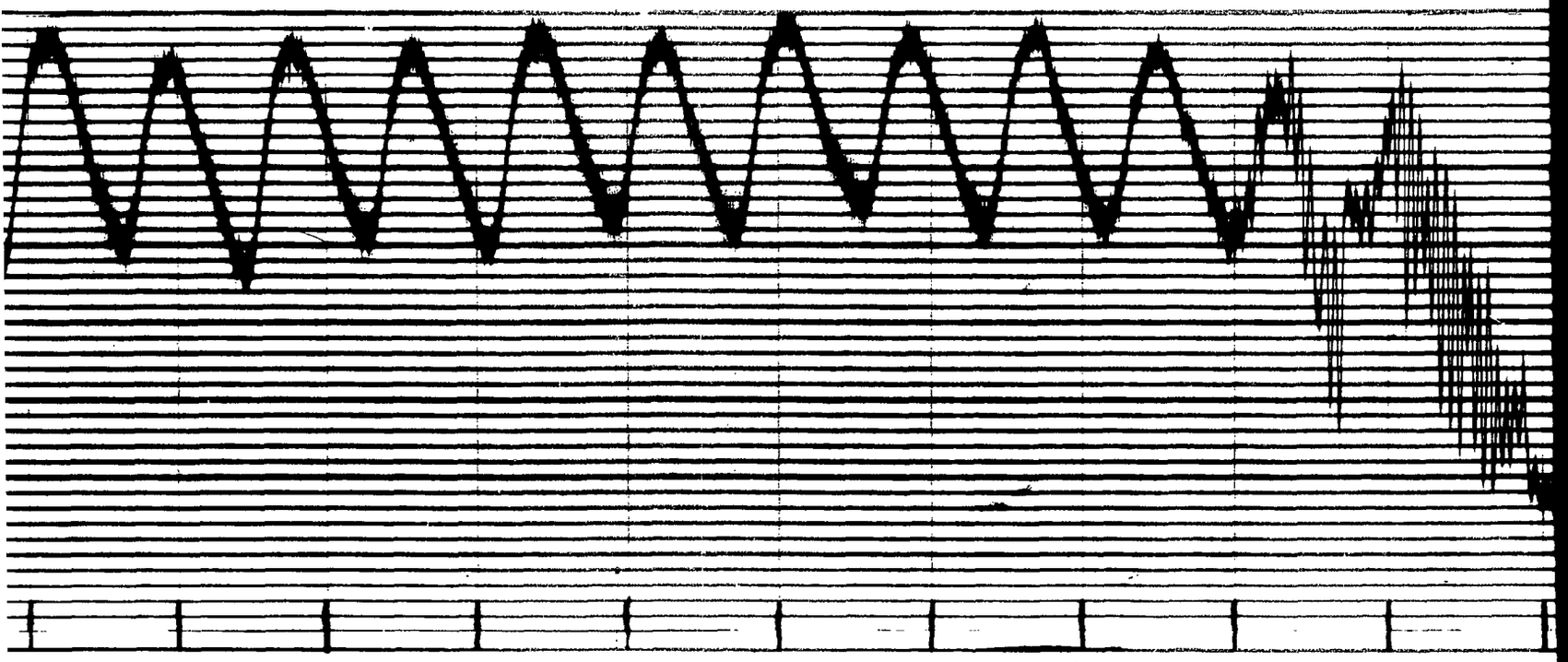

Section C-C Expanded

TRACK 7 May 63

Satellite 62 E

Russian Rocket

4

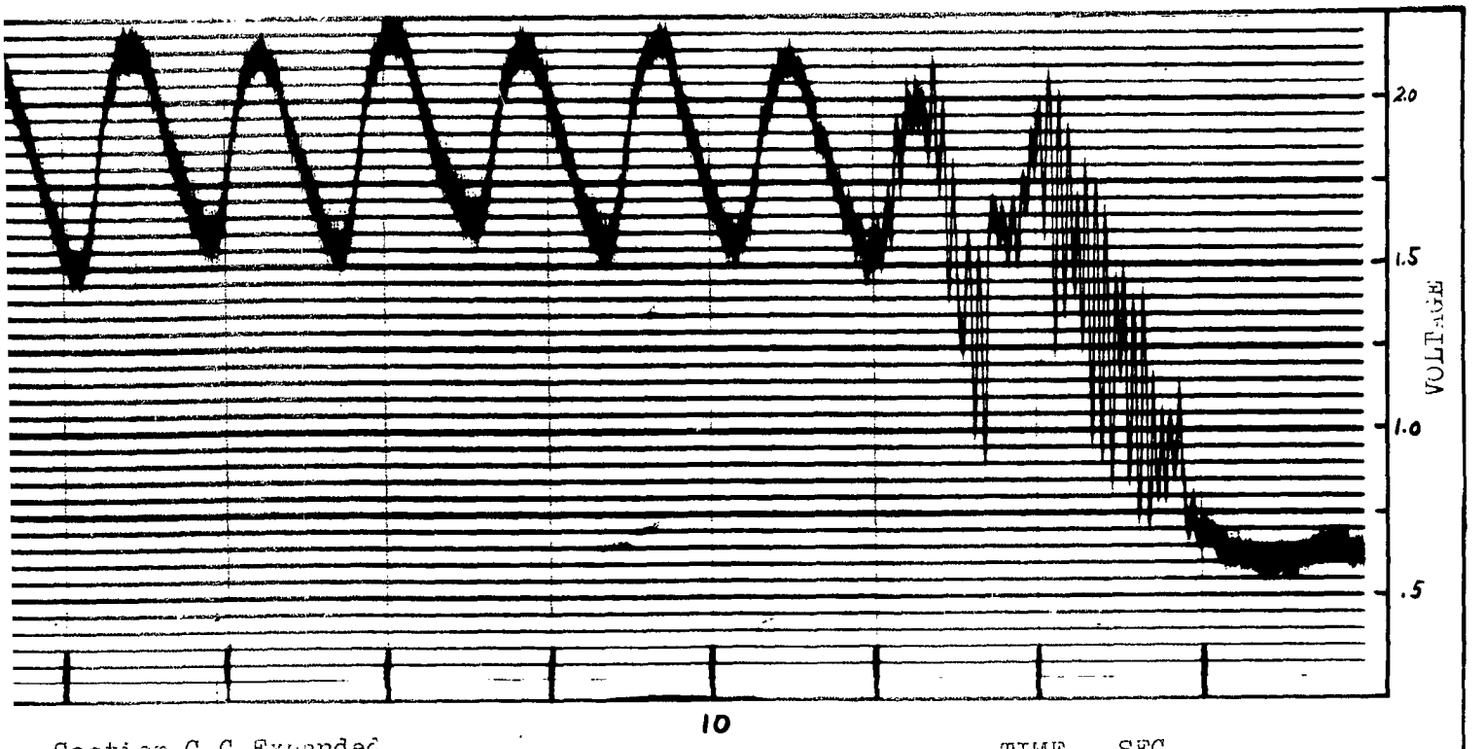

Section C-C Expanded

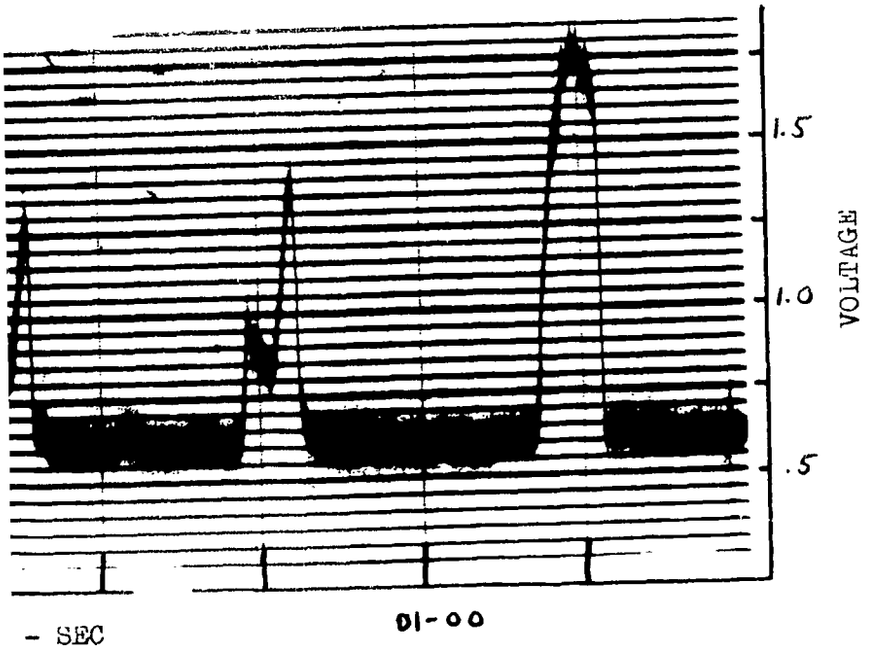

TRACK 7 May 63

Satellite 62 BETA THETA 2

Russian Rocket Body

5

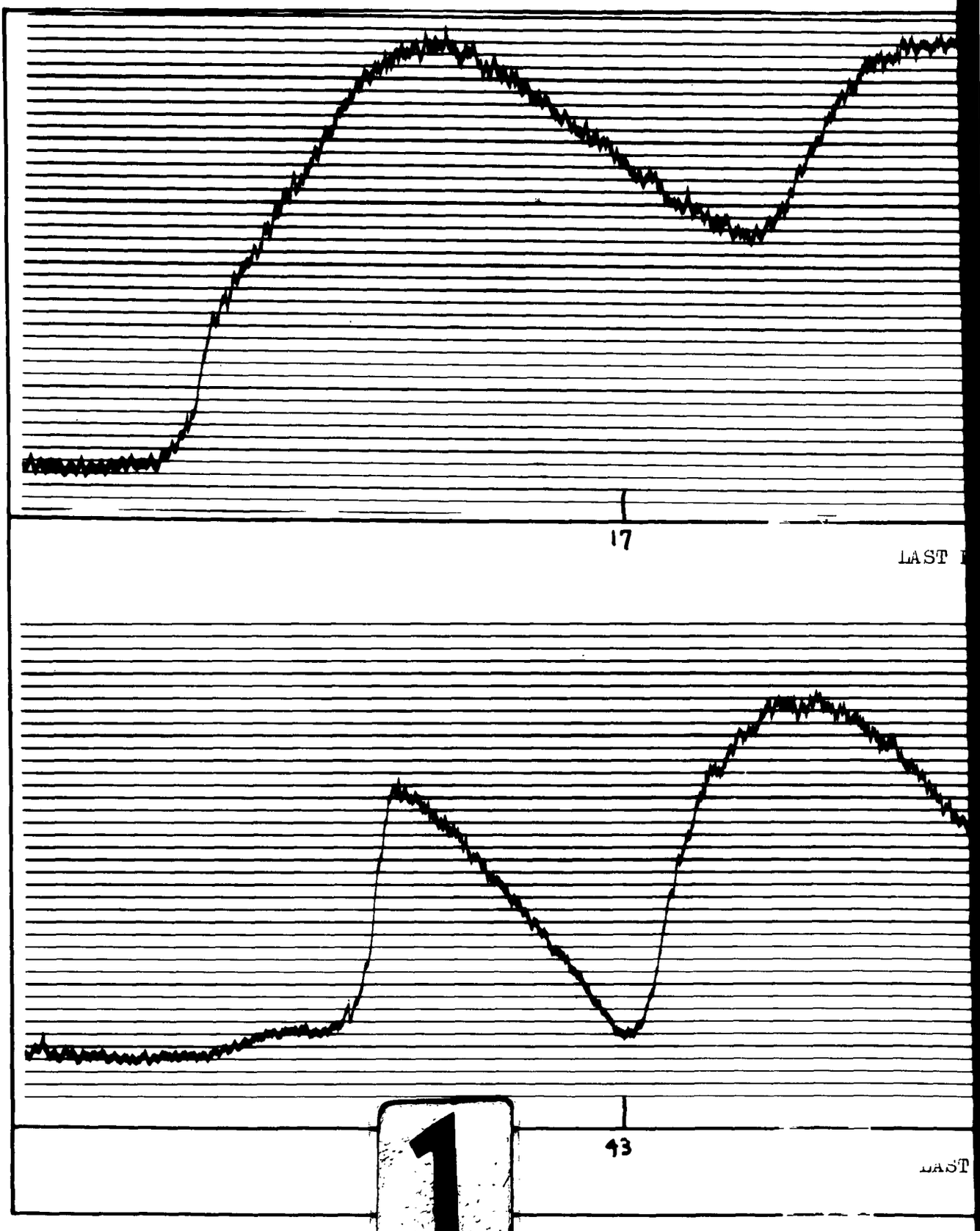
17
LAST
43
LAST
1

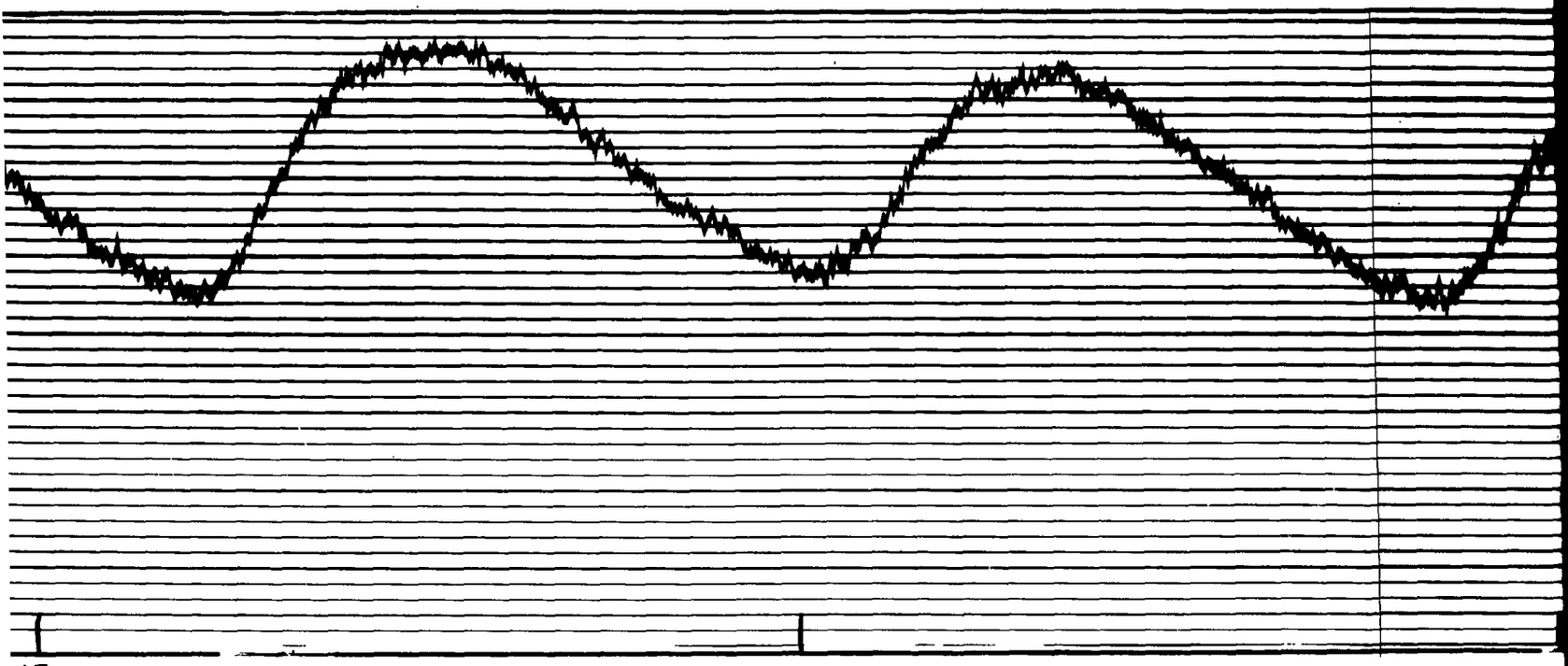

17

LAST FIVE PEAKS OF SECTION C-C EXPANDED TO FIVE INCHES PER SEC

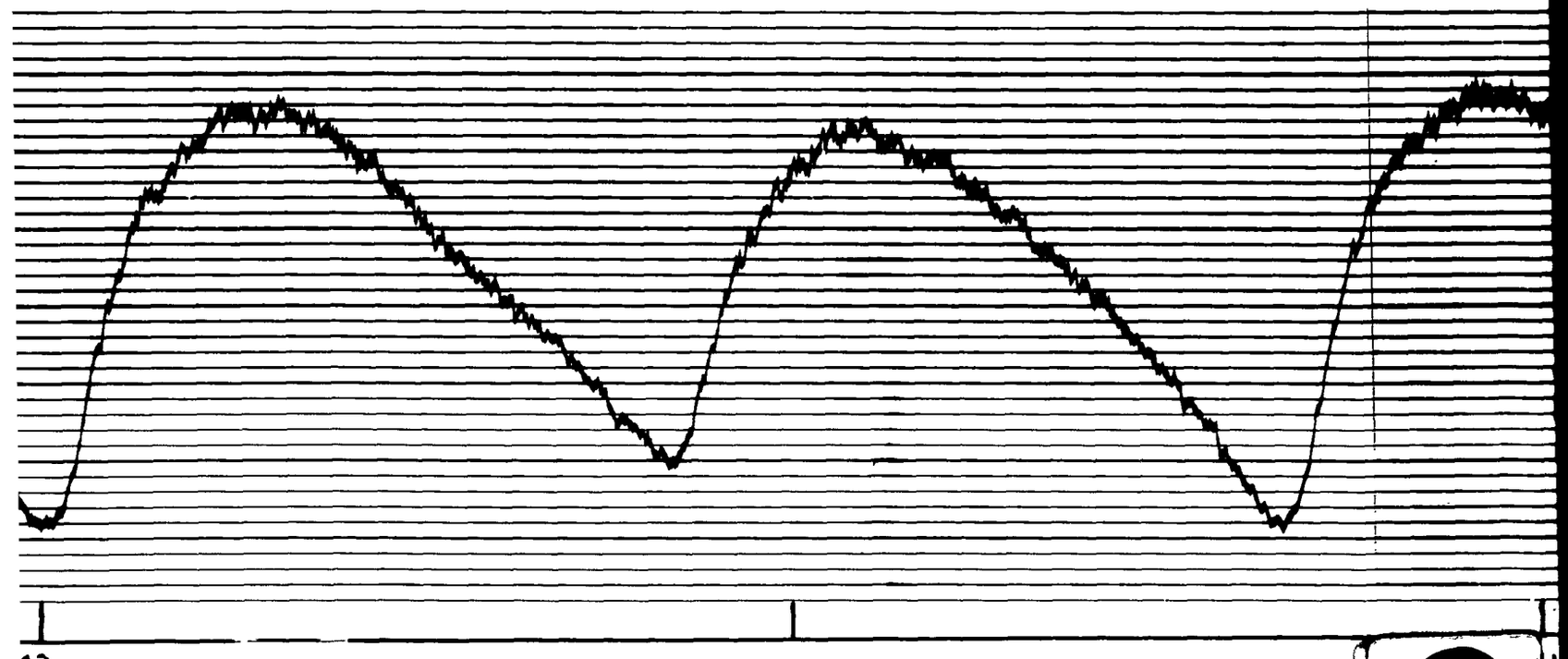

43

LAST FOUR PEAKS OF SECTION D-D EXPANDED TO FIVE INCHES PER SE

2

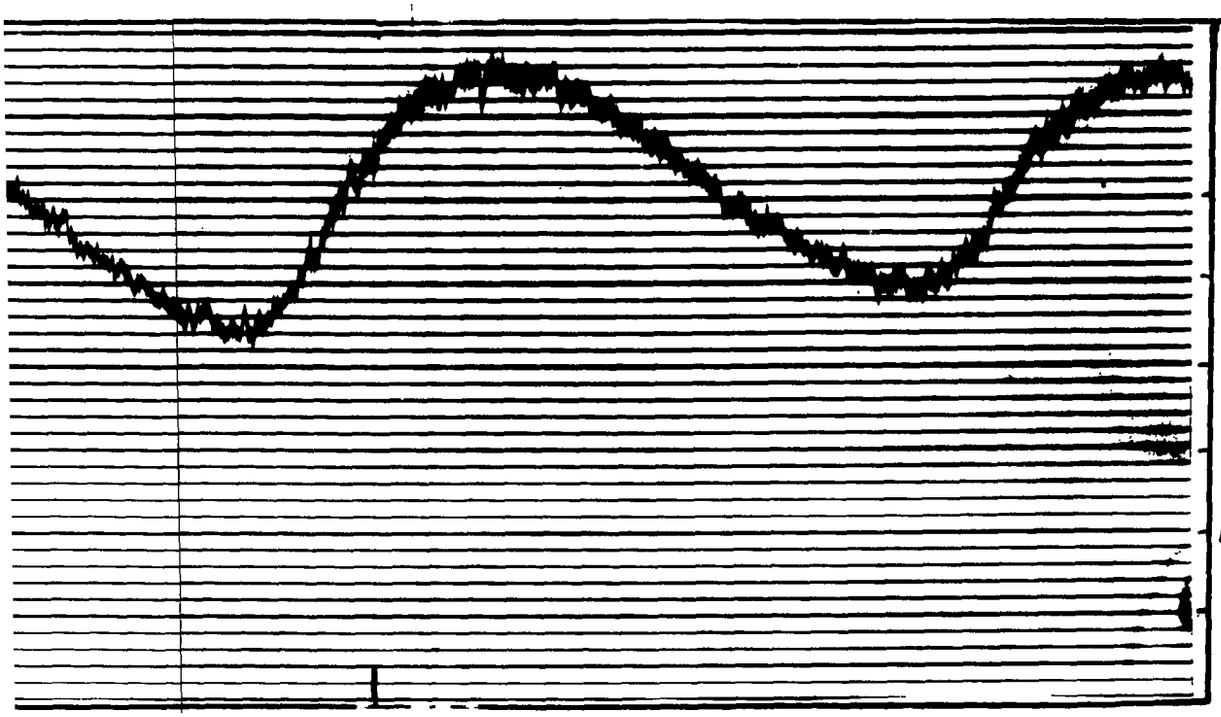

TRACK 7 May 63

Satellite 62 BETA THETA 2

Russian Rocket Body

PER SEC

15

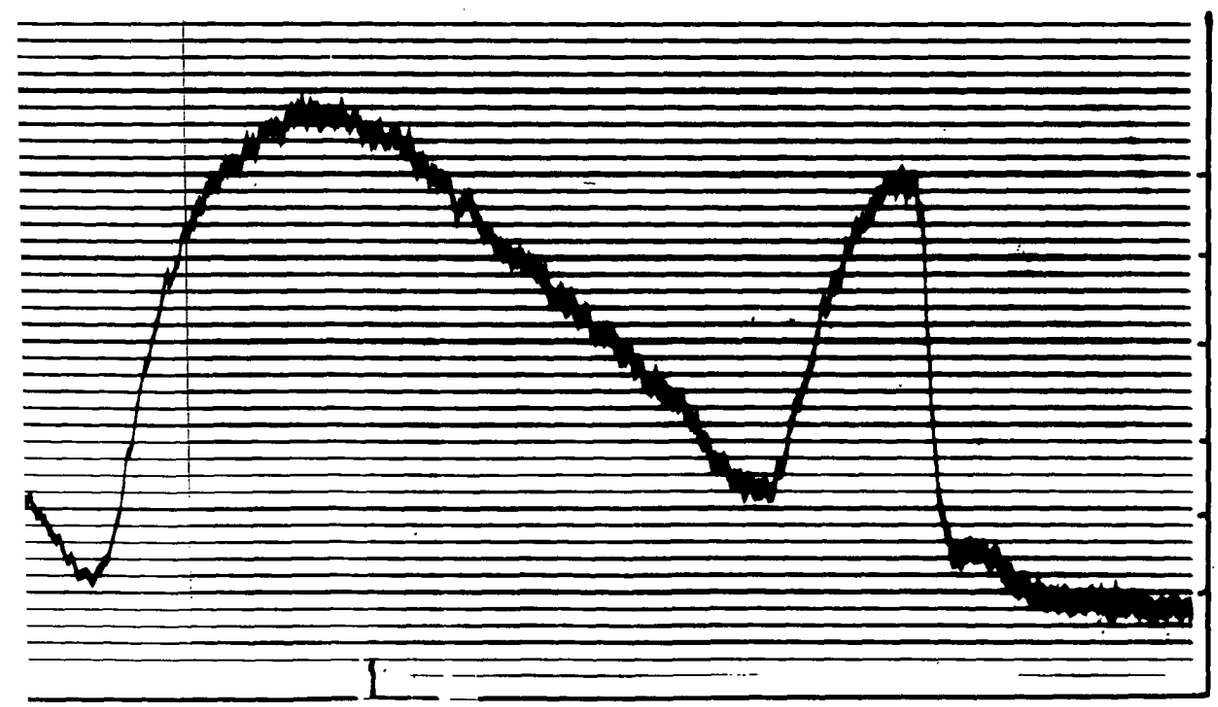

41

S PER SEC

3